Controls on hydrocarbon column-heights in the north-eastern North Sea

Ole Christian Engdal Sollie

Master thesis in Petroleum Geology

Department of Earth Science

University of Bergen

June, 2015

Abstract

Knowledge about the controls on hydrocarbon column-heights is important in hydrocarbon exploration, as such column heights are the main controlling factor for in-place volumes of prospects. The north-eastern Viking Graben comprises an overpressured and a close to- normally pressured area, and commercial and sub-commercial discoveries as well as dry structures have been drilled in both areas. Both oil and gas is present in reservoirs in the study area and the aim of the present study was to investigate the controls on the hydrocarbon column-heights and the distribution of oil and gas. A regional seismic interpretation of the main reservoir unit in the area, the Brent Group, has been carried out based on 3D seismic and published exploration well data. Mapping of spill points and fluid contacts within the different reservoirs in the area resulted in identification of both filled and underfilled traps. The seismic amplitude variations of cap rocks above underfilled and dry traps were investigated in search for evidences of underlying and column-restricting leaky faults or fault intersections.

An overpressured area without lateral pressure communication between hydrocarbon-bearing and dry structures has been identified in the deep basinal parts, while a close to normally pressured area with possible communication between the reservoirs is present on the eastern flank of the Viking Graben. Previously open fill-spill routes are suggested to be closed at present day in the overpressured area due to extensive quartz cementation during burial. This has resulted in a limited supply of gas from the deep grabens to the shallow terraces. It is inferred that the oil that is preserved in the shallow structures is present because of closure of the migration routes for gas from the graben areas, combined with oil charge from shallower areas.

A total of six structures in the study area have been found to leak, of which four are underfilled. One of the reportedly dry structures within the study area is suggested to contain hydrocarbons up-dip from the well location. Leakage through faults and especially fault intersections are suggested to control the hydrocarbon column heights in the leaky structures, and such leakage can be the cause of emptied reservoirs. The suggested leaky faults have different orientations from the faults that delineate the filled structures. However, most of the leaky faults are not critically oriented for failure in the present day stress regime. Seismic bright amplitude anomalies in the Kyrre Formation are present above four of the four column-restricting leaky faults or fault intersections in the deep overpressured area. It is suggested that analysis of amplitude variations in the Kyrre Formation should be applied to future volume and prospect risking of structural traps in the study area.

Acknowledgements

The present study was conducted at the Department of Earth Science, University of Bergen. I would like to acknowledge several people that have been important during this study and my time at the University.

First I would like to thank my supervisor, Christian Hermanrud, for providing me with this interesting and challenging project. He has been very enthusiastic and helpful, giving me rapid and constructive feedback during this project. I would also like to thank all the members of the PESTOH group for valuable discussions.

Statoil ASA is thanked for providing the 3D seismic data and well data needed to conduct this project.

I would like to express my gratitude to my lab mates and friends, Audun Aas Hegna and Alice Vie. They have made a positive atmosphere in the seismic lab, even during stressful periods. I also wish to thank all my fellow students at the University of Bergen for five eventful years and lots of great memories. My friend, Birgitte Opås is thanked for taking her time to proofread my thesis.

I am also very grateful to my family for all their support and encouragement throughout these years.

The most special thank goes to my girlfriend, Ragnhild, for being so supportive and cheerful during difficult times.

Bergen, 29 June 2015

Ole Christian Engdal Sollie

Table of Contents

1 Introduction

The Northern North Sea has been subject to extensive hydrocarbon exploration for several decades and is today a highly mature area, with a total of 26 producing fields and a number of fields in development (NPD, 2015). Major rotated fault blocks and horst structures on the western and eastern side of the Viking Graben, namely the Tampen Spur and Horda Platform, host some of the largest oil and gas accumulations on the Norwegian Continental Shelf (Fig. 1.1a). The majority of these large-scale Jurassic traps were discovered with the use of simple 2D seismic data already in the 1970s (e.g. Statfjord, Snorre, Gullfaks, Oseberg and Troll fields).

As the most evident and large hydrocarbon traps in the Northern North Sea were discovered several decades ago, methods and knowledge that could lead to new commercial discoveries are of high value in the industry. During the last three decades, improved imaging of the subsurface due to the introduction of 3D seismic data, has allowed for mapping of more complex geological structures and screening of subsurface processes. Although great advances in technology and geological knowledge have led to new discoveries, the occurrence of sub-commercial discoveries and dry traps is still a major concern for oil companies.

The present study covers an area in the north-eastern region of the Northern North Sea (within quadrant 35), approximately between $61°00 - 61°65'$N and $2°90' - 3°70'$E (Fig. 1.1a). It encompasses the north-eastern part of the Viking Graben (Flatfisk Slope) and southern part of the Sogn Graben, including the Marflo Spur, northern part of the Lomre Terrace and the western part of the Uer Terrace. Small-scale rotated fault blocks and horst structures in this area form a transition from the shallow, normally pressured Horda Platform to the deeper, overpressured Viking Graben (section X-X' in Figure 1.1c). Since exploration of this area started in the early 1980s, both commercial, sub-commercial and dry traps have been encountered.

The column diagram in Figure 1.1b presents all the drilled structures within the study area, sorted per decade (for simplification, appraisals and post near field wells are left out in this presentation). So far, the only discoveries that have been developed in this region, are the Vega and Fram fields. These relatively small fields were discovered in the most active period of exploration, during the 1980s and 1990s. Of 14 individual structures drilled during this period, only six proved to contain commercial volumes (i.e. Vega and Fram). Five structures, namely Aurora, 35/11-5, Afrodite and 35/10-2, were sub-commercial discoveries. The four remaining wells: 35/11-1, 35/11-3S, 35/10-1 and 35/4-1, proved dry structures, of which the latter three wells recorded residual hydrocarbons within the reservoirs.

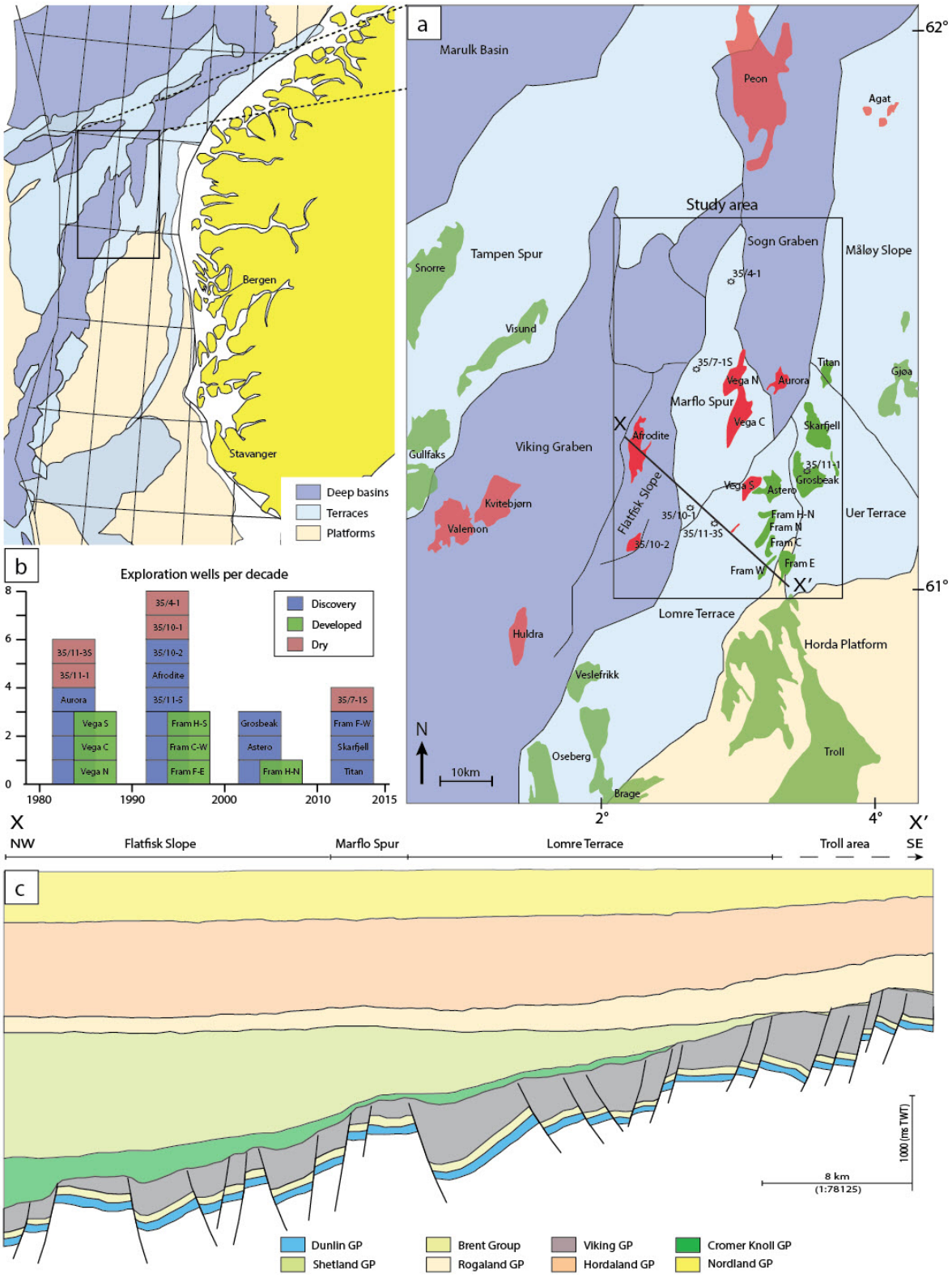

Figure 1.1: a: Overview of the study area and locations of discoveries and dry wells (modified after fact maps in NPD, 2015). **b:** Diagram presenting a simplified exploration history of the study area. **c:** Section from NW to SE showing the structural configuration through the study area (based on interpretation of current data set).

By the year 2000, few Early to Middle Jurassic traps remained untested, resulting in decreased exploration activity in the following decade. However, of three structures drilled during this period, all proved to contain commercial volumes. The Fram H-N and Astero discoveries are both accumulations in local Late Jurassic turbiditic sands, derived from collapsed delta fronts on the shallow terraces (Holgate *et al.*, 2013). These discoveries thus represent a relatively new play type in this area, compared to the Early to Middle Jurassic pre-rift reservoirs (e.g. Brent, Cook, Statfjord Formations). Interestingly, the Grosbeak discovery, which was proven by well 35/12-2, were drilled slightly further up-dip from the previously dry well 35/11-1 (drilled in 1984).

Due to the introduction of the new petroleum plays in this area, exploration has been quite successful during the last five years, with three commercial discoveries: Titan, Skarfjell, and another discovery in the Fram area (Fram F-W). Similar to Fram H-N and Astero, Titan and Skarfell both represent oil accumulations in Late Jurassic turbiditic sequences. Only well 35/7-1S, targeting the Apollon prospect, was unsuccessful. Unlike most of the dry structures in this area, this structure did not contain residual hydrocarbons.

In relative recent years, much attention has been paid to explaining the mechanisms and processes that could potentially lead to hydrocarbon leakage and reduced in-place volumes, and fault reactivation has been suggested as a main cause (Hermanrud & Bolås, 2002; Wiprut & Zoback, 2002; Gartrell *et al.*, 2004; Bolås *et al.*, 2005). Modelling of recent stress changes in the Northern North Sea has been conducted based on well data, in attempts to find influencing factors on trap integrity (Fjeldskaar *et al.*, 2000; Grollimund & Zoback, 2003). Also, 3D seismic data has been extensively investigated in search for relationships between reduced hydrocarbon column-heights, seismic anomalies and other characteristics of leaking structures (Heggland, 2013; Løseth *et al.*, 2013; Hermanrud *et al.*, 2014). Although such studies have been conducted both in the Barents Sea (Georgescu, 2013) and at the Halten Terrace (Ersland, 2014), similar studies are yet to be conducted in the north-eastern North Sea.

Borge (2000) investigated the controls on fluid dynamics and overpressures in Jurassic reservoirs by 3D numerical modelling of fault bounded pressure compartments in the Northern Viking Graben. He suggested that the dominating factor for generation of overpressures during Tertiary was quartz cementation and that reduced overpressure, and leakage from pressure compartments was attributed to hydraulic fracturing of the cap rocks. This study was however limited in the sense that leakage was solely associated with high overpressures. Also, the study did not include analyses of fault orientations or amplitude anomalies in the overburden. More recent studies in other areas have showed that leakage is often caused by reactivation of faults due to stress changes (Bolås & Hermanrud, 2002; Wiprut & Zoback, 2002; Teige *et al.*, 2002; Bolås

et al., 2005). Therefore, evaluation of structural characteristics and current stress state is necessary to assess different leakage mechanisms.

Teige & Hermanrud (2004) conducted a seismic study on one of the sub-commercial discoveries in the area, the B-structure, which were drilled by well 35/10-2. Based on the location of the gas-water contact relative to the structural spill point of this structure and the presence of residual hydrocarbons below the gas-water contact, they concluded that the structure is underfilled. Seismic investigation of the structure indicated that the hydrocarbon column-height could potentially be controlled by vertical leakage through one or more of the faults that delineate the structure. Reduced in-place volumes caused by vertical fault leakage have also been associated with other underfilled structures, both on the Tampen Spur in the Northern North Sea and in other oil provinces (Wiprut & Zoback, 2000, 2002; Gartrell *et al.*, 2003; Kristiansen, 2011; Georgescu, 2013; Ersland, 2014). However, these papers have only investigated structures in local areas, thus it is not known if these findings are applicable for hydrocarbon traps elsewhere.

There are several dry wells with residual hydrocarbons within the study area, and residual hydrocarbons have been recorded below the hydrocarbon columns in other structures. This indicates that one or several geological processes have resulted in reduced column-heights in relative recent geological time. However, what processes that control hydrocarbon column-heights in the area have apparently not been documented.

This study aims to investigate the controls on hydrocarbon column-heights in the northeastern North Sea. Spill routes, fluid contacts and pressure regimes have been mapped in an attempt to get an understanding of the plumbing system and the oil versus gas distribution in the area. Seismic and structural characteristics, including reservoir pressures of the different traps have been investigated in an attempt to distinguish the traps with reduced hydrocarbon column-heights from the filled structures. Evaluations on the different leakage mechanisms which could explain the underfilled and dry traps have also been performed.

2 Geological evolution of the Northern North Sea

The tectonic evolution of the North Sea can be traced back to the mid-Ordovician, when the continental elements of Baltica and Avalonia converged and collided with Laurentia. The collision persisted well into Devonian, resulting in the closing of the Iapetus Ocean and the formation of the Caledonides (Ziegler, 1975; Bluck, 2000). Sinistral shearing between the continents during the Caledonian phase resulted in the formation of NE-SW-oriented structural lineaments in the crystalline basement (Whipp *et al.*, 2014). Some of theses lineaments later acted as zones of crustal weakness and were reactivated as normal faults during post-orogenic collapse in the Devonian and Carboniferous (Ziegler, 1992; Whipp *et al.*, 2014). It has also been suggested that these reactivated zones had geometrical constraints during rifting phases in Mesozoic and even during the passive, thermally driven subsidence in Cenozoic (Bartholomew *et al.*, 1993; Whipp *et al.*, 2014).

Mesozoic

Throughout the Mesozoic era, the Viking Graben along with surrounding terraces and platform areas in the Northern North Sea underwent two major episodes of lithospheric stretching, separated by a period of tectonic quiescence (Nøttvedt *et al.*, 1995; Færseth, 1996). Both episodes were approximately of the same magnitude and of equal importance for the structural evolution of the Northern North Sea. However, due to a change in orientation of the extensional stress fields, the structural expression between the two rifting episodes differ significantly (Færseth, 1996).

The first major rifting phase initiated in Late Permian to Early Triassic, triggered by the break-up of Pangea. Regional E-W to ENE-WSW oriented extension in the Northern North Sea resulted in the formation of a 130-150 km wide basin, consisting of high displacement N-S oriented basement-involved fault systems, such as the Snorre, Visund and Sogn Graben faults (Færseth, 1996). Throughout Triassic, the E and W dipping asymmetric half-grabens comprising the basin, were continuously filled with (syn- and intra-rift) alluvial, fluvial and lacustrine sequences of the Hegre Group (Steel & Ryseth, 1990; Steel, 1993; Ravnaas *et al.*, 2000). Towards the end of Triassic and into the Early Jurassic period, fluvial deposits of the Statfjord Formation dominated throughout the Northern North Sea (Fig. 2.1) (Steel & Ryseth, 1990).

Associated with early Triassic rifting and subsequent compaction- and thermally induced basin subsidence, the depositional environment in the Northern North Sea gradually passed from continental to marine conditions in the Jurassic period (Nøttvedt *et al.*, 1995; Ravnaas *et al.*, 2000). A major marine flooding in Middle Sinemurian led to the

establishment of the shallow Dunlin Sea, allowing marine shales of the Dunlin Group, the Amundsen and Drake Formations, to deposit throughout the Northern North Sea. Sandy near-shore and inner shelf deposits of the Johansen and Cook Formations separating the Dunlin shales, indicates intervening periods of relative sea-level fall. These sandy sequences prograded westwards into the basin and are believed to be derived from the Norwegian hinterlands (Steel, 1993).

Major tectonic uplift in the Middle Jurassic, coupled with active erosion of the southern and eastern reaches, namely the mid-North Sea dome and the Northern North Sea rift margins, led to the evolution of the Brent Delta System of the Northern North Sea. The Brent delta prograded northwards, covering the Viking Graben including its western and eastern flanks (e.g. Tampen Spur and Lomre/Uer Terrace) and reached its progradational limit approximately at $61,5°$N, where it shales out into marine mudstones (Helland-Hansen *et al.*, 1992; Steel, 1993; Nøttvedt *et al.*, 1995; Graham *et al.*, 2003). Today the Brent Group form excellent reservoir rocks and spill routes for petroleum in the North Sea, and the majority of the producing fields and prospects within the Lomre/Uer Terrace area is presented by the Brent sands.

As a response to the tectonic uplift and erosion of the Horda Platform and Norwegian hinterlands in the Latest Toarcian/Earliest Aalenian, fan-deltas prograded west- and north-westwards into the basin, covering major parts of the Lomre/Uer Terrace. These shallow marine sandstones are known as the Oseberg Formation (and its British equivalent: Broom Formation). Although the Oseberg Formation is formally a part of the Brent Group, it is widely recognized as being separated from the main components of the Brent Delta System (Helland-Hansen *et al.*, 1992; Steel, 1993). In the Latest Aalenian/Earliest Bajocian, a marine flooding produced an extensive marine basin, drowning the Oseberg sand systems in the Northern North Sea. This maximum flooding resulted in renewed accommodation space in the basin and denotes the beginning of the progradation of the proper Brent Delta System (Helland-Hansen *et al.*, 1992).

The progradational part of the Brent Delta is represented by the Rannoch-Etive Formations and the lower part of the Ness Formation. The Rannoch-Etive deposits are delta front facies, more specifically deposition in the the lower/middle shoreface to upper shoreface/foreshore realm, respectively. The lower Ness is the terrestrial equivalent of the Rannoch-Etive sequence, characterized by a fluvial depositional environment and comprises a somewhat more heterolithic interval with mixed sequences of sandstone, mudrock and coal (Helland-Hansen *et al.*, 1992). The progradation of the Brent Delta was relatively rapid and the retreat commenced already in late Early Bajocian (Steel, 1993), continuing into Early Bathonian. The transgressive part of the Brent Delta is represented by the Tarbert Formation, marked by the first appearance of shoreline sediments, and its continental equivalent, the upper Ness Formation (Helland-Hansen

et al., 1992).

The second and last major rifting phase in the northern North Sea started in Late Bajocian-Early Bathonian and marks the cessation of the Brent Delta System (Helland-Hansen *et al.*, 1992; Steel, 1993; Whipp *et al.*, 2014). Regional NW-SE oriented extension led to reactivation of old Permo-Triassic faults (e.g Snorre, Visund and Sogn Graben faults) and the formation of new Jurassic faults throughout the basin (Færseth, 1996). In the area north-east of 61°N, which underwent maximum stretching (Færseth, 1996), new Jurassic terraces developed between the Viking Graben and Horda Platform (Graham *et al.*, 2003; Holgate *et al.*, 2013). The Lomre and Uer Terrace are both examples of such terraces, exhibiting primarily NNE-SWW-trending faults, forming a mosaic of narrow sub-basins and structural highs throughout the area (Gabrielsen *et al.*, 2001).

As a result of mid-Late Jurassic rifting and subsequent basin deepening, a major marine flooding led to the deposition of the fully marine Viking Group throughout the northern North Sea (Whipp *et al.*, 2014). Pulsed rifting during mid-Late Jurassic, accompanied with several transgressive-regressive cycles, resulted in the progradation of three major sandstone units in the shallow sea of the rift margins: the Krossfjord, Fensfjord and Sognefjord Formations (Steel, 1993; Holgate *et al.*, 2013). Sourced from the uplifted Norwegian Hinterlands, these deltas covers the Horda Platform and pinches out westwards into the shaly Heather Formation, towards the Lomre/Uer Terrace (Holgate *et al.*, 2013). These units, each 100-200 m thick, form the reservoirs of the giant Troll field on the Horda Platform (Holgate *et al.*, 2013), including the Fram fields and the recently discovered Grosbeak accumulation on the Uer Terrace.

Sourced from the collapse of Late Jurassic delta fronts, turbidity currents transported sands from the Horda Platform, north-east- and north-westwards into the deeper basins. These Callovian and Oxfordian turbiditic sequences form relatively good reservoirs and their reservoir sequences host several oil and gas discoveries at the Lomre/Uer Terrace (e.g. Fram H-N, Astero, Skarfjell, Aurora and Titan) (Graham *et al.*, 2003; Holgate *et al.*, 2013). The thicknesses of these turbidites varies and can be up to 200 m in proximal parts, however, mapping of these units is challenging due to their lateral and vertical thickness variation (Bugge *et al.*, 2001).

As the rate of extension and tectonic-induced subsidence reached its peak in Kimmeridgian times, a new marine flooding of the Viking Graben led to deposition of the deep-marine mudstones of the Draupne Formation (Steel, 1993; Holgate *et al.*, 2013; Whipp *et al.*, 2014). Restricted bottom water circulation in the rift-related subbasins allowed for the accumulation and preservation of organic material, thus making the Draupne Formation a highly potent source rock unit throughout the North Sea (Keym *et al.*, 2006). By the mid-Late Ryazanian (Early Cretaceous), practically the

entire basin was flooded, resulting in a less isolated and more oxygenated environment, which in turn favoured deposition of less organic shales throughout the Cretaceous time (Badley *et al.*, 1988; Bugge *et al.*, 2001).

Sedimentation throughout the Cretaceous was highly influenced by the structural relief formed during late Jurassic rifting and post-rift basin subsidence (Bugge *et al.*, 2001). The lower Cretaceous Cromer Knoll Group, comprising the Åsgard, Sola and Rødby Formations, reflects an overall transgressive trend in the northern North Sea (Bugge *et al.*, 2001). This group mainly consists of calcareous claystones, siltstones and marls with occasional layers of limestones and sands, represented by the Mime Formation (basin margins (Kjennerud *et al.*, 2001)) and Agat Formation (in the northern part of the area) (Gabrielsen *et al.*, 2001). The lower Cretaceous deposits onlap the Upper Jurassic shales and are mainly present in the deeper parts of the basin and in structural lows at the terraces.

Towards the Horda Platform and on structural highs, the Lower Cretaceous Cromer Knoll Group is nearly absent and the Draupne shale and Sognefjord sands are in some places directly overlain by the Upper Cretaceous deposits. As basin subsidence increased in the Upper Cretaceous, deposition of the dominantly shaly and marly Shetland Group (Svarte, Blodøks, Tryggvason, Kyrre and Jorsalfare Formations) gradually smoothed the Jurassic rift relief. Also, regional subsidence continuously shifted eastwards towards the Horda Platform, resulting in a wider and deeper basin with a much lower gradient than before. By the end of Cretaceous, thermal equilibrium was reached and tectonic subsidence ceased (Bugge *et al.*, 2001; Gabrielsen *et al.*, 2001; Kyrkjebø *et al.*, 2001; Kjennerud *et al.*, 2001; Faleide *et al.*, 2002).

Cenozoic

The Cenozoic Era is characterized by repeated uplift of the North Sea basin margins and surrounding landmasses (e.g. British and Scandinavian continents). As a result, large amounts of sediments (up to ca. 2500 m) were deposited in the continuously subsiding North Sea basin (Jordt *et al.*, 1995; Martinsen *et al.*, 1999; Faleide *et al.*, 2002; Head *et al.*, 2004; Gregersen & Johannessen, 2007). These major sequences of Cenozoic post-rift sediments are divided into the Rogaland, Hordaland and Nordland Groups (Isaksen & Tonstad, 1989). During Paleocene time, water depth reached 800 m in the deepest parts of the basin and most of the sediments derived from the Norwegian mainland were deposited in the north-eastern North Sea.

The first period of flank uplift and subsidence of the Viking Graben is attributed to compressional stress caused by the opening of the North Atlantic Ocean in Late Paleocene-Early Eocene times (Skogseid *et al.*, 2000). Explosive volcanism related to

the North Atlantic rifting led to the deposition of volcanic ashes throughout the North Sea (Balder Formation) (Isaksen & Tonstad, 1989). Extensive subsidence during the Eocene period led to a major transgression and deposition of mud and sand (Hordaland Group) on top of the volcanic material (Rogaland Group) (Thyberg *et al.*, 2000; Martinsen *et al.*, 1999).

As sea floor spreading between Greenland and the Norwegian mainland initiated in the Late Eocene, associated compression resulted in a relative sea-level fall and erosion of the basin flanks. Erosional material, derived from the the East Shetland Platform and Norwegian mainland, were transported by submarine fans into the deeper parts of the basin. The sandy Grid Formation is interpreted to represent such deposits (Isaksen & Tonstad, 1989; Rundberg & Eidvin, 2005). At the Eocene-Oligocene boundary, a global shift from greenhouse to icehouse conditions resulted in formation of icecaps on Antarctica and Greenland and enhanced flux of sea-level (Zachos *et al.*, 2001; Rundberg & Eidvin, 2005; Rasmussen *et al.*, 2008).

During Oligocene, deposition in the North Sea was dominated by mud and pulses of coarse clastic sediments, transported through gravity flows from the repeatedly uplifted basin margins (Isaksen & Tonstad, 1989; Rundberg & Eidvin, 2005). In some parts of the Northern North Sea, the Late Oligocene Skade Formation represents such sandy and shaly deposits in the upper part of the Hordaland Group (Rundberg & Eidvin, 2005; Eidvin *et al.*, 2013a). This part of the Hordaland Group has been found to be modified by post-depositional processes in many locations in the North Sea (Løseth *et al.*, 2003, 2013).

The Hordaland and Nordland Groups are separated by the Mid-Miocene Unconformity (MMU), reflecting another phase of tectonic compression and associated uplift of the North Sea basin, and fall in relative sea-level (Martinsen *et al.*, 1999; Galloway, 2002; Rundberg & Eidvin, 2005; Eidvin *et al.*, 2013a; Løseth *et al.*, 2013). Large volumes of sand, sourced from the East Shetland Platform, were deposited in the shallow marine areas of the Northern North Sea. This sand is termed the Utsira Formation and extends 450 km north-south, 75-130 km east-west and reaches its maximum thickness of 300 m in the southern Viking Graben (Rundberg & Eidvin, 2005; Gregersen & Johannessen, 2007; Eidvin *et al.*, 2013a).

A new connection between the North Sea and the Norwegian-Greenland Sea was established as the North Sea basin subsided during the Pliocene (Fyfe *et al.*, 2003; Head *et al.*, 2004). During Pleistocene, another uplift of the surrounding landmasses was accompanied with glacial advantages, depositing large sedimentary wedges, prograding eastwards in the North Sea basin (Eidvin & Rundberg, 2007; Gregersen & Johannessen, 2007). Above these wedges, a succession of clay forms the last deposits below the present day seafloor (Gregersen & Johannessen, 2007).

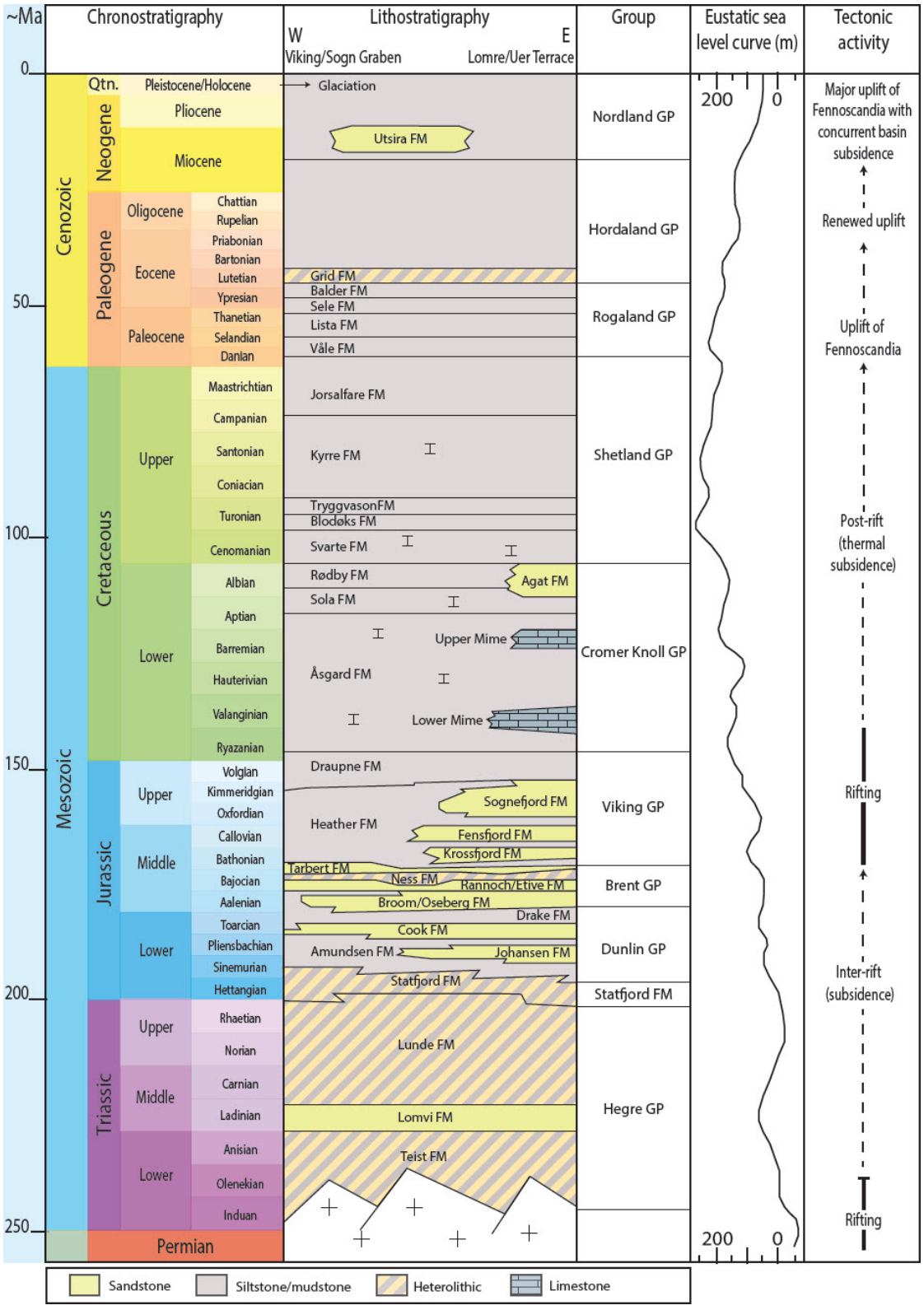

Figure 2.1: Complete lithostratigraphy of quadrant 35: north-eastern Viking Graben and surrounding areas (Lomre/Uer Terrace). Based on previous work from Dahl & Solli (1993); Steel (1993); Skibeli *et al.* (1995); Færseth (1996); Odinsen *et al.* (2000); Ravnaas *et al.* (2000); Graham *et al.* (2003). Nomenclature and color codes are in accordance with the International stratigraphic chart (ICS, 2014), with slight modification based on Northern North Sea literature.

3 Background theory

This chapter provides a brief review of some concepts and definitions regarding pore pressure, fluid flow, stress, and trapping and leakage mechanisms of hydrocarbons in the subsurface. These are all relevant topics related to accumulation of hydrocarbons and controls on hydrocarbon column-heights.

3.1 Pore pressure

Pore pressure, also referred to as formation pressure, is the fluid pressure within a porous network of a geological formation. In deep sedimentary basins (e.g. North Sea basin) pore pressures often varies in magnitude both laterally and vertically. Because of this variation, pore pressures are commonly compared with the hydrostatic pressure at the same depth, which is the pressure of a column of formation water from the sea surface (Osborne & Swarbrick, 1997). The increase of hydrostatic pressure with depth is close to linear and is commonly referred to as the *hydrostatic* gradient (Fig. 3.1).

Normally pressured formations are plotted along the hydrostatic gradient, implying that the formation pressure is in equilibrium with the hydrostatic pressure (Fig. 3.1). In such a scenario, the pore network in the reservoir is interconnected with the overburden, allowing formation fluids to escape. Normally pressured formations are thus often referred to as *open systems* (Buhrig, 1989). However, as will be discussed in section 3.4.3, hydrocarbons in normally pressured reservoirs are often trapped by capillary forces.

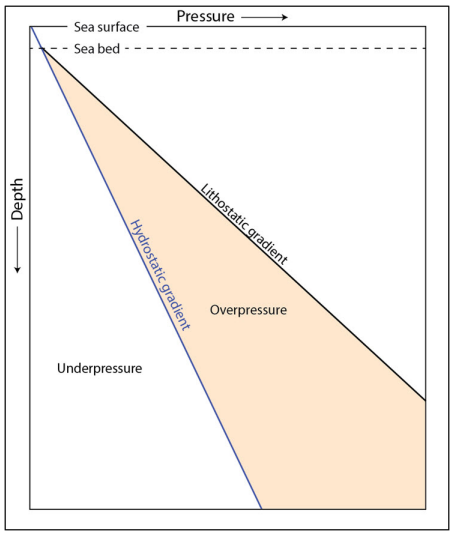

Figure 3.1: Conceptual pressure vs depth plot showing the hydrostatic and lithostatic gradients, including the area of underpressure and overpressure.

Geological formations with pore pressures significantly above the hydrostatic pressure at a given depth are referred to as *overpressured* (Fig. 3.1). Such abnormal pressures are principally formed as a response to disequilibrium compaction (caused by rapid burial) and/or fluid volume expansion in the reservoir (caused by cracking/generation of gas). Other processes that might cause overpressure in a reservoir are hydrocarbon buoyancy, hydraulic head and diagenesis (Osborne & Swarbrick, 1997). Overpressured formations have limited communication with the surface and is often referred to as *restricted* (moderately overpressured) or *closed* (highly overpressured) *systems* (Buhrig, 1989).

Although less common, if the pore pressure is significantly lower than the hydrostatic pressure the formation is referred to as *underpressured* (Fig. 3.1). Aside from pressure decrease related to gas/oil production, such pressure regimes are usually associated with basins which have experienced unloading of sediments by erosion and uplift (Osborne & Swarbrick, 1997).

3.1.1 Pore pressure in the Northern North Sea

In major parts of the Northern North Sea basin, regional stratigraphic units, such as late Jurassic and Cretaceous shales, act as vertical barriers, separating the deeper overpressured Jurassic interval from the normally pressured overburden sandstones. Based on a number of exploration wells in the Northern North Sea, Borge (2000) mapped the regional pressure regimes in this area. A trend of increasing overpressure in the Middle Jurassic Brent Group, from the near-normally pressured Horda Platform towards the deeper parts of the Viking Graben is evident (Fig. 3.2). Lateral variations of pore pressures within a sedimentary basin are often a result of lateral impermeable barriers caused by the presence of sealing faults.

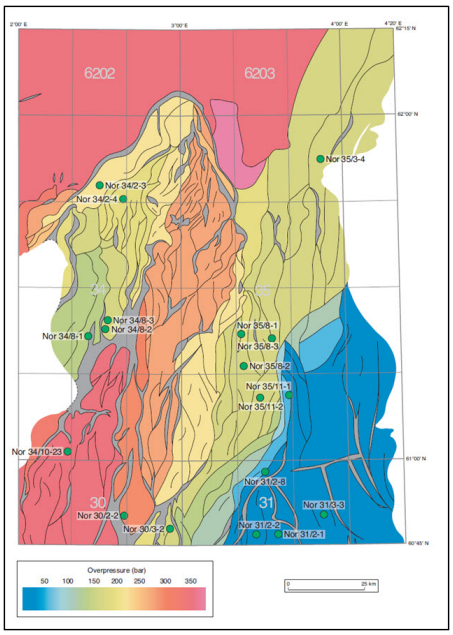

Figure 3.2: A model showing the variations of present day pressure in the middle Jurassic Brent Group. After Borge (2000), modified by Graham *et al.* (2003).

3.1.2 Measurement of pore pressure

Pore pressures can be measured with a range of tools and methods. One of the most reliable and efficient tools is the repeat formation tester (RFT), a wireline formation tester tool that allows for multiple and accurate pressure measurements from any permeable unit during drilling (Graham *et al.*, 2003). However, in low permeable units, such as shales and mudstones (<1,0 milliDarcy), the tool often fails to record the formation pressure (Osborne & Swarbrick, 1997).

Pore pressure gradients (or fluid pressure gradients) can be established by plotting measured pore pressures in a formation. Different fluids (e.g. oil, gas and water) have different pore pressure gradients due to variation in density, making this method quite efficient in detecting hydrocarbons and locating fluid contacts in a reservoir. Moreover, overpressure gradients are the main drivers for subsurface fluid flow (including hydrocarbon migration), a topic which will be discussed in the following section.

3.2 Hydrocarbon generation, migration and accumulation

Generation of hydrocarbons occurs in deeply buried organic rich shales and coal layers, and the major controlling factors for their generation are temperature and time. In the Northern North Sea, the primary source rock is the organic rich Late Jurassic Draupne Formation, including parts of the Heather Formation. There is also a source potential (gas) in parts of the Middle Jurassic Brent Group (Ness Formation) and in the Early Jurassic Dunlin Group. However, the contribution from these relative to the Draupne Formation is rather small and thus usually ignored (Goff, 1983).

According to Goff (1983), the Draupne Formation reached oil maturity 70-80 Ma ago in the most deeply buried areas (>4500 m). Peak oil generation occurred 55-65 Ma ago, and cracking of oil into gas began 40 Ma ago. Large quantities of oil and gas have thus been generated during the Cenozoic Era. The transport of hydrocarbons out of the source rock and into the reservoirs in which they are found is called migration. Migration of hydrocarbons can be divided into primary migration and secondary migration (Tissot & Welte, 1984; Gluyas & Swarbrick, 2003; Minescu *et al.*, 2010).

3.2.1 Primary migration

Primary migration is the transport of hydrocarbons out of the source rock, where they are generated, and into adjacent rocks (Fig. 3.3). The presence of thin layers of silt and sand within the source rock can serve as migration pathways, allowing the hydrocarbons to flow out through interstitial pores (Darcy flow). However, if such lithologies are absent, petroleum generation will cause pressure to build up until fractures are created. Fractures results in increased permeability and allows hydrocarbons to migrate towards permeable units (Bjørlykke, 2010). The formation mechanisms of fractures will be discussed in section 3.4.1.

3.2.2 Secondary migration

Secondary migration is the subsequent movement of hydrocarbons within the porous and permeable sandstone beds towards the reservoir/trap (Fig. 3.3). Although regional pressure gradients are important for fluid flow in general, migration of oil and gas is mainly driven by buoyancy. Because of this, oil and gas phases will flow upwards, in the upper parts of the sandstone beds, along pathways where petroleum is concentrated. As the hydrocarbons reach a trap and accumulate, capillary resistant force of the cap rock (impermeable shale, membrane seal) will prevent further upward flow (Bjørlykke, 2010).

The North Sea basin is heavily faulted, resulting in juxtaposition between permeable sandstones and impermeable shales in many areas. Although this is fortunate for accumulation of hydrocarbons, such features might hinder migration to shallower traps. In places where sand juxtaposes sand, hydrocarbons can often flow laterally through the fault. However, clay smear and/or cementation along such fault planes may reduce the permeability and increase the capillary entry pressure, preventing further migration (Lothe *et al.*, 2006; Bjørlykke, 2010).

3.2.3 Spill point

Hydrocarbons can only accumulate down to a certain point of a trap, which is commonly referred to as the "spill point". A trap can be controlled by a *structural spill point* and/or a *fault spill point* (Fig. 3.3). The structural spill point is associated with the deepest point of an anticline, while the fault spill point is where two reservoir beds are juxtaposed and in contact with each other, letting fluids flow through. If the fault spill point is sealing, hydrocarbons can accumulate down to the structural spill point.

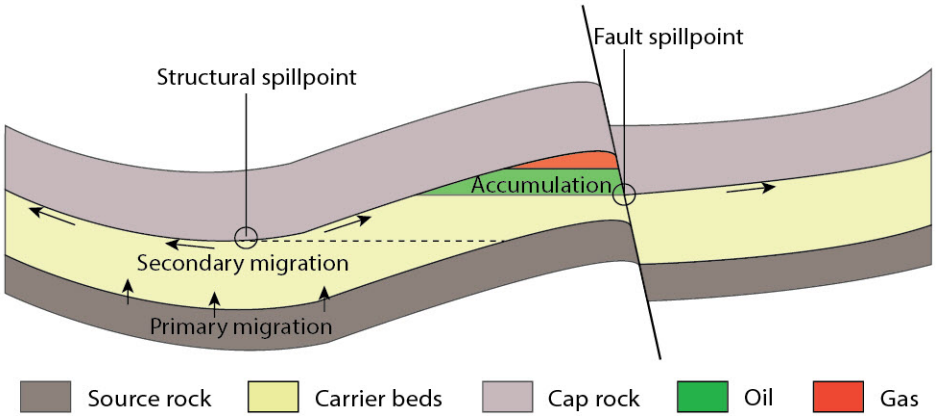

Figure 3.3: A conceptual sketch showing primary and secondary migration, and accumulation of hydrocarbons controlled by spill points.

3.3 The principal stress components

Knowledge about the stress state of the subsurface is highly relevant for hydrocarbon exploration, as changes in stress can influence the integrity of hydrocarbon traps (Wiprut & Zoback, 2002; Gartrell *et al.*, 2003; Grollimund & Zoback, 2003; Bolås *et al.*, 2005). There are three principal stress components, usually referred to as the *vertical stress* (S_V), the *least horizontal stress* (S_h) and the *maximum horizontal stress* (S_H) (Bolås & Hermanrud, 2002). These components in most cases work at right angles to each other. With knowledge of the magnitude of these components, one can deduce which faulting regime prevails.

Anderson (1905) defined three different stress regimes based on the relative magnitude of the principal stress components: 1) if the vertical stress component (S_V) is the largest, the rocks are in an extensional regime, 2) if the maximum horizontal stress component (S_H) is the largest and the least horizontal stress component (S_h) is smallest, the rocks will be in a strike-slip regime, 3) if the vertical stress component (S_V) is the smallest, a compressive regime prevails. In the subsequent sections, these stress components and their use will be described.

3.3.1 Vertical stress

In sedimentary basins, the vertical stress component is commonly defined as the weight of the overburden, including the weight of the pore fluids. The increase of vertical stress per meter of depth is commonly referred to as the *lithostatic gradient* (Fig. 3.1)(Bjørlykke, 2010). Regional lithostatic gradients are usually determined by integration of density logs from several wells in the applicable areas. A lithostatic gradient of $2.3\,g/cm^3$ is also commonly used. Although this is sufficient in many cases, this approximation is not very accurate, as shallow sediments with high porosity are less dense than deeply buried sediments with low porosity (Bolås & Hermanrud, 2002).

3.3.2 Least horizontal stress

In normal or strike slip stress regimes, the least horizontal stress is commonly referred to as the *least principal stress* (S_3). Associated with exploration, the magnitude of this stress component can be measured while drilling from *leak off tests* (LOT's). This test measures the pressure required to create fractures at a given depth, by pumping fluids into the geological formation until fracturing is initiated (Bolås & Hermanrud, 2002).

Gaarenstroom *et al.* (1993) used leak off pressure (LOP) measurements from a number of exploration wells to create a regional least principal stress envelope for the Central North Sea (Fig. 3.4). They suggested that this envelope, made by a smoothed line

through the lowest LOP values, represents the upper limit of the least principal stress in the area. Moreover, he implied that reservoir pressures exceeding this envelope would initiate hydrofracturing of the cap rock and result in leakage.

Bolås & Hermanrud (2002) illustrated that leak off test taken from various exploration wells are of mixed quality, and that the least principal stress estimated based on these measurements can be both over- and underestimated. They argue that because of large variations in LOT measurements, Gaarenstroom *et al.* (1993)'s LOP-envelope most likely gives too low values for the regional least principal stress. Bolås & Hermanrud (2002) therefore suggested that an averaged curve through the individual LOP data would be more appropriate, and give a more correct estimate of the least principal stress.

The location of the LOT envelope is important, as it is often used to estimate the retention capacities of traps. This is a measure of the pore pressure a trap can tolerate before the seal fails (provided that tensile (and not shear) failure occurs, and that the seal has no tensile strength)(Bolås *et al.*, 2005). The retention capacity is defined as the least principal stress minus the pore pressure:

$$RC = S_3 - P \tag{3.1}$$

If the retention capacity approaches zero, this may indicate that the trap is close to fracturing. However, according to Bolås *et al.* (2005), the retention capacity alone is not a satisfactory indicator for seal failure in general. This will be discussed further in section 3.4.

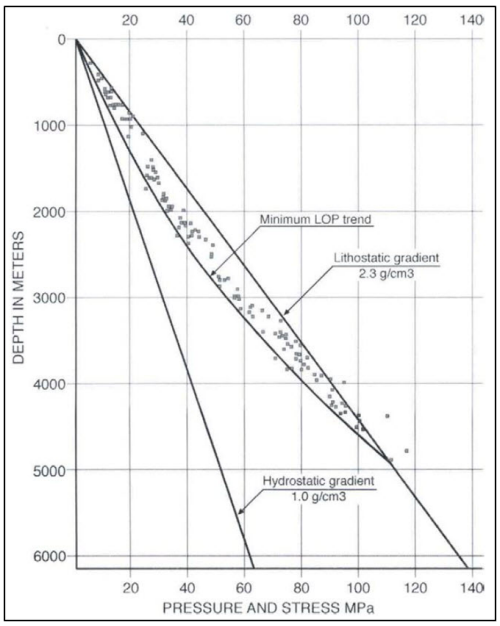

Figure 3.4: Minimum LOP trend from the Central North Sea. Bolås & Hermanrud (2002) argued that this envelope underestimates the regional least horizontal stress From Gaarenstroom *et al.*, 1993, adapted by Bolås & Hermanrud, 2002

3.3.3 Maximum horizontal stress

The magnitude of the maximum horizontal stress is more difficult to determine than the other two components, as it can not be measured directly in exploration wells (Bolås & Hermanrud, 2002). However, estimations on the magnitude of this stress component have been attempted with a range of methods (Zoback *et al.*, 1985, 1995a,b; Brudy *et al.*, 1997). Common for most methods on S_H -magnitude determination, is that they are based on the knowledge on the other principal stresses: S_V and S_h. However, as estimates of these stress components can be erroneous, there are high uncertainties regarding the value of S_H (Bolås & Hermanrud, 2002).

Based on borehole breakout data in the Visund field in the Northern North Sea, Wiprut (1998) suggested that the present day magnitude of S_H is 30% higher than S_V, implying that the Northern North Sea is currently in a strike-slip regime. Aadnoy *et al.* (1994), on the other hand, suggested that the present day magnitude of S_H is 0-20% lower than S_V, based on data from the neighbouring Snorre field, implying an extensional regime. A decrease of stress anisotropy with depth was also suggested, which is in accordance with the suggestions of Hermanrud & Bolås (2002).

The orientation of the maximum horizontal stress is fairly well constrained on a regional scale, along the Norwegian Continental Shelf. Brudy & Kjørholt (2001) found that the orientation of the maximum horizontal stress in the North Sea is in a ENE-WSW direction, based on inspection of borehole failures from high resolution borehole imaging logs.

3.3.4 Recent stress perturbations in the Northern North Sea

As hydrocarbon migration in the Northern North Sea commenced in the Early Cenozoic and increased in the Pliocene (Goff, 1983), stress changes before this time period is not relevant for hydrocarbon leakage. The following events are believed to have caused stress anisotropy in recent geological time (Bolås *et al.*, 2005):

- Thick, westward prograding sedimentary wedges during Pliocene-Pleistocene, causing increased vertical and horizontal stress in the underlying sediments. More pronounced stress anisotropy in the Halten Terrace and Central Graben areas (1500 m thick wedges) than in the Viking Graben (about 600 m thick wedges).
- Glacial advance and withdrawal during Pleistocene caused crustal flexuring and increased stress anisotropy. Sediments under the hinge zone of the flexuring were most influenced. The position of the hinge zone is given by Doré & Jensen (1996)

and is shown in Figure 3.5a. It is apparent that this affected the north-eastern Viking Graben more than the Halten Terrace.

- Abrupt changes in vertical stress at the shelf edge, due to loading and unloading of glaciers. The location of the shelf edge is shown in Figure 3.5b. This affected the Halten Terrace more than the north-eastern Viking Graben.

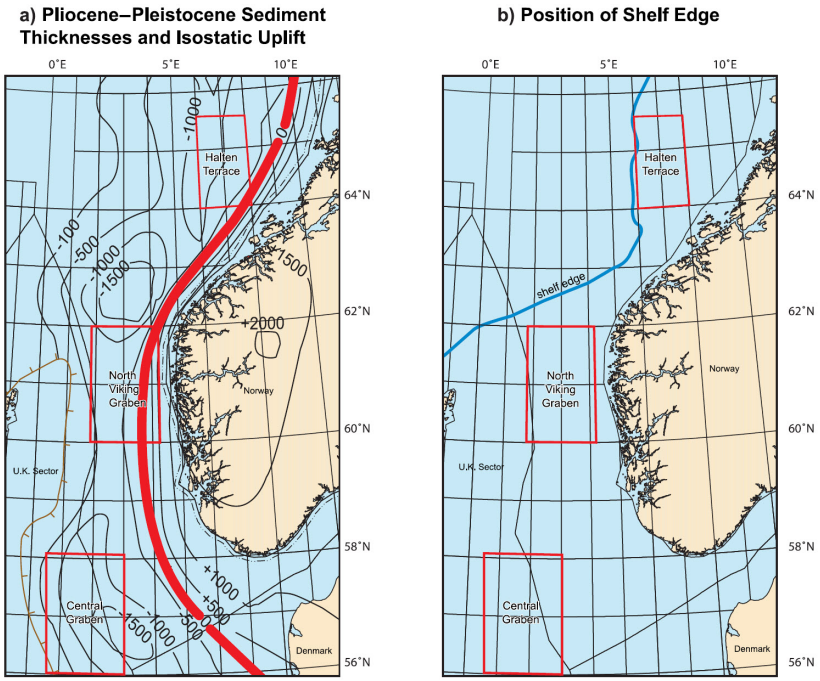

Figure 3.5: The location of the hinge zone caused by crustal flexuring (**a**) and the present-day shelf edge (**b**) in the North Sea and Norwegian Sea. From Bolås *et al.* (2005) (figure a is originally from Doré & Jensen (1996))

3.4 Trap integrity and seal failure

Analysis of trap integrity is an important aspect of hydrocarbon exploration, as seal failure might influence in place hydrocarbon volumes. Seal failure and leakage of pore fluids is of often associated with faults or fractures, caused by stress perturbations in the subsurface (Bolås & Hermanrud, 2002). In the following sections, some important aspects regarding these topics will be discussed.

3.4.1 Shear and tensile failure

The sealing characteristics of a trap can be significantly influenced by the mode of failure, which is most commonly associated with faulting (shear failure) or fracturing (tensile failure). Being able to estimate the likelihood for such events to occur is essential, as failure can result in seal breaching and leakage. Faulting or fracturing may initiate when the failure conditions for the rock is met (Hermanrud *et al.*, 2005). A very common way to illustrate stress and failure conditions is with Mohr's diagram (Fig. 3.6).

The Mohr's diagram is made up in such a way that rock failure will initiate if Mohr's circle touches the failure envelope. This can either occur by increased differential stress (circle expands) or by increased pore pressure (circle moves to the left). Two different failure envelopes are presented in this diagram, both of which are commonly applied. The linear *Mohr-Coulomb* failure envelope is favouring shear failure, as Mohr's circle will always touch the failure envelope before least principal stress reaches zero. The other envelope, *Griffith-Coulomb*, describes intact rocks with a cohesive strength. In this case, increased pore pressure (circle moves to the left) might induce tensile failure (hydrofracturing) before shear failure (Hermanrud *et al.*, 2005).

According to Wiprut & Zoback (2002), well oriented faults will slip before pore pressure can rise to the level of the minimum principal stress and cause hydrofracturing. Thus they suggest that hydrocarbon leakage due to hydrofracturing is unlikely.

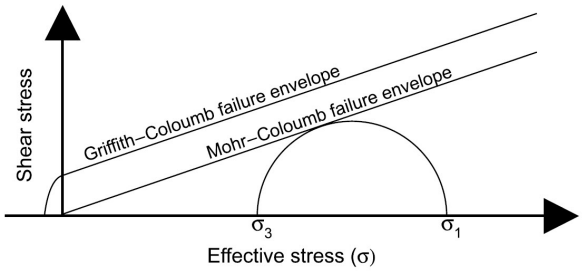

Figure 3.6: Mohr's circle with linear (Mohr-Coulomb) and curved (Griffith-Coulomb) fracturing criteria. σ_1 is the largest effective stress (stress minus pore pressure), and σ_3 is the least. (From Hermanrud *et al.*, 2005)

3.4.2 Faults and fault intersections as fluid conduits

Wiprut & Zoback (2000, 2002) conducted a study on hydrocarbon column heights and leakage potential in the Visund field and three other unnamed fields in the Northern North Sea. Based on a number of wells, they analysed the present magnitude and orientation of all three principal stresses in each field. They found that hydrocarbon leakage in this area might be related to fault reactivation. Three factors were suggested to control fault reactivation: *"1) locally elevated pore pressure in the reservoir , 2) fault orientations that are nearly optimal oriented for frictional slip in the present-day stress field, 3) a relatively recent perturbation of the compressional stress caused by post-glacial rebound*" (Wiprut & Zoback, 2002).

Based on a study of the Skua oil field in the Timor Sea, Australia, Gartrell *et al.* (2003, 2004) demonstrated that fault intersections might play a significant role in trap integrity and fluid leakage. The oil-water contact in this underfilled field appeared to correspond with the depth and position of a fault intersection bounding the structure. Seismic interpretation and modelling of fault patterns in the area showed that zones of high dilation were generated in the vicinity of the fault intersections during contraction. They suggested that these zones would probably contain high concentrations of open fractures, providing effective paths for fluid leakage.

3.4.3 Capillary leakage

Hydrocarbons can in theory leak through a water wet seal by Darcy flow (movement of hydrocarbons through interstitial pores). For this to happen, the buoyancy of the hydrocarbon phase (oil or gas) has to overcome the capillary entry pressure of the seal (Berg, 1975):

$$Pc_e < (\rho_w - \rho_{hc})gh \tag{3.2}$$

where Pc_e is the capillary entry pressure, ρ_w and ρ_{hc} are the densities of water and hydrocarbons respectively, g is the gravitational acceleration and h is the height of the hydrocarbon column. The capillary entry pressure is determined by the radius of the largest interconnected pore throats of the seal (Berg, 1975):

$$Pc_e = 2\gamma/r_s \tag{3.3}$$

where γ is the interfacial tension between water and hydrocarbons, and r_s is the radius of the largest connected pore throats.

3.5 Geological significance of seismic amplitude variations

Seismic surveying is the most powerful geophysical exploration method to date, allowing for relatively detailed geological mapping of the subsurface. The method is based on the recording and analysis of acoustic waves as they travel through the Earth. Variation of lithology and pore fluids in the subsurface results in density and velocity changes (e.g. changes in acoustic impedance), forming boundaries on which the seismic waves reflect and return to the surface (Badley, 1985). The timing and strength of these reflected waves is recorded and further processed into the final product, a seismic volume (2D line or 3D cube). A seismic volume allows for imaging and interpretation of the subsurface.

Local variations of pore fluids in the subsurface, for instance hydrocarbons replacing formation water, might results in local changes in acoustic impedance. Seismic surveying is quite sensitive to such variations, thus the presence of hydrocarbons in the subsurface is often imaged on seismic data as amplitude anomalies (bright spots and dim zones), hydrocarbon related diagenetic zones (HRDZ) and seismic chimneys (Badley, 1985; Avseth *et al.*, 2005; Ligtenberg, 2005; Arntsen *et al.*, 2007; Løseth *et al.*, 2009; Heggland, 2013). A brief review of hydrocarbon leakage and accumulation expressed in seismic data will be presented in the following sections.

3.5.1 Bright spots and dim zones

In seismic data, bright spots and dim zones are amplitude anomalies that appear due to acoustic impedance contrasts in the subsurface (Fig. 3.7). Bright spots are due to their high amplitude and negative phase anomalies, often associated with changes of fluids within the rocks. Within water bearing sandstones or shales, local presence of hydrocarbons will cause local differences in densities, which in some cases can be viewed in seismic data as bright spots. Moreover, hydrocarbon-water contacts with some reservoirs can be expressed as flat spots in seismic data (Løseth *et al.*, 2009).

In some cases, the amplitude of a seismic reflector is locally reduced, reflecting a lowered impedance contrast between two different lithologies. Such features are referred to as dim zones and might be caused by the presence of gas or oil, cancelling the impedance contrast between the layers (Løseth *et al.*, 2009).

Bright spots, flat spots and dim zones, are in some cases referred to as direct hydrocarbon indicators (DHI) (Badley, 1985; Avseth *et al.*, 2005; Ligtenberg, 2005). DHI's are often observed in the vicinity of leaking faults, above presumably leaking reservoirs, at shallow gas pockets, and along gas chimneys (Ligtenberg, 2005).

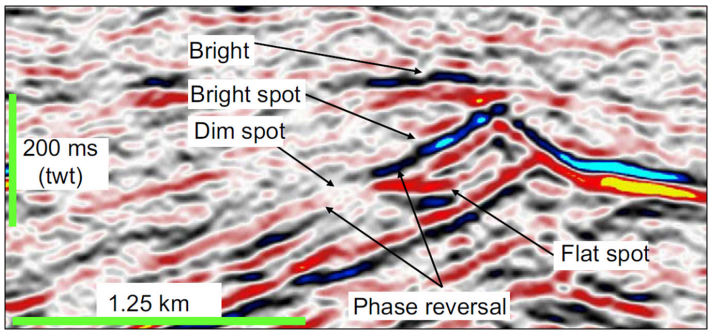

Figure 3.7: Presence of bright spots, dim spot and flat spots in seismic data. From Løseth *et al.* (2009)

3.5.2 Hydrocarbon-related diagenetic zones (HRDZ)

Hydrocarbons that leak into overburden rocks from deeper reservoirs will in some cases result in biodegradation and intense carbonate cementation. Due to the increased density caused by cementation, such zones results in an increase in acoustic impedance and a strong seismic response. Hydrocarbon-related diagenetic zones are often observed above local fluid conduits, such as faults and fault-intersections (O'Brien *et al.*, 2002; Ligtenberg, 2005).

3.5.3 Seismic chimneys

Seismic chimneys are associated with vertical to near-vertical columns of noisy seismic character (Ligtenberg, 2005). In the Northern North Sea, these features are often observed above highly overpressured structures (e.g. Gullfaks South) (Løseth *et al.*, 2009). It is suggested that seismic chimneys is a result of the presence of gas in the overburden rocks, caused by tectonically and hydraulic fracturing of the cap rock in hydrocarbon bearing structures. Seismic chimneys are therefore often referred to as *gas chimneys* and interpreted as indication of hydrocarbon leakage (Fig. 3.8) (Heggland, 1998, 2005; Ligtenberg, 2005; Løseth *et al.*, 2009; Heggland, 2013).

Heggland (2013) promoted a classification of different gas chimneys, based on their shape and location relative to the leaking structure (Fig. 3.9). Based on this classification, Heggland (2013) suggests a distinguished feature between hydrocarbon-charged traps and dry traps. In short, type 1 chimneys are narrow, concentrated chimneys and are associated with faults. These chimneys indicate that the fault is or has been open for vertical leakage of fluids. Type 2 chimneys are wider and located above the crest of the structure. According to Heggland (2013), type 2 chimneys are associated with hydrocarbon bearing structures.

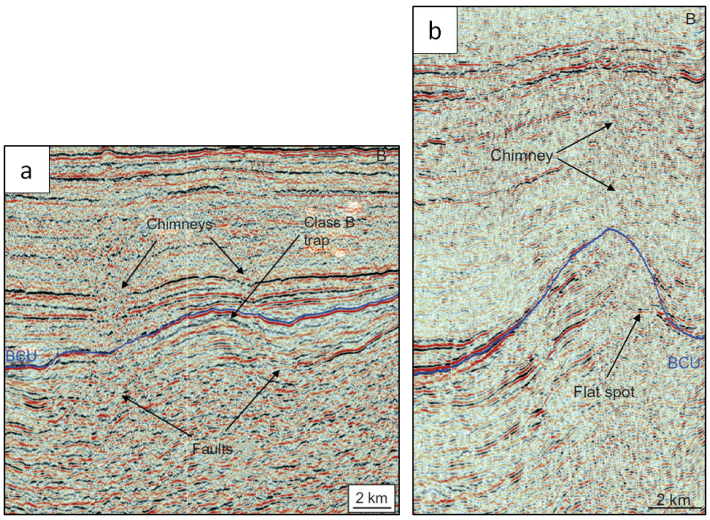

Figure 3.8: Different types of chimneys, **a**: fault related and **b**: top seal related. From Heggland (2013)

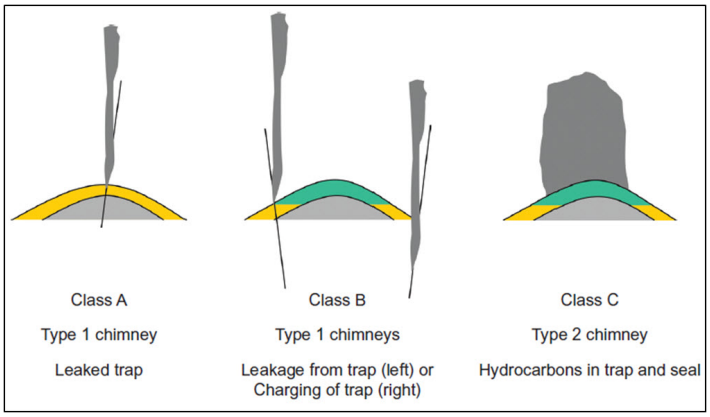

Figure 3.9: Trap classification based on associated gas chimneys. Type 1 chimneys are associated with faults, while type 2 chimneys are wider and located above teh crest of the structure. From Heggland (2013)

3.5.4 Seismic expressions associated with remobilized sediments

Shallow and deep occurrences of remobilized sediments are reported in many places in the North Sea, including the north-eastern region of the Northern North Sea (Løseth *et al.*, 2003, 2009, 2013) (Fig. 3.10). Internal generation of overpressure is believed to be the main triggering mechanism of these features. Such overpressures might be generated by invasion of fluids from external sources (i.e. leaking structures) (Løseth *et al.*, 2009).

The shallow remobilized sediments are commonly found in the upper part of the Hordaland Group, and are characterized by a highly chaotic seismic reflection pattern, with an irregular, mound- and bowl-shaped upper boundary (Løseth *et al.*, 2009). Below these zones, so-called V-brights are commonly observed. These are believed to represent carbonate-cemented sand injection structures and thicker sand units (Huuse *et al.*, 2004; Huuse & Mickelson, 2004; Løseth *et al.*, 2003; Cartwright *et al.*, 2007).

The deep remobilized sediments might have a slightly different expression in the seismic data. They often appears as reflection free or chaotic reflection patterns, where small segments of the primary beds act as randomly distributed reflection planes (Løseth *et al.*, 2009). These deep situated features are often associated with connected feeder dikes to mud volcanoes at the surface, expressed as reflection free areas in seismic data (Graue, 2000). Above and at the flanks of the mud diapirs and feeder pipes high amplitude anomalies are often observed (Stewart & Davies, 2006).

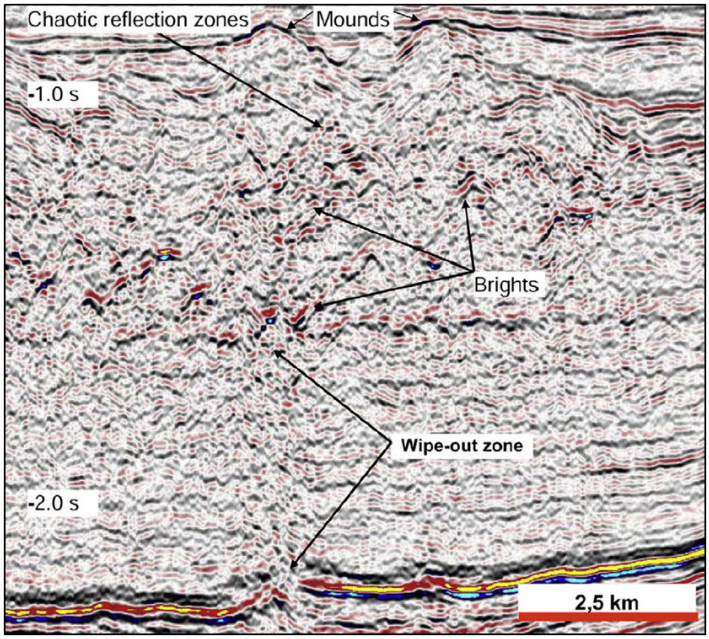

Figure 3.10: Chaotic reflection zone with brights distributed in a random pattern, associated with remobilized sediments. The narrow wipe out zone is interpreted as a gas chimney with focused fluid flow. From Løseth *et al.* (2009)

4 Data and methodology

This chapter gives a brief overview of the data and tools, as well as the work methods utilized in this project.

4.1 Seismic data

The seismic database were provided by Statoil ASA, and consists of four overlapping 3-D seismic cubes: NH9402, BPN9301, SG9603 and ST13M03. The seismic data covers an area of $3510km^2$ in the north-eastern North Sea, and defines the extent of the study area (Fig. 4.1). The area coverage, attributes and line orientations/spacing of the individual seismic cubes can be viewed in Table 4.1.

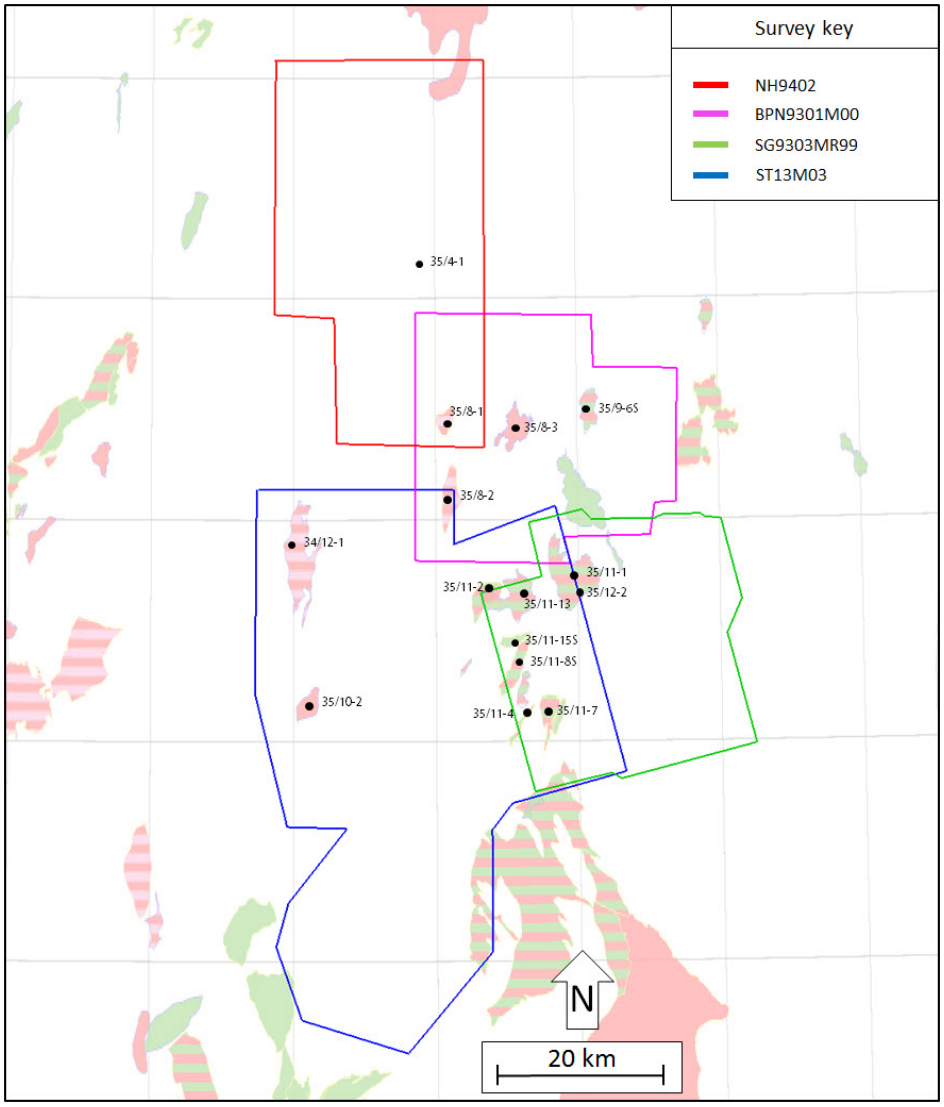

Figure 4.1: Map showing the location of the 3-D seismic surveys and exploration wells used in this study.

Table 4.1: Overview of the seismic surveys utilized in this study, including their phase, polarity, resolution, area coverage, line orientation and line spacing.

Survey	Phase	Polarity	Resolution	Area (km^2)	Line orientation	Line spacing (m)
NH9402	Minimum	Reverse	Poor	1265	Iln = E-W	25
					Xln = N-S	12.5
BPN9301M00	Zero	Normal	Moderate	1008	Iln = E-W	25
					Xln = N-S	25
SG9603MR99	Zero	Normal	Poor	1125	Iln = NNW-SSE	25
					Xln = ESE-SNS	25
ST13M03	Zero	Normal	Moderate	3295	Iln = N-S	25
					Xln = E-W	12.5

Iln, inline; Xln, crossline

Seismic survey BPN9301, SG9603 and ST13M03 are zero-phase time migrated and presented with normal polarity (SEG Convention). In these data sets, a downward increase in acoustic impedance is represented by a peak (red reflection), while a downward decrease in acoustic impedance is represented by a through (blue reflection) (Fig. 4.2a). Seismic survey NH9402 has been processed differently than the other data sets, resulting in a 90° phase rotation (minimum phase) and reverse polarity. A downward increase in acoustic impedance is thus represented by a peak (red reflection) and a downward decrease is represented by a through (blue reflection) (Fig. 4.2b). The vertical axis of all surveys are in the time domain (two-way time, TWT ms), thus seismic sections presented in this study are in TWT.

In general, the data quality in this area varies from moderate to poor (Table 4.1). Higher quality seismic data in this area was not obtainable, as these could not be published.

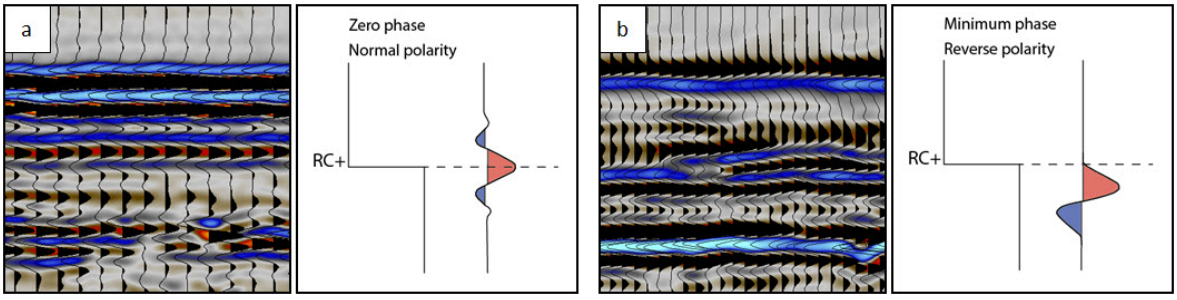

Figure 4.2: Phase and polarity of **(a)** seismic survey BNP9301, SG9603 and ST13M03, and **(b)** seismic survey NH9402

4.2 Well data

The well database were also provided by Statoil ASA, and comprises digital conventional well logs (i.e. gamma ray, sonic, density), check-shots and RFT-pressure measurements from 17 exploration wells within the study area (Table 4.2). Locations of the wells are displayed in Figure 4.1. Also, leak-off tests, lithological logs and information on fluid contacts and shows recordings have been obtained from published well reports in the well section of the Norwegian Petroleum Directorate's web pages (NPD, 2015). The use and uncertainties of these data will be described in the following sections.

Table 4.2: List of wells in the study area. Note that some wells do not contain information on fluid contacts (N).

Wells	**Field**	**TD** (fm)	**TD** (m)	**Fluid contacts**	**Shows**
35/8-1	Vega North	Statfjord	4344	Y	Y
35/8-2	Vega Central	Statfjord	4334	Y	Y
35/11-2	Vega South	Statfjord	4024	Y	Y
35/8-3	Aurora	Rannoch	3944	N	Y
35/9-6S	Titan	Lunde	3689	N	Y
35/11-1	Grosbeak	Hegre	3360	Dry	Y
35/12-2	Grosbeak	Etive	2541	Y	Y
35/11-13	Astero	Heather	3292	Y	N
35/11-15S	Fram H-North	Heather	2987	Y	N
35/11-8S	Fram H-South	Drake	3355	Y	Y
35/11-4	Fram F-East	Statfjord	3125	Y	Y
35/11-7	Fram C-West	Statfjord	2895	Y	N
34/12-1	Afrodite	Cook	4711	N	Y
35/10-2	B-structure	Statfjord	4675	Y	Y
35/4-1	Dry	Hegre	4924	Dry	Y
35/10-1	Dry	Statfjord	3982	Dry	Y
35/11-3S	Dry	Statfjord	4025	Dry	Y

4.2.1 Check-shots and conventional well logs

Check-shots and digital well logs have been used for seismic interpretation in the software Petrel 2013 (developed by Schlumberger).

Well tops were generated based on formation tops, obtained from published well reports in the well section of the Norwegian Petroleum Directorate's web pages. Depth (m) to time (TWT ms) conversion of the well tops have been performed with the use of digital check-shots. As an assisting tool for seismic interpretation, digital well logs (i.e. gamma ray, sonic and density logs) were used to distinguish lithological boundaries in areas with weak seismic responses.

4.2.2 Formation pressures

RFT-pressure measurements from all wells have been used in this study. Plotted in pressure versus depth plots, each geological structure is represented with the highest quality RFT-pressure measurement close to top reservoir. Based on these pressure measurements, the magnitude of overpressure and retention capacity in each structure were calculated and are presented in their respective table. As discussed in section 3.3.2, calculation of retention capacities is based on the estimated magnitude of least horizontal stress (S_3), which again is based on leak-off tests (LOT) measurements.

4.2.3 Leak-off tests (LOT)

Leak-off tests (LOT) from all exploration wells within the study area make the basis for creating the least horizontal stress (S_3) envelope in the pressure vs. depth plots. As pointed out by Bolås & Hermanrud (2002), LOT data are highly uncertain and can lead to both under- and overestimation of the regional least horizontal stress. Therefore, an averaged curve through the individual LOP data has been performed with a polynomial of 3rd order best-fit line for all wells. Based on least horizontal stress values from the best-fit line, retention capacities were calculated for each individual structure in the area.

In addition to retention capacities, a ratio between the overpressure and the least horizontal stress estimate has been calculated for every structure. This is here referred to as the "overpressure factor". Formula:

$$OpF = Overpressure/(LOT - hydrostatic\,pressure) \tag{4.1}$$

The output from this formula gives a number between 0 to 1, where 0 is corresponds to no overpressure, while 1 is largest overpressure possible before failure (as pore pressure $>$ least principal stress). These calculations will be listed in tables throughout the result chapter.

4.2.4 Lithological well logs, fluid contacts and hydrocarbon shows

For illustrative purposes, lithological logs of each well were digitalized and attached with respective information on fluid contacts (GOC/OWC/GWC) and recordings of hydrocarbon shows. In some wells, gas levels are also attached were they are found informative. Note, however, that some wells do not contain recording of fluid contacts or hydrocarbon shows (shown in Table 4.2).

4.3 Methodology

4.3.1 Seismic interpretation

Interpretation of the seismic data was performed with the software Petrel 2013, developed by Schlumberger. Figure 4.3 illustrates the interpretation workflow.

A fairly detailed regional interpretation of the main reservoir unit in the area, the Brent Group, has been conducted. For consistency, the reflection pick of the top Brent Group unit was based on an increase in acoustic impedance, corresponding to a red reflection in all seismic surveys. Other regional seismic interpretations include: Base Cretaceous Unconformity (BCU), Top Shetland Group and Seabed.

In the south-eastern part of the study area, additional reservoir units are represented by the Sognefjord and Fensfjord Formations, and Intra Heather Formation turbidites. Due to poor seismic resolution in this area, especially below Base Cretaceous, no regional interpretations have been performed on these reservoirs. As a consequence, this affects the mapping of spill routes and analysis of column heights in these reservoirs. However, rough interpretations of these units are still presented in the seismic sections.

In general, the different seismic units were manually interpreted and 2-D tracked with an inline density of 2-32 lines, depending on the complexity and data quality. Occasionally, interpretation in crossline and random lines were conducted to tie inline interpretations. The final interpretations were used to generate surface grids, which form the basis for location of spill routes and analysis of structural characteristics.

In general, the main uncertainties regarding seismic interpretation within the study area is poor vertical and lateral seismic resolution in some areas. The largest uncertainty is associated with interpretations in the northernmost part of the study area, due to the extremely poor data quality of seismic survey NH9402. Also, the data quality within the eastern part of seismic survey SG9603 and in the south-eastern part of seismic survey ST13M03, is poor.

4.3.2 Attribute analysis

Attribute analyses were performed in order to enhance important features in the seismic data. These attributes include RMS (root mean square) and Variance. The RMS attribute features were used for mapping/displaying the extent and strength of bright and dim areas observed in seismic sections. A common workflow for this was to interpret the closest overlaying or underlying continuous seismic reflector of the bright, generate a surface grid, and then lower or elevate the surface grid by an X number of ms TWT, until it becomes positioned in bright zone. The interval used for RMS extraction

depends on which features one wish to include. In this study, an interval of +/-10 to +/-20 ms TWT was commonly utilized. Variance extraction was mainly used as a support tool for seismic interpretation, in structural complex areas.

4.3.3 Visualization of data

The software Adobe Illustrator CS6 has been used to make figures, lithological well logs and interpretations on 2-D seismic sections. The seismic surfaces that are displayed in this project are usually shown in 2D view with a vertical exaggeration of 5 and an artificial light source to highlight the features of interest. Key fault orientations of the studied structures are plotted in the software Stereonet 9.2.3, and presented in rose diagrams.

4.3.4 Workflow chart

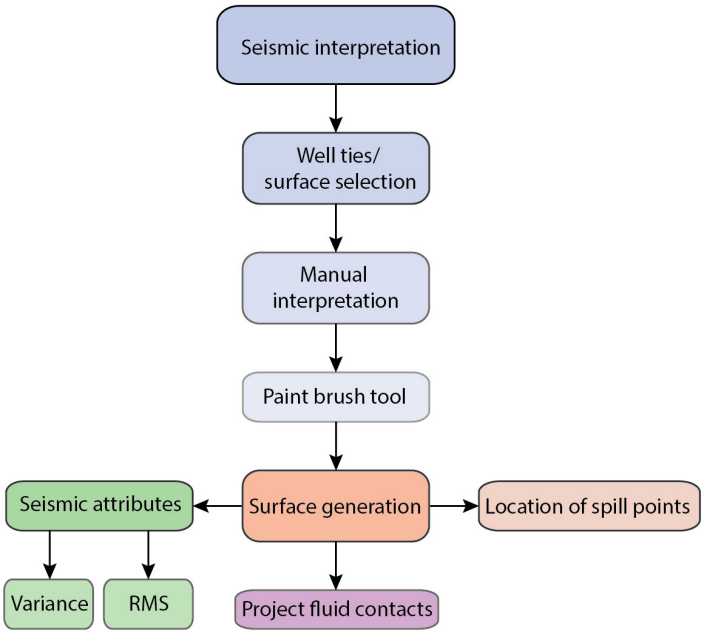

Figure 4.3: Overview of the interpretation workflow.

5 Results

In this chapter seismic observations and interpretations as well as analysis of reservoir pressures will be presented. Due to the large number of wells and structures, they are divided into seven areas based on their location and/or spill-routes (Table 5.1). Each area will be presented in their respective sub-chapter, accompanied with a seismic section and lithological well logs with interpretations of reservoirs and fluid contacts. The seismic sections have been carefully picked with emphasize on giving the reader insight into the structural setting and geology in the area, as well as presenting key observations in the overburden.

Table 5.1: Overview of areas and wells. The 17 wells are categorized based on their presence in seismic transects through this chapter.

Area		Wells					Seismic section	
1.	Vega	35/8-1	35/8-2	35/11-2			1.	C - C'
2.	Aurora - Titan	35/8-3	35/9-6S				2.	D - D'
3.	Grosbeak	35/12-2	35/11-1				3.	E - E'
4.	Fram - Astero	35/11-7	35/11-4	35/11-8S	35/11-15S	35/11-13	4.	F - F'
5.	Afrodite - B-structure	34/12-1	35/10-2				5.	G - G'
6.	Dry north	35/4-1					6.	H - H'
7.	Dry south	35/10-1	35/11-3S				7.	I - I'

The study area is presented in Figure 5.1 with (**a**) regional Top Brent Group and (**b**) regional Base Cretaceous Unconformity surface maps, including locations of main seismic sections and key wells. Location of the seismic surfaces and main structural elements is displayed in Figure 5.2.

The area is generally deepening towards the north and west, from the shallow Horda Platform towards the Viking and Sogn Graben. The structural configuration throughout the area is well displayed by the Top Brent map, showing evidence of N-S and NE-SW trending normal faults, which are predominantly of Jurassic origin. These fault systems form local highs and traps that are responsible for most of the hydrocarbon accumulation in the Jurassic sands throughout the area. Although most of the reservoirs are situated in the Middle Jurassic Brent Group, accumulations in Late Jurassic sands represented by the Krossfjord, Fensfjord and Sognefjord Formations, as well as local turbiditic sands, are present in the shallower eastern region. Interpretations of these reservoir units will only be presented in the 2-D seismic sections.

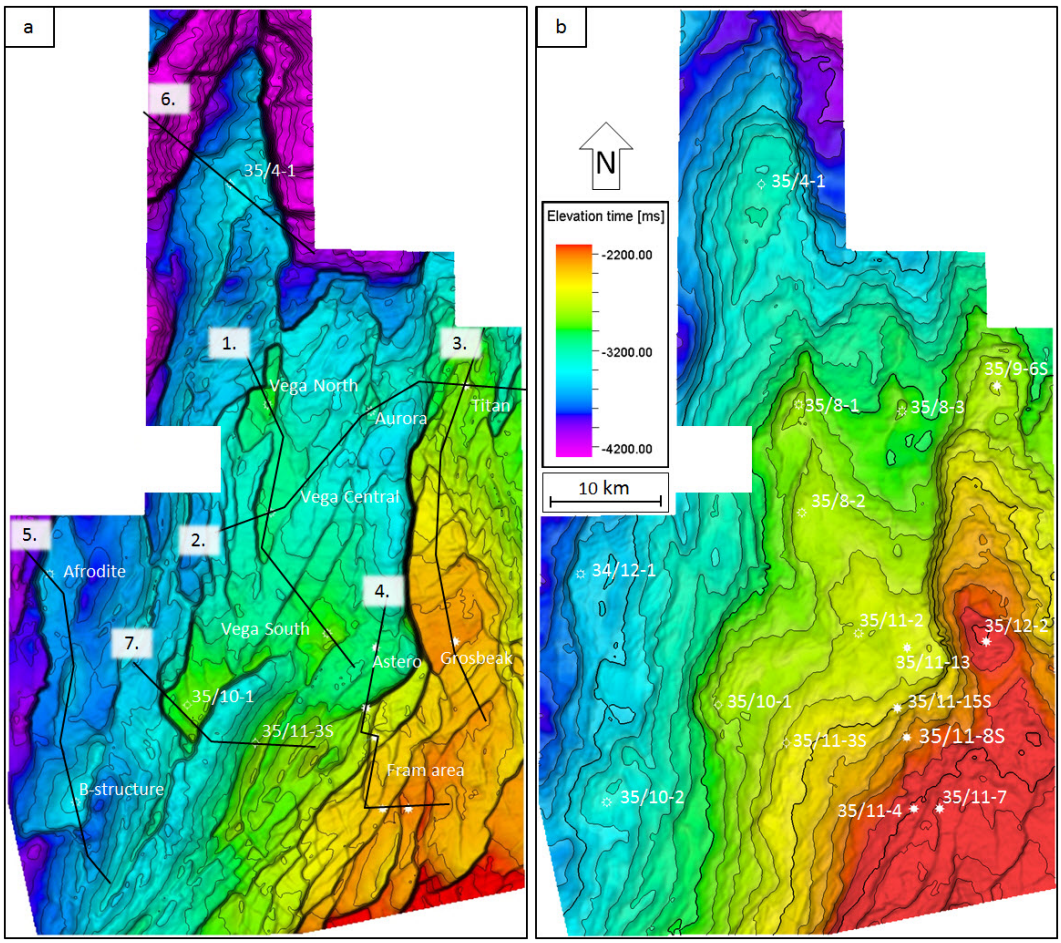

Figure 5.1: Overview of the study area, presented by **a**: regional top Brent Group surface map with location of seismic sections, and **b**: regional Base Cretaceous surface map with well locations.

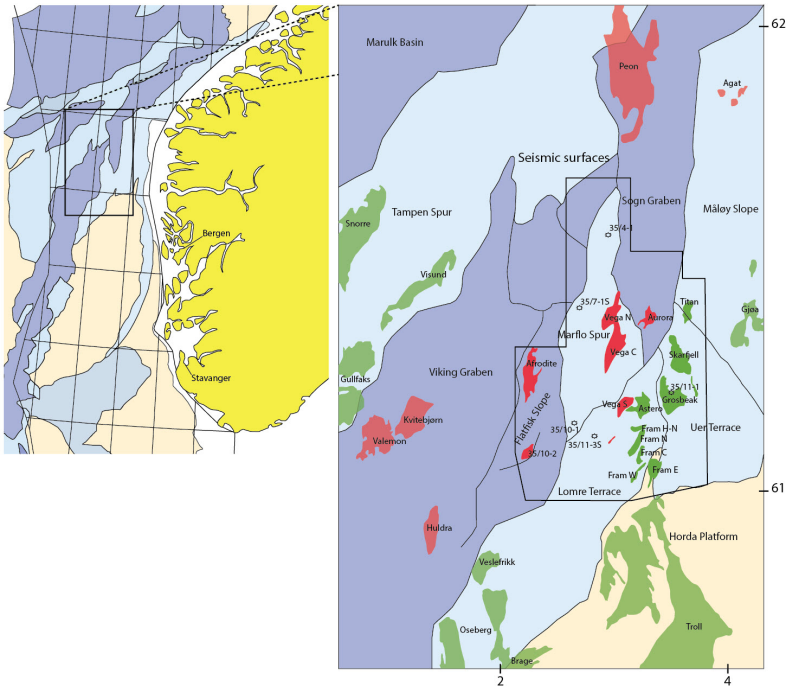

Figure 5.2: Names of structural elements and location of fields. The location of the seimsic surfaces in Figure 5.1 i marked with black outline.

5.1 Vega area

The Vega area encompasses three producing gas/condensate fields: Vega North, Central and South. The northern structure was drilled first by well 35/8-1, and it was followed by drilling of the central (35/8-2) and southern (35/11-2) structures (Fig. 5.3a). The reservoirs in this area are overpressured, with a decreasing overpressure from the northern to the southern structure (Fig. 5.3b). Figure 5.4 shows a seismic section with interpretation from Vega North to South (location of seismic section marked by black line in Figure 5.3a). The Middle Jurassic Brent Group is the only hydrocarbon bearing sands in this area and is overlain by the predominantly shaly Viking Group. Pressures and gas-water contacts within the Brent Group are listed in Table 5.2, and the presence and extent of hydrocarbon shows is presented in the lithological well logs in Figure 5.5.

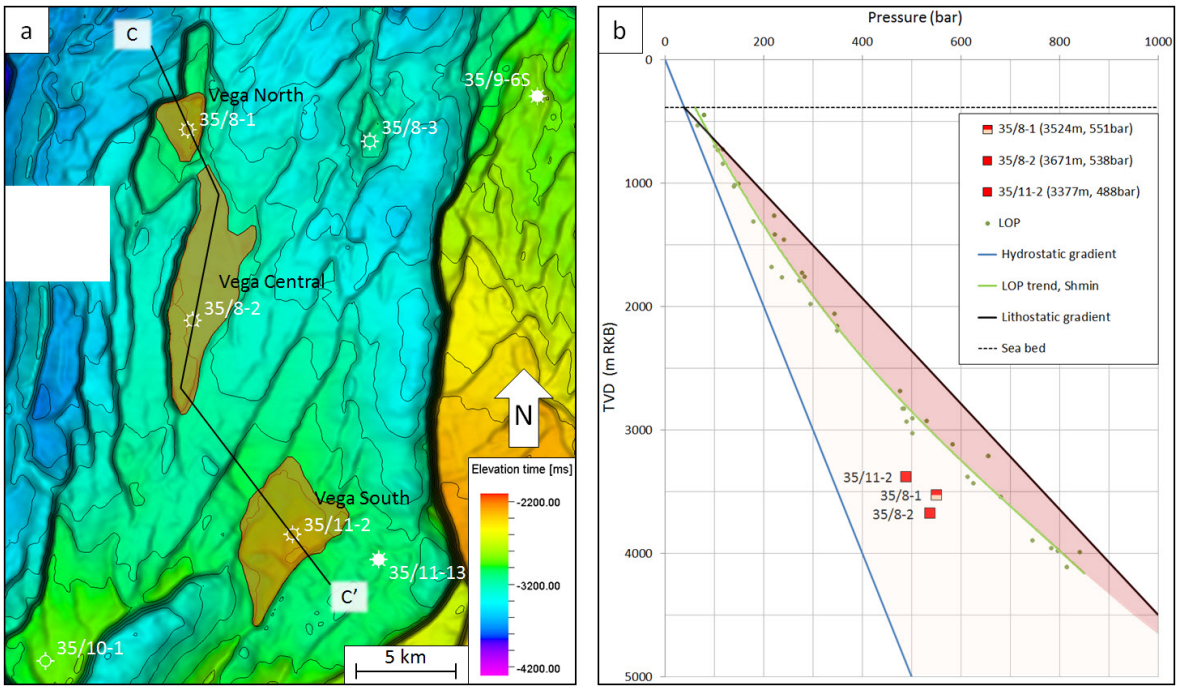

Figure 5.3: Overview of the Vega area. **a**: Top Brent surface map (100 m contour spacing) superimposed by red field outlines, based on gas-water contacts. Black line represents the path of seismic section C-C'. **b**: Reservoir pressures in the Vega structures presented in a pressure vs. depth plot

Table 5.2: Summary of fluid contacts, spill points and pressure measurements close to top reservoir in the Vega structures.

Well	GWC		Spill point			Pressure			
	TVD	TWT	TVD	TWT	TVD	Pore	Overpressure	RC	Op/LOT-Hydr
35/8-1	3657	-3070	3830	-3165	3524	551	199	129	0.61
35/8-2	3733	-3144	3738	-3148	3671	538	171	192	0.47
35/11-2	3545	-3023	3550	-3026	3377	488	150	142	0.51

Units: TVD (True Vertical Depth, m RKB); TWT (Two Way Time, ms); Pressure (bar)

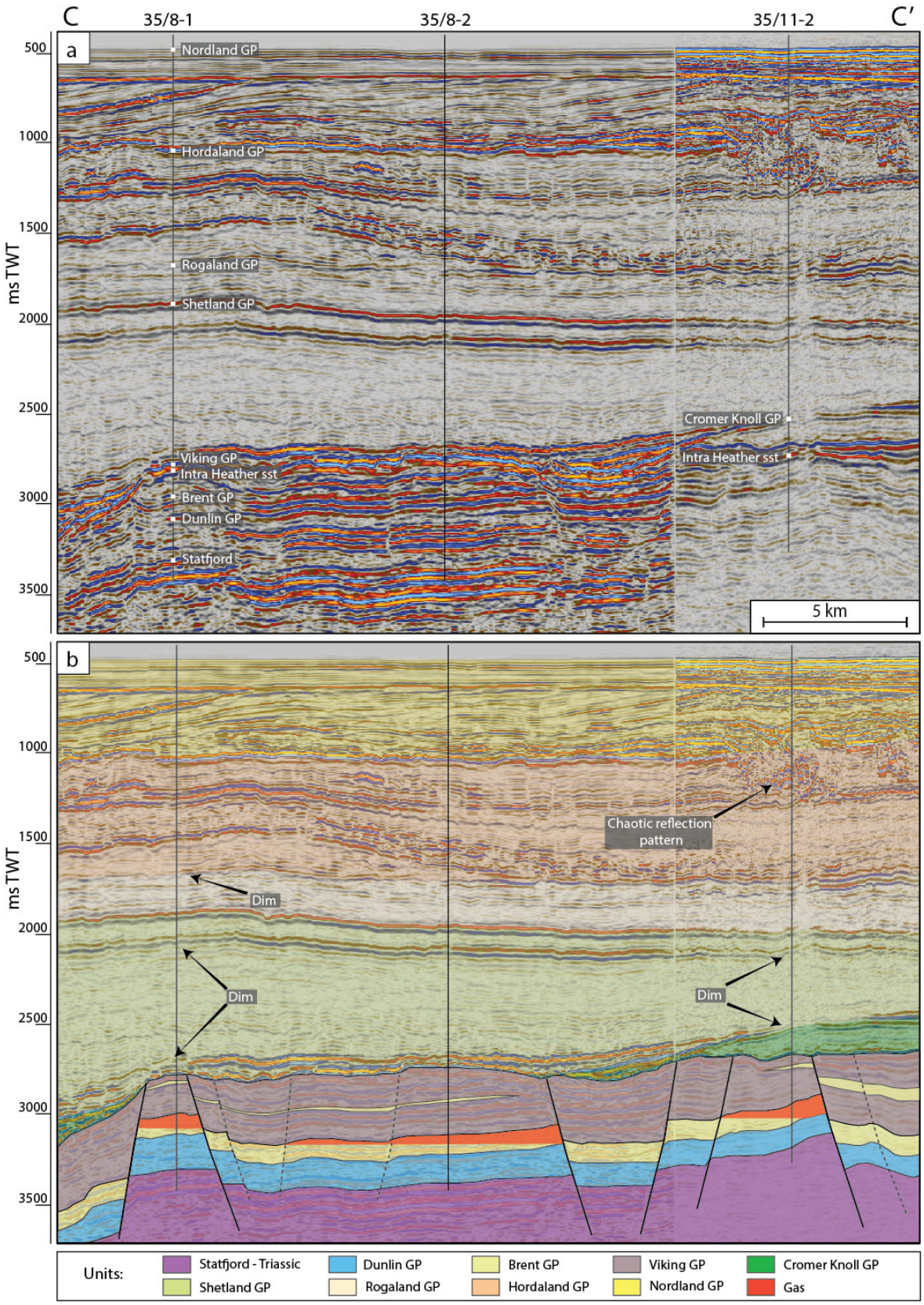

Figure 5.4: Seismic section C-C' shows an uninterpreted (**a**) and interpreted (**b**) version from NW to SE through the Vega area, including key observations in the overburden. Note the reduced reflectivity (dim) above Vega North and Vega South and the chaotic reflection pattern in the Hordaland group.

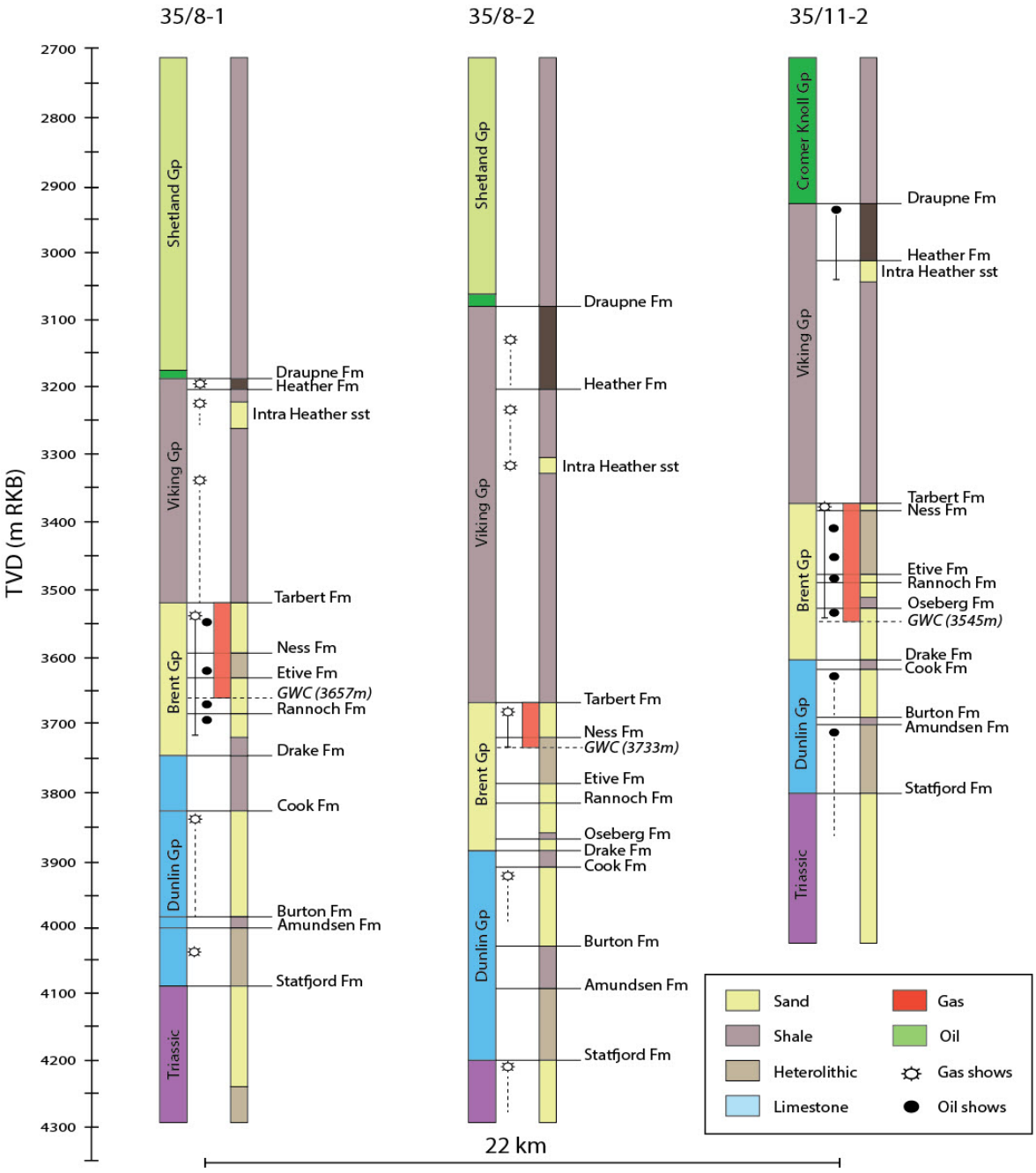

Figure 5.5: Lithological well logs corresponding to the wells in seismic section C-C', with recordings of hydrocarbon shows and fluid contacts.

5.1.1 Vega North - 35/8-1

Vega North resides on the north-eastern edge of the Viking Graben, between the Lomre Terrace and Marflo Spur. The structure is a small horst, bound and intersected by a number of normal faults, trending N-S, NE-SW and ENE-WSW (Fig. 5.9a and 5.10). The Viking Group is dominantly shaly, interbedded with a 40 m thick Intra Heather Formation sand that contains gas shows, illustrated in the interpreted seismic section and in the lithological well log (Fig. 5.4b and 5.5). The Brent Group was penetrated

at 3516 m and contained a gas column through the Tarbert Formation and into the upper part of the Etive Formation, down to a gas-water contact at 3657 m (Fig. 5.5). Pore pressure in the top of the Brent Group was measured to 551 bar by RFT pressure sampling, corresponding to an overpressure of 199 bar (Table 5.2). High background gas and distinct hydrocarbon shows were recorded below the gas column through the remainder of the Brent Group and in the Early Jurassic Cook Formation (Fig. 5.5).

The structure spills to the south-east towards Vega Central at 3830 m (marked by dotted line in Figure 5.9a). The large vertical difference between the gas-water contact and the structural spill point (173 m) suggest that the structure is underfilled. Further investigation of the position of the gas-water contact shows that it coincides with a fault intersection bounding the north-western part of the structure (Fig. 5.6). The orientations of these faults are marked with red colour in the rose diagram in Figure 5.10. A subtle flat spot is observed at -3070 ms TWT. Converted to true vertical depth, this corresponds to 3657 m, which is the depth of the gas-water contact (Table 5.2). A dim zone and subtle inclined bright spots are observed above the fault intersection (Fig. 5.6a).

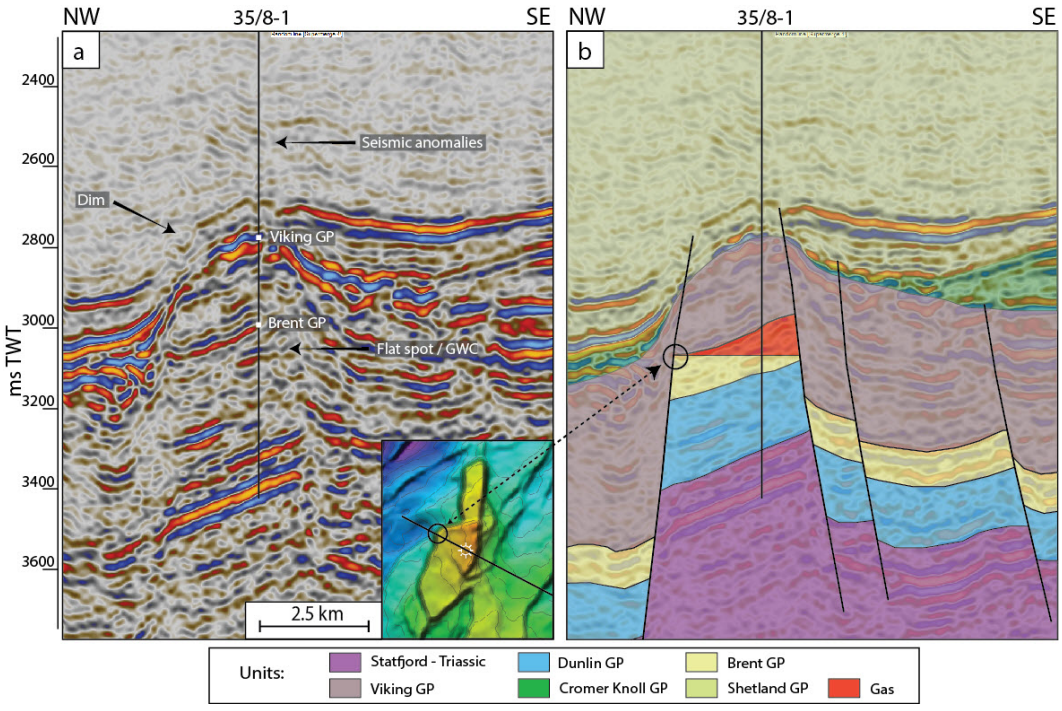

Figure 5.6: NE-SE seismic section through the fault intersection in the north-western part of the structure. Note the flat spot within the Brent Group and dim above the western fault.

The seismic data was analysed in search for other amplitude variations that could indicate vertical leakage and presence of gas in the overburden near Vega North. Although no distinct chimneys or brights were observed, slight dimming of the top Balder Formation (Rogaland Group) and top Kyrre Formation (Hordaland Group) reflectors

are apparent directly above the structure (Fig. 5.4). An RMS amplitude map of the top Kyrre Formation reflector, displayed in Figure 5.9b, shows that the dim is a local event, concentrated above the structure and two of the faults.

5.1.2 Vega Central - 35/8-2

Vega Central is the southern neighbour of Vega North. The structure is bound by a large W-dipping, N-S to NE-SW-trending normal fault, and a smaller E-dipping, NE-SW-trending normal fault (Fig.5.10). These two faults intersect each other to the south, forming a pointy three-way structural closure (Fig. 5.9a). The whole structure is slightly tilted towards north-east and the crest of the structure is located along the westerly dipping N-S fault, towards the south. Well 35/8-2 penetrated the Brent Group at 3666 m and core analyses indicated a gas-water contact at 3733 m, resulting in a gas-column extending through the Tarbert Formation and into the upper part of the Ness Formation (Fig. 5.5). According to the well log, no shows were recorded below the gas-water contact in the Brent Group contrary to what was observed in Vega North, however, shows do appear in the Early Jurassic Cook and Statfjord Formations.

The structure spills south-east towards Vega South at 3738 m, 4 m below the gas-water contact (marked by dotted line in Figure 5.9a and c). This indicates that Vega Central most likely is filled to spill-point. However, this is a fault spill-point, which means that south-eastward migration relies on permeable faults for across-fault fluid flow and on sand-sand juxtaposition of the Brent Group between Vega Central and South. Investigation of this spill route shows that sand-sand juxtaposition is likely (Fig. 5.7). Pore pressure in Vega Central is at top reservoir measured to 538 bar, corresponding to an overpressure of 171 bar.

No amplitude anomalies have been observed in the overburden above Vega Central, as shown in the seismic section (Fig. 5.4) and the RMS amplitude map (Fig. 5.9b).

5.1.3 Vega South - 35/11-2

Vega South is the shallowest structure in the Vega area. It is confined by NE-SW - trending normal faults, dipping to the east and west, forming a low relief horst-structure (Fig. 5.9c and 5.10). The primary target of well 35/11-2 was an Early Cretaceous fan, which proved to consist of only marl and clay. However, a 31 m thick Intra Heather Formation sand with oil shows was encountered in the otherwise shaly Viking Group. The Brent Group was penetrated at 3370 m and contained a 175 m gross hydrocarbon column down to a gas-water contact at 3545 m in the upper part of the Oseberg Formation (based on RFT pressure measurements) (Fig. 5.5). Oil and gas shows were

not recorded below the gas-water contact in the Brent group, however, weak shows do appear in the Early Jurassic Cook and Statfjord Formations.

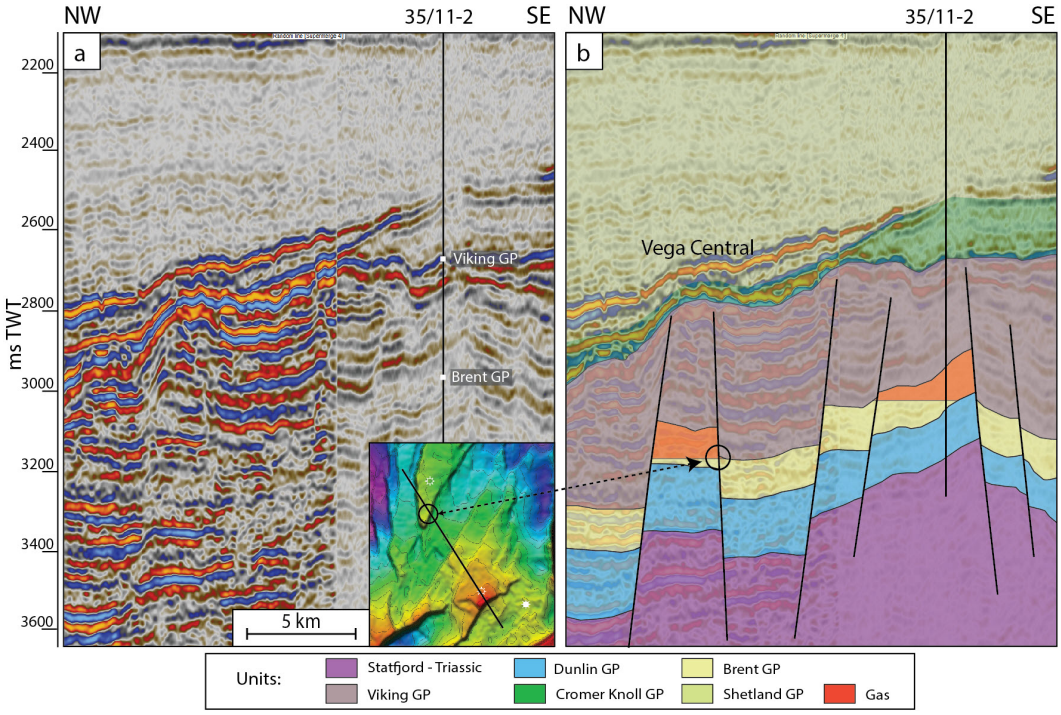

Figure 5.7: NW-SE seismic section along the spill route from Vega Central to Vega South. Juxtaposition between the Brent Group is suggested to be present between these structures.

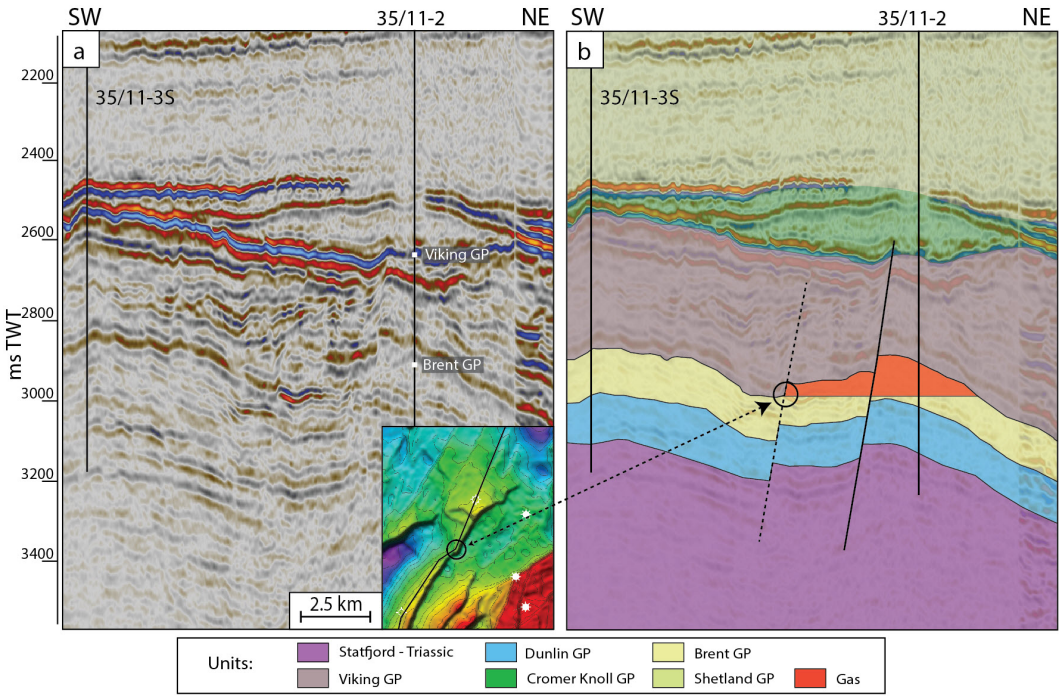

Figure 5.8: NE-SW seismic section of Vega South, illustrating the depth of the gas-water contact in relation to the spill point.

The structure spills south-westwards at 3550 m into a lower pressured westerly dipping

rotated fault block (35/11-3S), which is 5 m below the gas-water contact. This may indicate that Vega South is filled to its structural capacity (Fig. 5.8). The pore pressure was measured to 488 bar at the top of the reservoir, which corresponds to an overpressure of 150 bar. According to organic geochemical analysis, the penetrated source intervals in the Draupne and Heather Formations were immature to marginally mature, and certainly less mature than the sampled petroleum in the Brent Group.

A thin vertical "pipe" with reduced reflectivity is apparent directly above the crest of the structure, through the Cromer Knoll and Shetland Groups and into the lower part of the Hordaland Group (5.4b). The lateral extent and character of this effect is displayed in the RMS amplitude map of the top Kyrre Formation reflector (Shetland Group) (Fig. 5.9d). It is evident that the event is somewhat concentrated above the very crest of the Vega South structure. Furthermore, this concentrated dimming feature is followed by a chaotic reflection pattern in the upper part of the Hordaland Group (Fig. 5.4b).

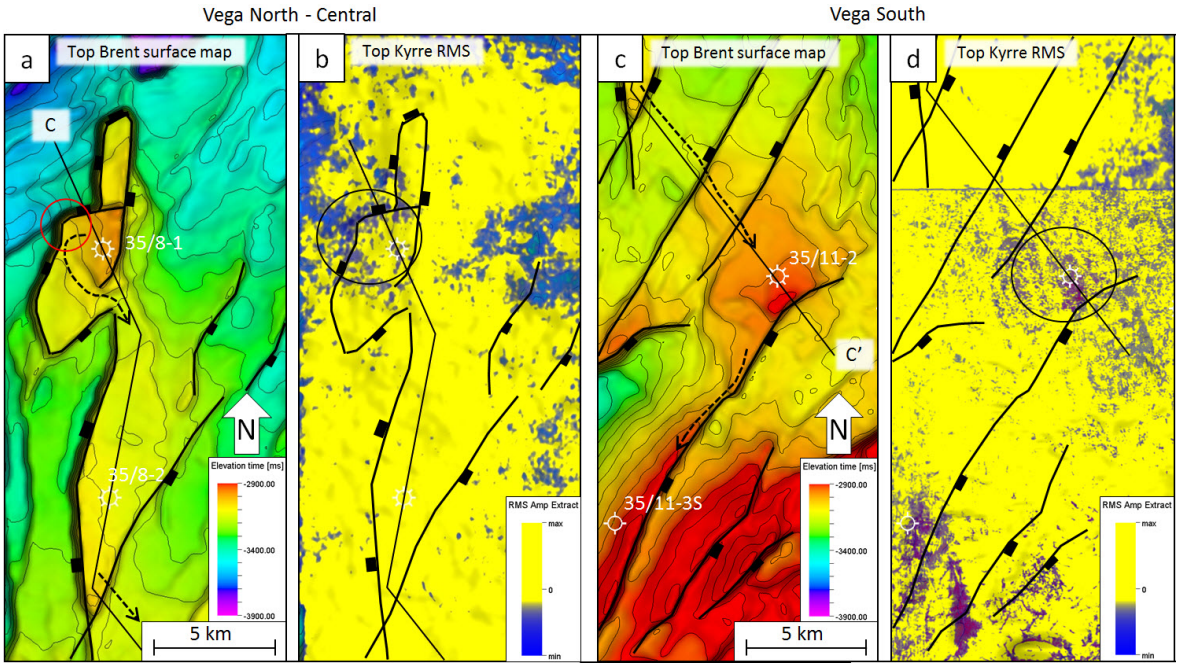

Figure 5.9: Close-up of the Vega structures. **a**: Top Brent map (50 m contour spacing) showing the structural configuration and spill routes of Vega North and Central. **b**: Superimposed RMS amplitude map of the top Kyrre reflector over Vega North and Central, including outline of main faults (note the reduced reflectivity over the Vega North structure and above two of the faults, marked by black circle) **c**: Top Brent map showing the structural configuration and spill route of Vega South. **d**: Superimposed RMS amplitude map of the top Kyrre reflector over Vega South, including outline of main faults (note reduced reflectivity over the crest of the structure, marked by black circle). Suggested migration routes are marked with dotted black arrows.

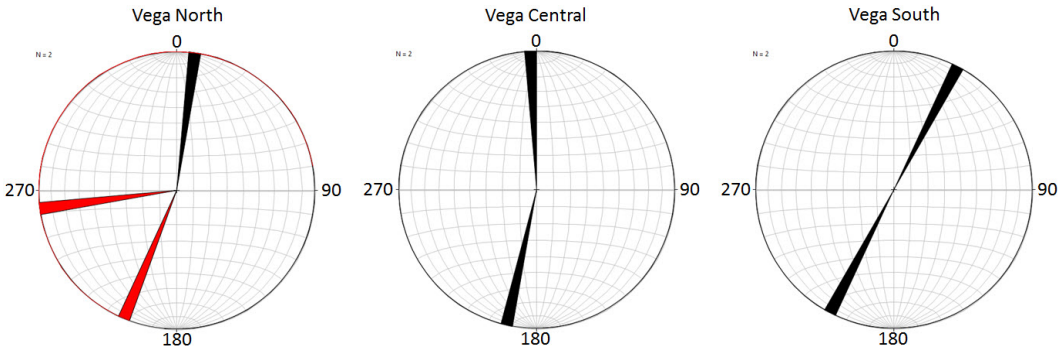

Figure 5.10: Rose diagram with the main fault trends in Vega area. Note the red fault trends in Vega North, which intersects and coincide with the gas-water contact.

5.1.4 Summary of the Vega area

Based on observations done in the Vega area, the following suggestions are made:

- Vega North is suggested to be underfilled, with the gas-water contact coinciding with a fault intersection that delineates the north-western part of the structure. This is supported by a large vertical distance (173 m) form the gas-water contact to the mapped spill point, and the presence of residual hydrocarbon shows beneath the gas-water contact in the Brent Group. Weak amplitude anomalies (brights and dim zone) are observed above the fault intersection. Whether this feature is directly related to leakage is uncertain.

- Vega Central and Vega South is suggested to be filled to their structural capacity. This is based on the fact that the gas-water contacts coincides with the depth of the mapped spill points. Moreover, no distinct hydrocarbon shows are recorded beneath the gas-water contacts in these structures (except from in the Dunlin Group). A vertical pipe of dimming is observed above Vega South, which might be related to the chaotic reflection in the upper part of the Hordaland Group. Whether the chaotic reflection pattern causes the reduced reflectivity in the underlying sections or vice versa is uncertain.

5.2 Aurora - Titan

The Aurora and Titan discoveries are located in the northern part of the Lomre/Uer Terrace, bordering the deeper Sogn Graben (Fig. 5.11a). The Aurora structure was drilled by well 35/8-3, which encountered gas in Intra Heather Formation sandstones and a water bearing Brent Group with shows. The Titan discovery, drilled by well 35/9-6S, comprises oil and gas in five stratigraphic levels: sands in the Dunlin and Brent Groups, and Intra Heather Formation sandstones. Pressures within these units are listed in Table 5.3 (no fluid contacts were identified in either of these wells). The pressure vs. depth plot in Figure 5.11b displays a large variation in reservoir pressures in this area, both laterally between the Aurora and Titan structures, and vertically between the reservoirs within each structure. Seismic section D-D' in Figure 5.12 shows an interpretation over this area.

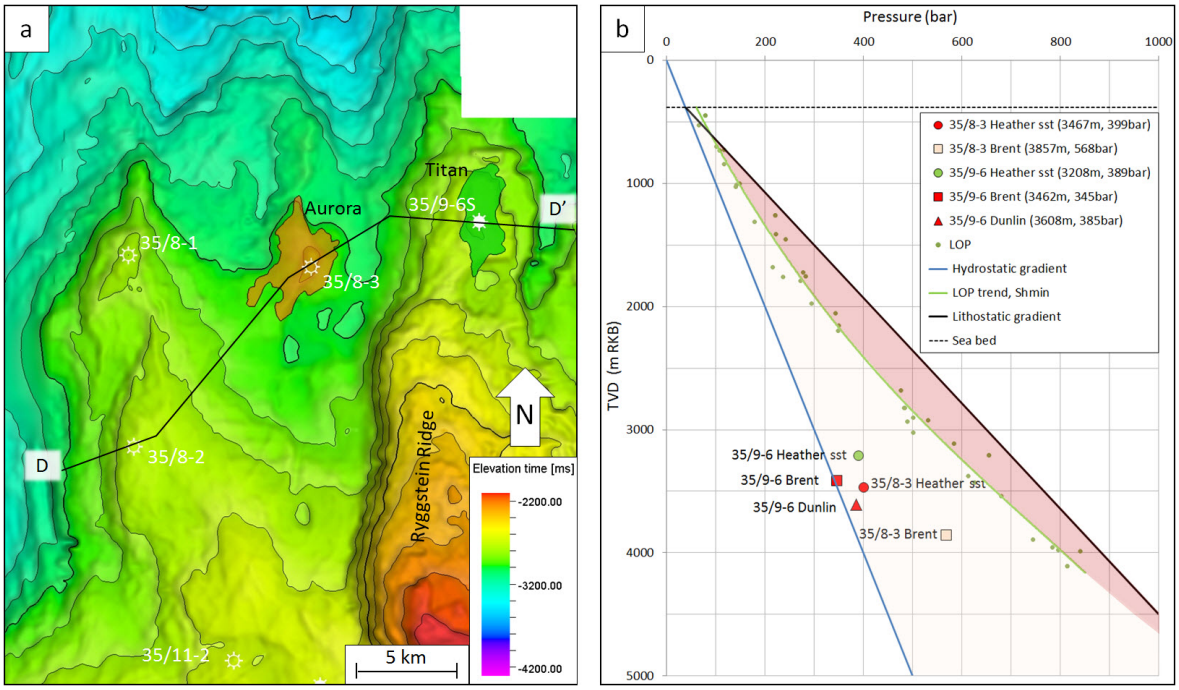

Figure 5.11: Overview of the Aurora - Titan area. **a**: Base Cretaceous Unconformity surface map (100 m contour spacing) superimposed by field outlines, based on the field outlines from the NPD fact-maps. Black line represents the location of seismic section D-D'. **b**: Reservoir pressures in the Aurora and Titan structures presented in a pressure vs. depth plot (note the large spread in pressures in this area).

Table 5.3: Summary of fluid contacts, spill points and pressure measurements close to top reservoir in the Aurora and Titan structures (note that no fluid contacts were found in these structures, and therefore intentionally left blank).

Well	Unit	GWC		Spill point		Pressure				
	Gp/Fm	TVD	TWT	TVD	TWT	TVD	Pore	Overpressure	RC	Op/LOT-Hydr
35/8-3	Heather sst	N/A				3467	399	52	261	0.17
	Brent	Dry			-3320	3867	568	182	202	0.47
35/9-6S	Heather sst	N/A				3208	389	68	191	0.26
	Brent	N/A		3408	-2880	3462	345	4	295	0.01
	Dunlin	N/A				3608	385	24	315	0.07

Units: TVD (True Vertical Depth, m RKB); TWT (Two Way Time, ms); Pressure (bar)

5.2.1 Aurora - 35/8-3

The Aurora discovery is located approximately 8 km east of Vega North. Structurally, Aurora appears as a small, pointy crest, bound by several soft-linking NE-SW-trending normal faults, dipping both to the east and west (Fig. 5.14a and 5.15). Well 35/8-3 encountered gas in a slightly overpressured 82 m thick sandstone unit in the Heather Formation, with an unknown gas-water contact (Table 5.3). Due to discontinuous reflectors in this area the distribution of this sand could not be mapped with confidence, thus determining a spill point is not possible. The Intra Heather sandstone is overpressured by 52 bar.

The underlying water bearing Brent Group is overpressured by 182 bar and spills south-west through a weakly faulted passage towards the slightly lower pressured Vega Central, indicated by the black dotted line in Figure 5.14a. The difference in overpressure between the Brent Group and the Intra Heather Formation sandstones is 130 bar.

Two concentrated vertical pipes with reduced reflectivity (dim) are observed in the overburden above the Aurora structure. (Fig. 5.12b). One of these is located in the vicinity of the eastern fault plane that delineates the structure. This feature appears as a circular low amplitude event in the RMS attribute map in Figure 5.14b. Interestingly, also larger, similar events are apparent in this area.

5.2.2 Titan - 35/9-6S

The Titan discovery is located on the northern tip of the Ryggstein Ridge, and it can be defined as a four-way structural closure at different stratigraphic levels, from Early to Late Jurassic age (the main fault trends are displayed in Figure 5.15). Oil and gas shows were recorded throughout the Viking, Brent and Dunlin Groups, and five different sandstone units contain accumulation of oil and gas (Fig. 5.13).

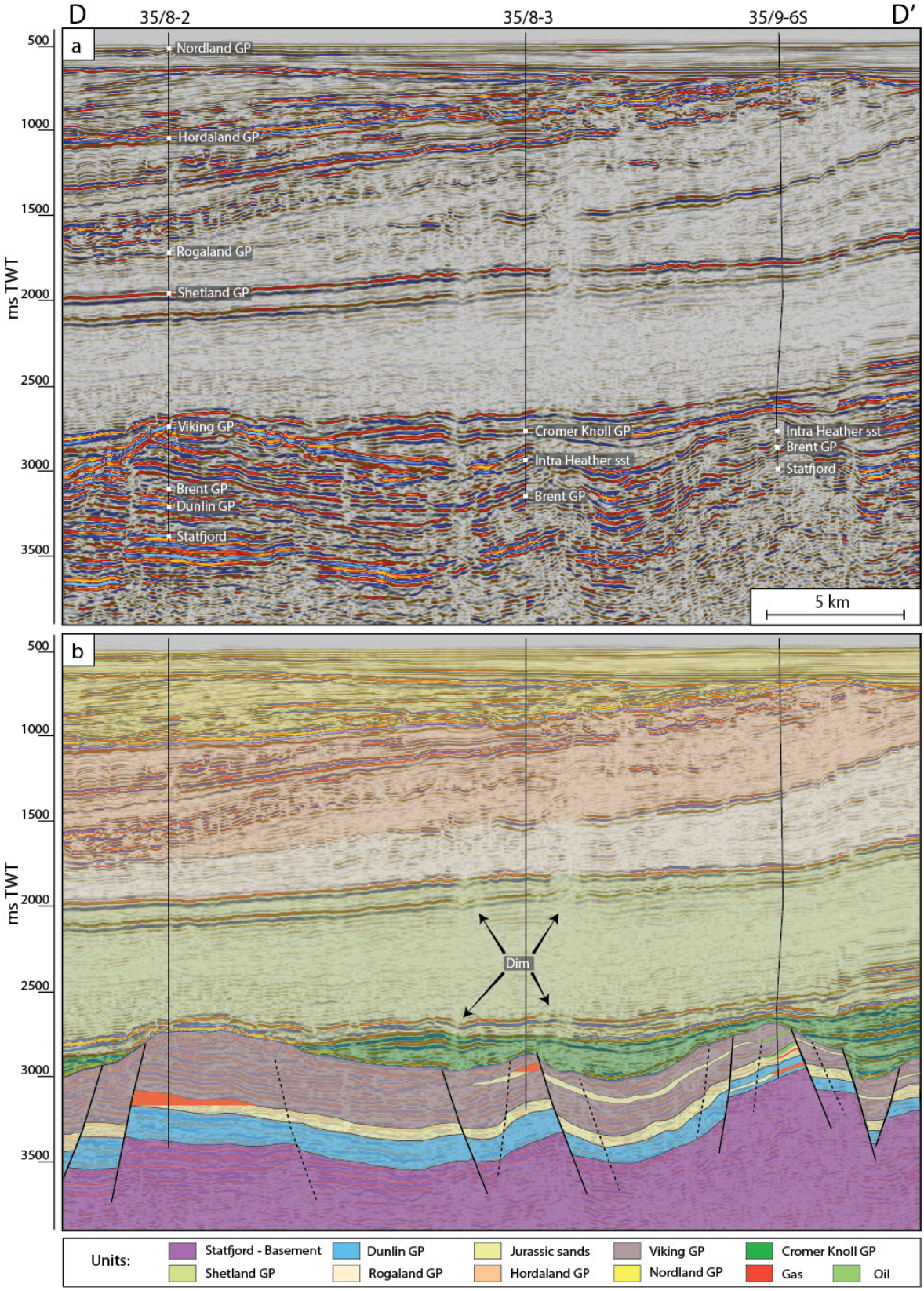

Figure 5.12: Seismic section D-D' shows an uninterpreted (**a**) and interpreted (**b**) version from W to E through the Vega Central, Aurora and Titan structures (including key observations in the overburden). Note the reduced reflectivity (vertical dim area) above the Aurora structure.

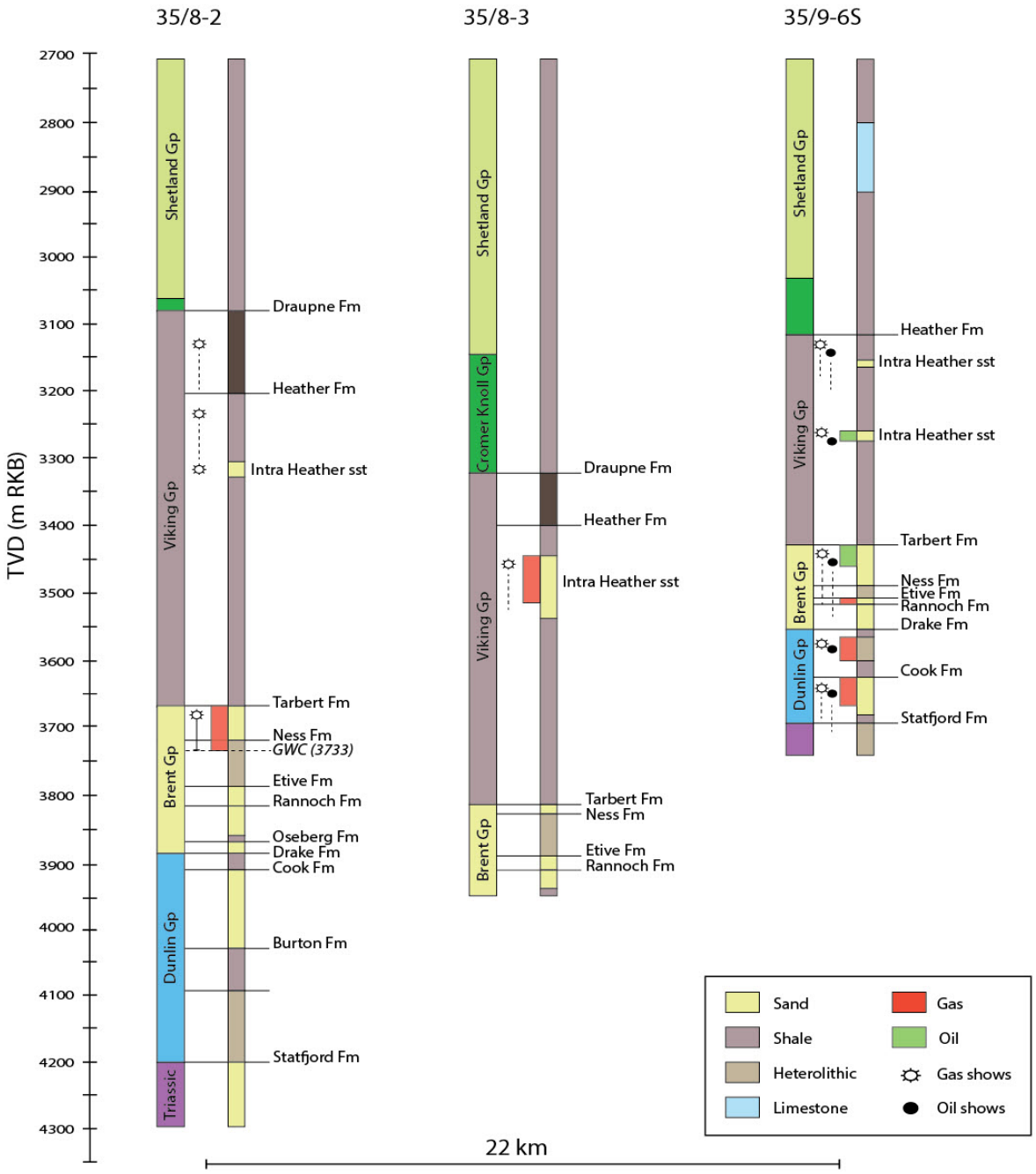

Figure 5.13: Lithological well logs corresponding to the wells in seismic section D-D', with recordings of hydrocarbon shows and fluid contacts. Note that no fluid contacts were identified in well 35/8-3 or 35/9-6S (oil and gas columns in the logs are only for illustration purposes).

As previously mentioned no fluid contacts have been identified in any of the hydrocarbon bearing reservoirs. This observation, and the variations of fluid pressures in the water phases between different sand, renders analyses of the degree of fill of this structure futile. The oil-bearing Intra Heather Formation sandstone is overpressured by 68 bar, while the deeper Brent Group is close to normally pressured, measuring an overpressure of 4 bar. The underlying sand in the Dunlin Group is slightly higher pressured than the Brent Group, with an overpressure of 24 bar. The Brent Group spills southwards at 3408 m along the Ryggstein Ridge into the lower pressured Grosbeak

structure.

Aside from chaotic reflection patterns in the upper part of the Hordaland Group, no strong amplitude anomalies were identified in the overburden directly above the Titan structure. However, significantly reduced seismic reflectivity was observed through the Shetland Group and particularly of the top Kyrre Formation reflector, southwards on the Ryggstein Ridge. This extensive dim event can be viewed partly in the southern part of the RMS attribute map in Figure 5.14b and in seismic section E-E' in Figure 5.17.

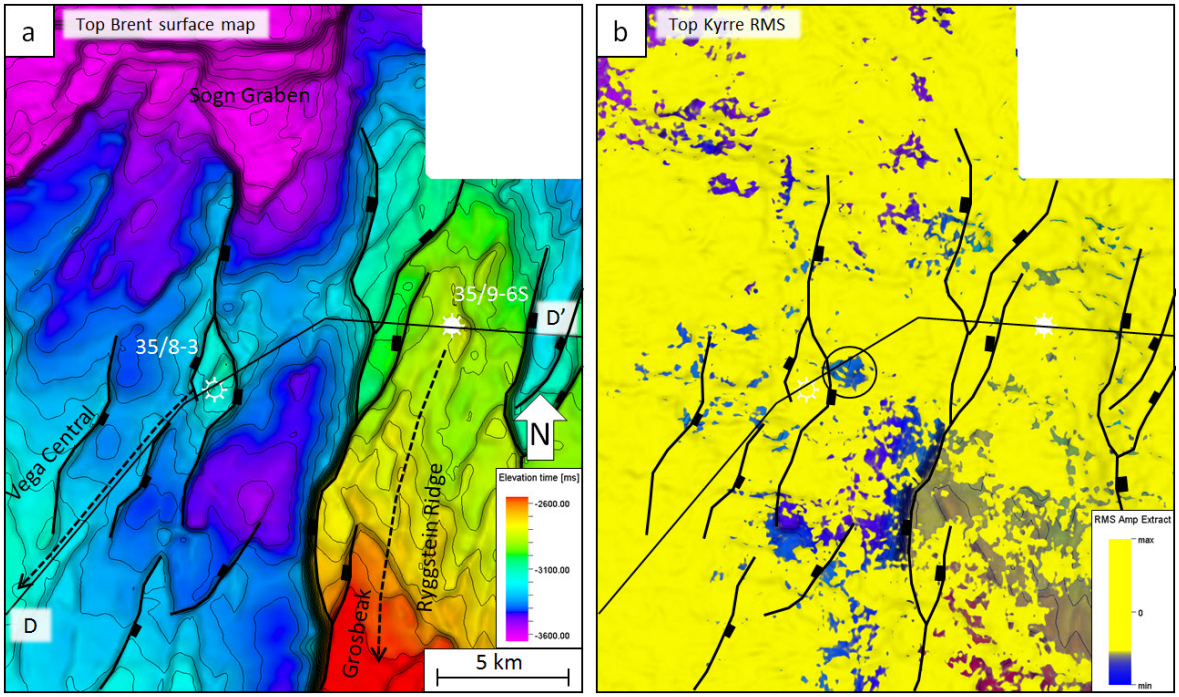

Figure 5.14: Close-up of the Aurora and Titans structures. **a**: Top Brent surface map (50 m contour spacing) shows the Middle Jurassic structural configuration in the area and spill routes from the respective structures. **b**: Superimposed RMS amplitude map of the Top Kyrre reflector, including outline of main faults (note the concentrated zone of reduced reflectivity adjacent to the Aurora structure, marked by black circle). Similar, but more widespread events are observed in the southern part towards the Ryggstein Ridge. Suggested migration routes are marked with dotted black arrows.

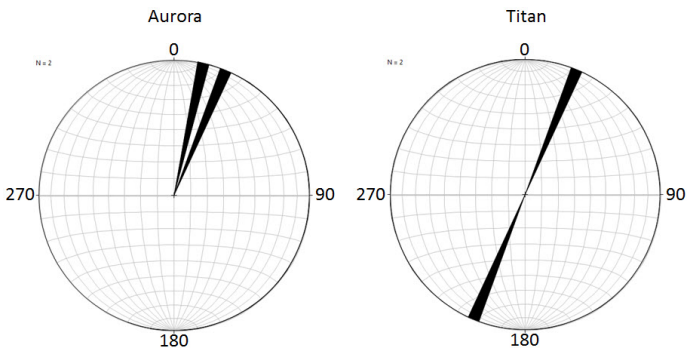

Figure 5.15: Rose diagram with the main fault trends in the Aurora and Titan structures.

5.2.3 Summary of Aurora - Titan

Due to unknown fluid contacts within the reservoirs in these structures, analysis on the controls on hydrocarbon column-heights can not be conducted in this area. Aside from that, the following can be deduced:

- Reduced reflectivity (dim) is observed above a fault plane that delineates the eastern part of the Aurora structure. Also, larger similar events are apparent south of the Titan structure, along the Ryggstein Ridge. Whether any of these anomalies are caused by leakage is unclear.
- Large variations in reservoir overpressures in the Aurora and Titan structures indicate a lack of communication between the reservoir sequences within each structure.

5.3 Grosbeak

The Grosbeak discovery is located on the Ryggstein Ridge, south of the Titan discovery and north-east of the Fram area (Fig. 5.16a). Well 35/12-2 encountered gas in the Late Jurassic Sognefjord Formation and oil in the Fensfjord Formations and Brent Group. Fluid contacts and pressures within these reservoirs are listed in Table 5.4, while the presence of hydrocarbon shows are illustrated in the lithological well logs in Figure 5.18. The pressure vs. depth plot in Figure 5.16b shows a close to normally pressured Brent Group and Fensfjord Formation overlain by a slightly overpressured Sognefjord Formation. Figure 5.17 displays a seismic section from north to south along the Ryggstein Ridge, coupled with an interpretation of the Grosbeak structure.

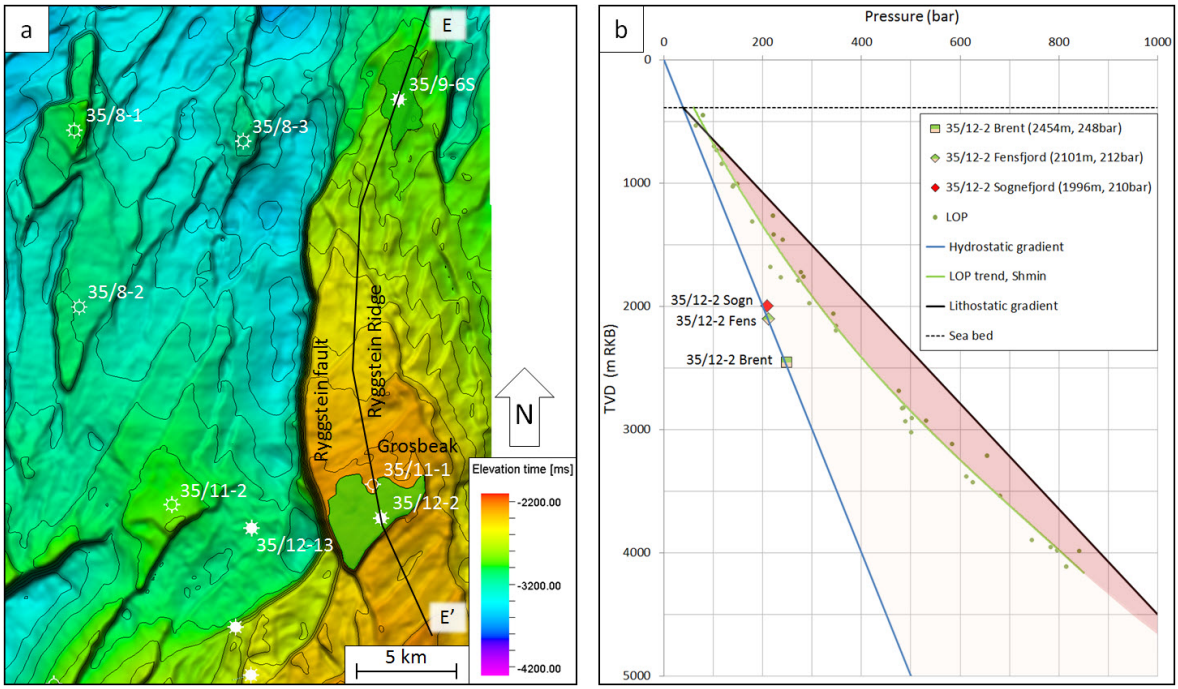

Figure 5.16: Overview of the Grosbeak structure. **a**: Top Brent Group surface map (100 m contour spacing) and field outline of the Grosbeak discovery base on the oil-water contact in the Brent Group. Black line represents the path of seismic section E-E'. **b**: Reservoir pressures in the Grosbeak structure presented in a pressure vs. depth plot. Note that the close to normally pressured oil-bearing Fensfjord Formation and Brent Group is overlain by a slightly overpressured gas-bearing Sognefjord Formation.

Table 5.4: Summary of fluid contacts, spill points and pressure measurements close to top reservoir in the Grosbeak structure. Note that the Sognefjord formation contains gas to its base (GTB).

Well	Unit	OWC		Spill point		Pressure				
	Gp/Fm	TVD	TWT	TVD	TWT	TVD	Pore	Overpressure	RC	Op/LOT-Hydr
35/12-2	Sognefjord	GTB		N/A		1996	209	9.4	111	0.080
	Fensfjord	2119	-2080	N/A		2101	212	1.9	128	0.015
	Brent	2485	-2305	2541	-2356	2454	248	2.6	162	0.016

Units: TVD (True Vertical Depth, m RKB); TWT (Two Way Time, ms); Pressure (bar)

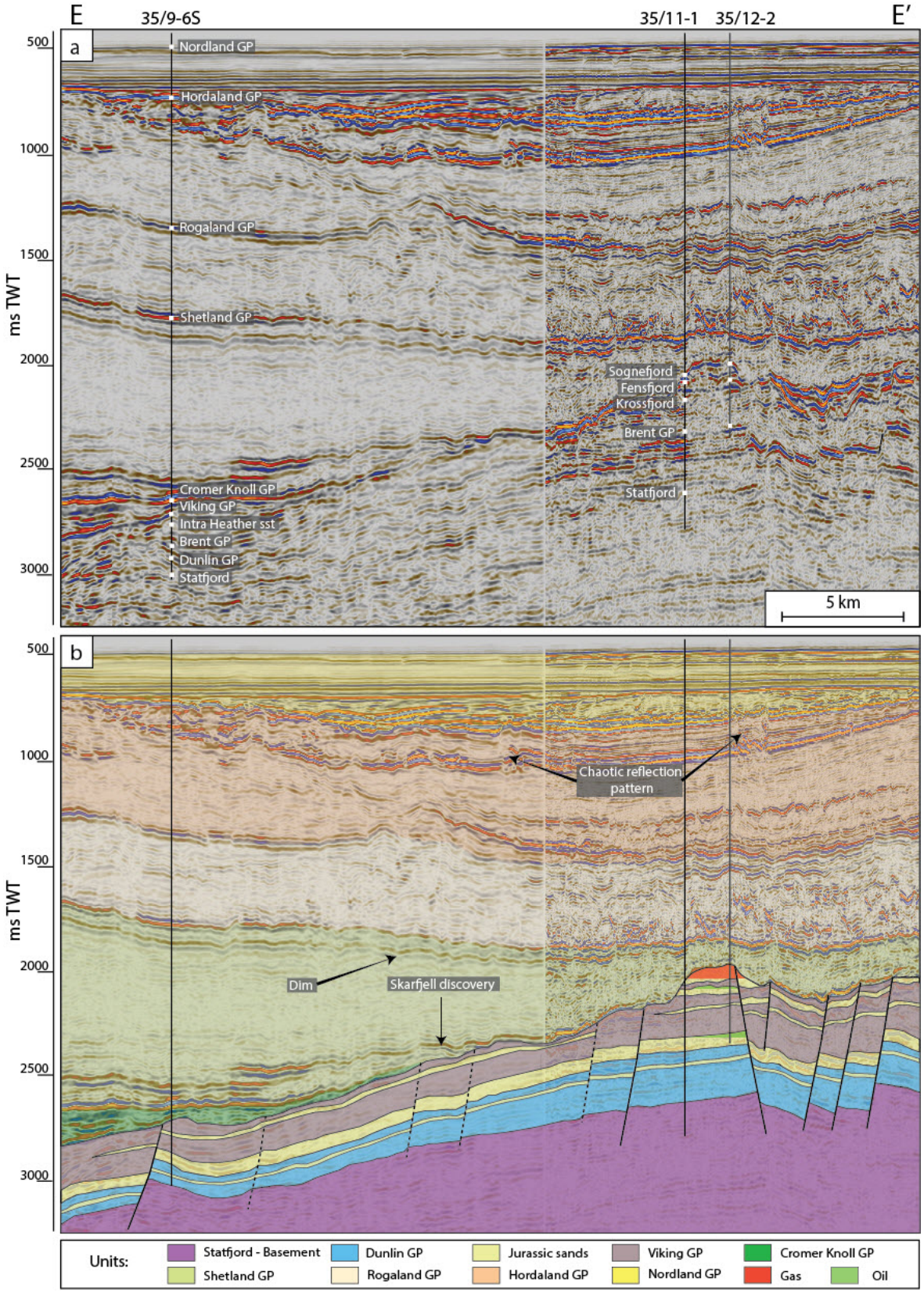

Figure 5.17: Uninterpreted (**a**) and interpreted (**b**) seismic section from N to S over the Ryggstein Ridge, from the Titan structure to the Grosbeak structure.

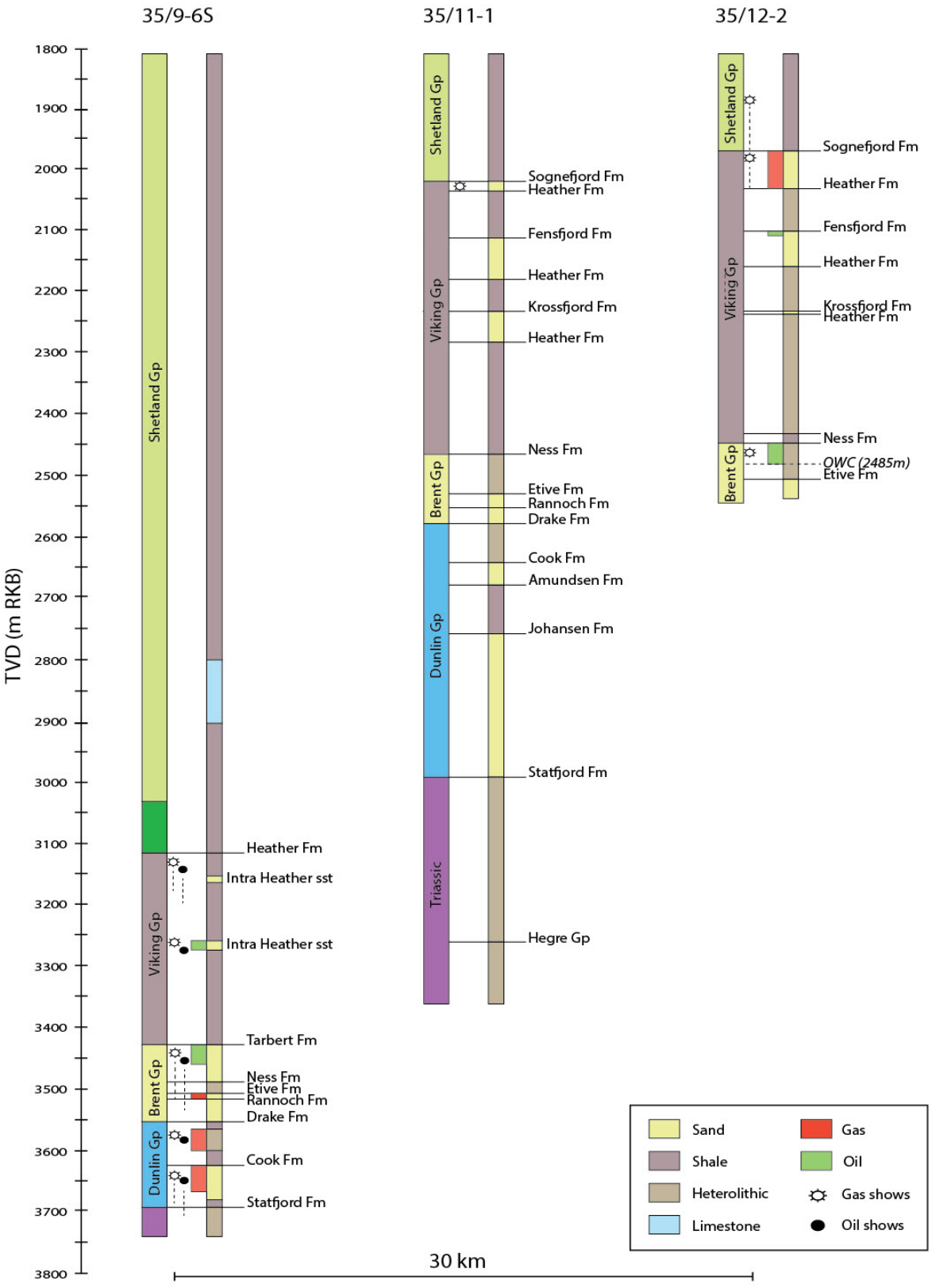

Figure 5.18: Lithological well logs corresponding to the wells in seismic section E-E', with recordings of hydrocarbon shows and fluid contacts.

5.3.1 Grosbeak - 35/12-2

The Grosbeak structure is a rather complex trap, formed by the large N-S trending and westerly dipping Ryggstein fault, and a number of smaller NE-SW trending normal faults dissecting the top of the Ryggstein Ridge (Fig. 5.19a and 5.20). The structure was first drilled by well 35/11-1 in a down-dip location, encountering a thin gas charged Sognefjord Formation, and thick water-bearing Fensfjord Formation and Brent Group.

Well 35/12-2 was spudded further south, targeting the crest of the Sognefjord Formation, which is unconformable overlain by Late Cretaceous shales of the Kyrre Formation. This erosional surface is well illustrated by the Base Cretaceous surface map in Figure 5.19b. Sandstones of the Sognefjord Formation proved to be much thicker (62 m) than in well 35/11-1 and contained gas to its base. The Fensfjord Formation contained oil in a two metre sandstone, passing into 13 m of shale, then into water-bearing sandstones. A lower oil-leg of 35 m gross was encountered in the Brent Group down to an apparent oil-water contact at 2485 m. No residual hydrocarbons were recorded below the oil-water contact in the Brent Group. Figure 5.16a shows how well 35/11-1 misses the oil-water contact in the Brent Group by only a few tens of metres.

The Brent Group spills southwards into the Fram area at 2541 m, which is 56 m below the oil-water contact. The spill point of the Fensfjord and Sognefjord Formations could not be determined.

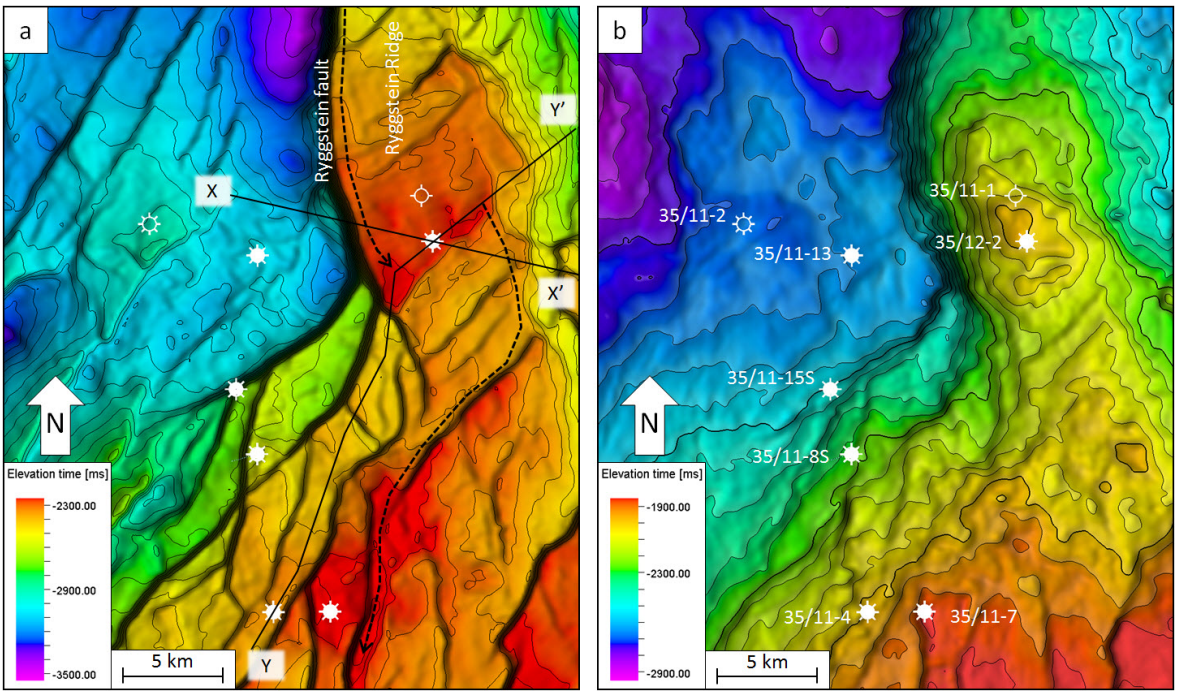

Figure 5.19: Close-up of the Grosbeak structure. **a**: Top Brent Group surface map (50 m contour spacing) shows the structural configuration in the area. **b**: Base Cretaceous surface map (50 m contour spacing) shows the unconformity between the Viking Group and the overlying Cretaceous shales. Suggested migration routes in the Brent Group are marked with dotted black arrows.

Seismic section Y-Y' in Figure 5.21, runs NE-SW through the Grosbeak structure and into the Fram area. Adjacent to the oil-bearing Brent Group, increased acoustic impedances (red reflections), which might indicate presence of sand, are observed. Based on a well tie with well 35/4-1, this reflection is interpreted to be part of the Fensfjord Formation. Note how the Fensfjord Formation is situated relative to the oil-water contact in the Grosbeak structure. This may indicate that the Grosbeak structure is filled to its capacity.

Several amplitude anomalies are observed in the overburden above the Ryggstein Ridge and the Grosbeak structure. However, due to poor seismic imaging in this area, it is difficult to distinguish noise from other seismic anomalies caused by lithology and fluid variations. Because of this, no RMS amplitude map of the overburden has been generated in this area. Nevertheless, for consistency, the overburden above the Grosbeak structure has been carefully scanned for any prominent seismic anomalies. Seismic section X-X' in Figure 5.21a shows the most prominent seismic features in the area, which are V-brights and a dim zone within the Rogaland Group.

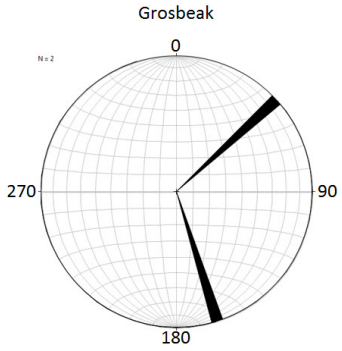

Figure 5.20: Rose diagram with the main fault trends in the Grosbeak structure.

5.3.2 Summary of Grosbeak

Based on analysis of fluid contacts and spill-points in the Grosbeak structure the following can be deduced:

- The Brent Group is suggested to be underfilled, with a vertical difference of 56 m between the oil-water contact and the structural spill point. However, there is no information on the presence of residual hydrocarbons below the oil-water contact. Juxtaposed sands could explain this.
- Whether the Fensfjord and Sognefjord Formations are underfilled or filled is highly uncertain, as no spill points could be determined in these units.
- V-brights and dim zones are observed above the top of the Grosbeak structure in the Rogaland Group.

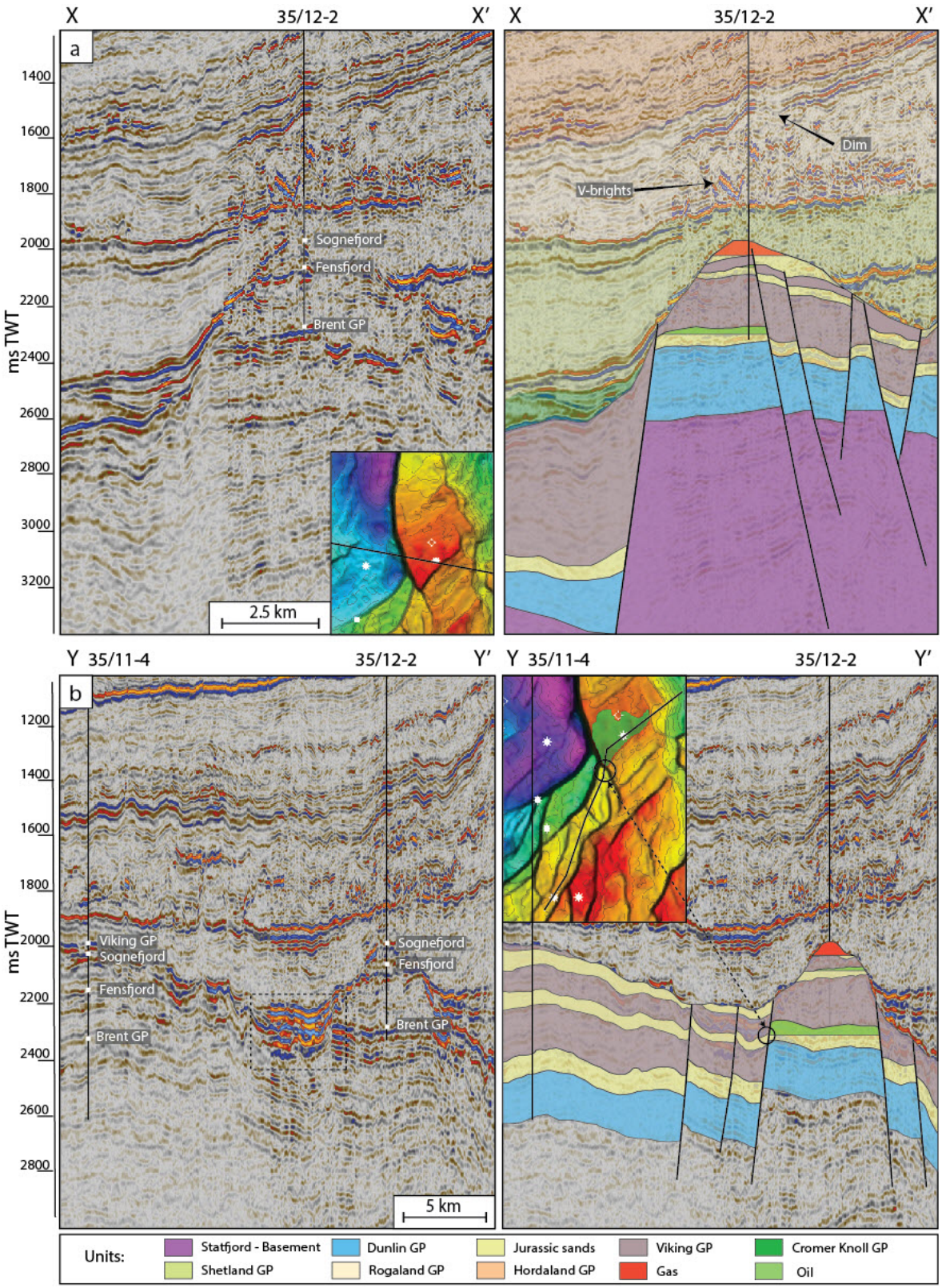

Figure 5.21: a: NW-SE seismic section through the Grosbeak structure shows locations of fluid contacts and amplitude anomalies in the overburden. **b:** NE-SW seismic section from the Grosbeak structure into the Fram area, show the possibility of juxtaposition between the Brent Group and Fensfjord Formation.

5.4 Fram - Astero

The Fram area is located in the eastern end of the Lomre Terrace and comprises several oil and gas discoveries in different stratigraphic levels. The area is structurally complex with a number of small down-faulted terraces, forming a transition zone from the deep part of the Lomre Terrace to the shallower Horda Platform, where the Troll field is situated further to the south (Fig. 5.22a). In contrast to the deeper situated fields in the Vega area, the Upper Jurassic Viking Group in the Fram area comprises several sandy units, represented by the Sognefjord and Fensfjord Formations, and Intra Heather Formation sandstones. However, due to poor seismic resolution in the area (and limited time available for detailed seismic analyses), interpretations of these units are only presented in the seismic section (Fig. 5.23). The poor data quality in this area is well illustrated in the seismic sections in Figure 5.26. Depth to fluid contacts and reservoir pressures are listed in Table 5.5. All reservoirs are close to normally pressured and plot along the hydrostatic gradient (Fig. 5.22b).

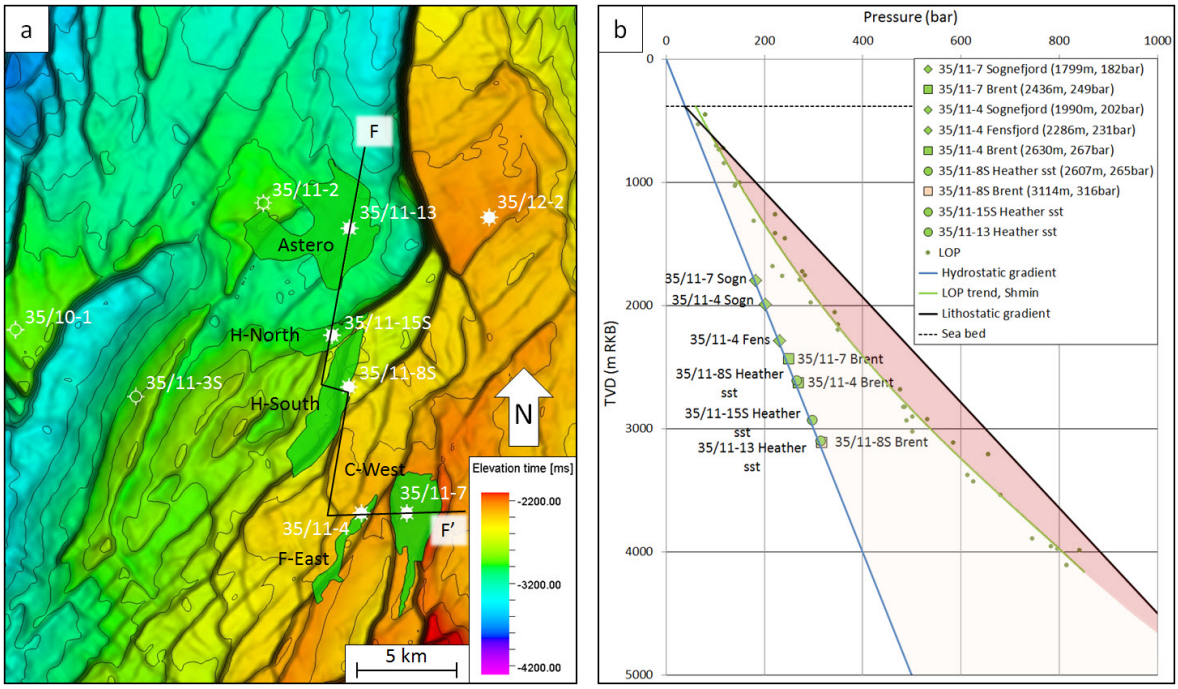

Figure 5.22: Overview of the Fram area with **a**: Top Brent surface map (100 m contour spacing) and field outlines (based on NPD) and **b**: Reservoir pressures presented in a pressure vs. depth plot. Note that the whole area is normally pressured, plotting along the hydrostatic gradient.

Table 5.5: Summary of fluid contacts, spill points and pressure measurements close to top reservoir in the in the Fram area.

Well	Unit	GOC		OWC		Spill point		Pressure			
	Gp/Fm	TVD	TWT	TVD	TWT	TVD	TWT	TVD	Pore	OP	RC
35/11-13	Heather sst	3128	-2765	3158	-2781	N/A		3096	314	4.4	166
35/11-15S	Heather sst	-	-	2941	-2640	N/A		2930	297	4.0	163
35/11/-8S	Heather sst	2626	-2428	2680	-2461	N/A		2607	265	4.3	155
	Brent	Dry w/shows				N/A		3114	316	4.6	169
35/11-4	Sognefjord	1994	-1990	2051	-2032	N/A		1990	202	3.0	118
	Fensfjord	-	-	2310	-2179	N/A		2286	231	2.4	154
	Brent	2670	-2390	2687	-2402	N/A		2630	267	4.0	158
35/11-7	Sognefjord	1800	-1834	1852	-1868	N/A		1799	182	2.1	103
	Brent	2470	-2246	2504	-2266	2504	-2266	2436	249	5.4	151

Units: TVD (True Vertical Depth, m RKB); TWT (Two Way Time, ms); Pressure (bar)

5.4.1 Astero - 35/11-13

The Astero discovery is located north of the Fram fields, approximately 5 km east of Vega South structure, and comprises oil and gas bearing Intra Heather Formation sandstones. These sands were encountered at 3096 m and measured 110 m thick, containing oil overlain by a thin gas cap. The gas-oil contact was inferred at 3098 m and the oil-water contact at 3137 m (Fig. 5.24). According to NPD, the reservoir sands are interpreted as Late Jurassic (Oxfordian age) high density turbidites derived from the Sognefjord delta in the east. The pore pressure close to top reservoir was measured to 314 bar, corresponding to an overpressure of 4.4 bar. According to the well log, no residual hydrocarbons were recorded below the oil-water contact (Fig. 5.24).

The depth to the structural spill point is unknown, however, based on the lack of residual hydrocarbons below the oil-water contact, the structure is suggested to be filled to its structural capacity. Considering the low reservoir pressure relative to the depth, the reservoir of the Astero structure might be in communication with the shallower Fram fields.

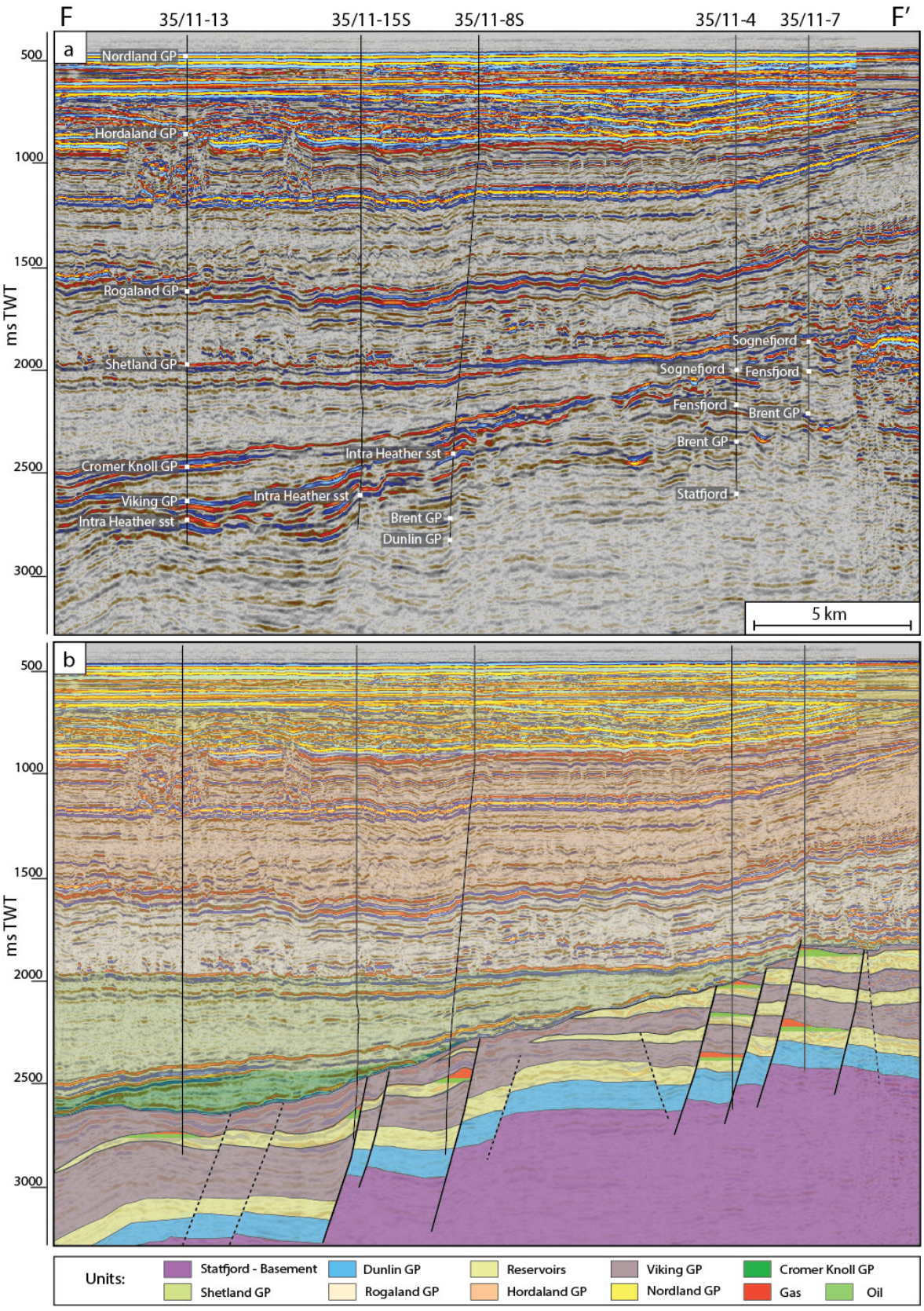

Figure 5.23: Seismic section F-F' shows an interpretation of the Fram area from NW to SE.

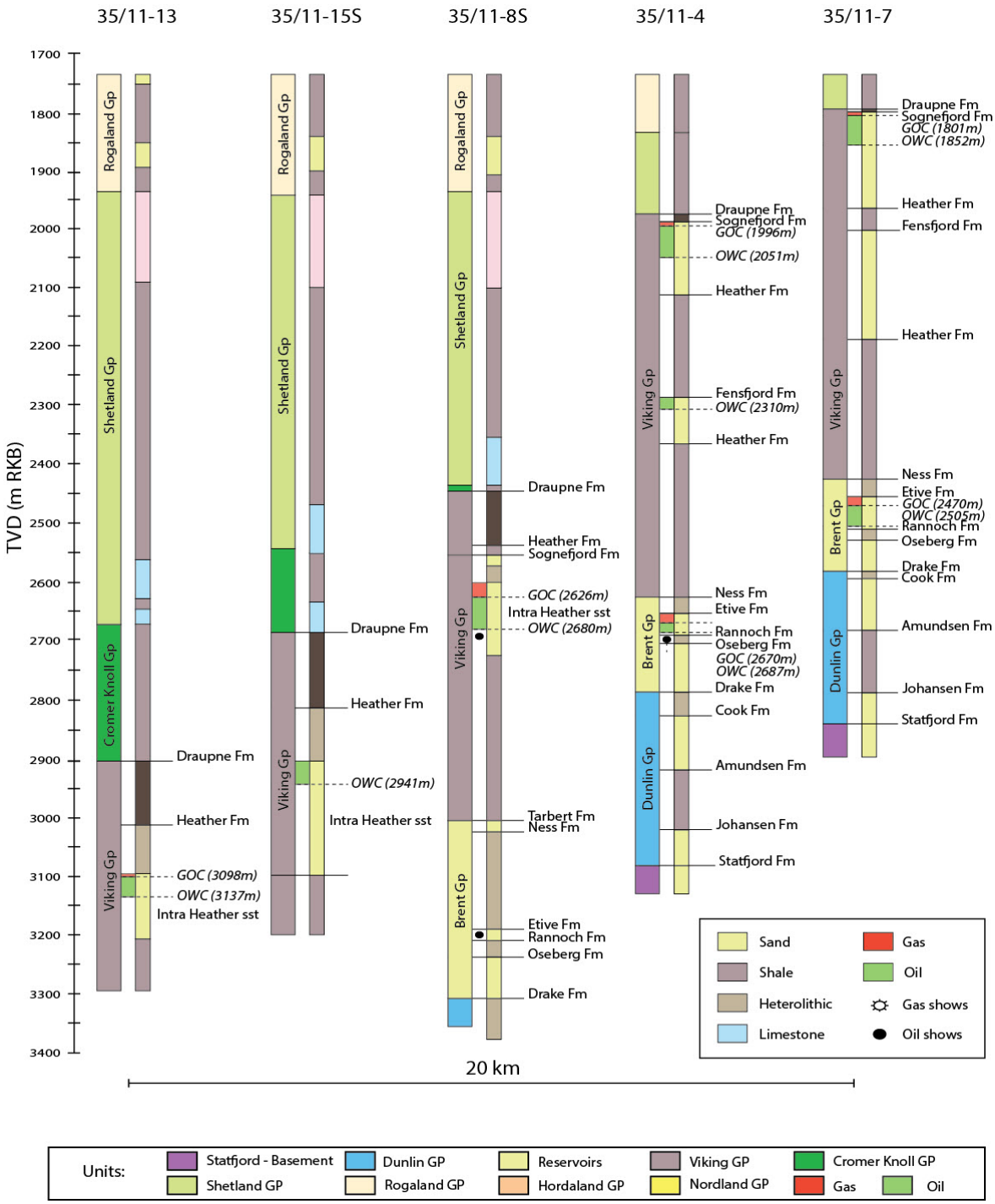

Figure 5.24: Lithological well logs with recordings of shows and fluid contacts corresponding to the wells in seismic section F-F' in Figure 5.23.

5.4.2 H-North - 35/11-15S

The H-North discovery, proved by well 35/11-15S, is located up-dip of the of the Astero discovery, adjacent to the Kinna fault (Fig. 5.25a). The reservoir in this structure consists of high density turbiditic sequences, and might be in communication with the deeper situated Astero structure. Well 35/11-15S encountered oil from top reservoir

down to an oil-water contact at 2941 m. The pore pressure close to top reservoir was measured to 297 bar, corresponding to an overpressure of 4.0 bar. There is not registered any residual hydrocarbons below the oil-water contact in this well, which might imply that the structure is filled to its capacity (Fig. 5.24).

5.4.3 H-South - 35/11-8S

The H-South discovery is located on the footwall of the Kinna fault, south of the H-North discovery (Fig. 5.25). Similar to the two previous discoveries, gas and oil was encountered in Intra Heather Formation sandstones (Oxfordian turbidites), with the gas-oil contact measuring at 2626 m and the oil-water contact at 2680 m. Hydrocarbon shows were recorded below the oil-water contact in this reservoir (Fig. 5.24). The Brent Group proved water bearing, also with residual hydrocarbons. Pressure close to top reservoir in the Intra Heather Formation sandstones and the Brent Group measured 265 and 316 bar, corresponding to overpressures of 4.3 and 4.6 bar, respectively.

As residual hydrocarbon were recorded below the oil-water contact in the Intra Heather reservoir and in the water-bearing Brent Group, further seismic investigation of this structure has been conducted. Seismic section X-X' and Y-Y' in Figure 5.26 runs through a fault intersection delineating the top of the Brent Group in this structure. A dim zone overlain by brights is apparent in the vicinity of the fault intersection. Further away from the fault intersection, no distinct seismic anomalies are observed in the overburden (section Z-Z' in Fig. 5.26). The NE-SW-trending fault in this intersection is marked with red colour in the rosediagram, while the other fault, oriented more towards N-S, is marked with black colour (Fig. 5.27).

5.4.4 F-East - 35/11-4

The F-East structure, located approximately 6 km south-east from the H-South discovery, contains oil and gas in three stacked reservoirs represented by the Sognefjord and Fensfjord Formations, and the Brent Group. Fluid contacts within these reservoirs are listed in Table 5.5. The spill points of the Sognefjord and Fensfjord Formations are not known. However, no residual hydrocarbons are reported beneath the fluid contacts, which might indicate that these reservoirs also are filled to their capacity (Fig. 5.24). The spill route in the Brent Group from F-East is suggested to occur along the terrace, through a relay ramp and into C-West (Fig. 5.25a). Residual hydrocarbons were recorded below the oil-water contact in the Brent Group, indicating that the structure might be underfilled.

Seismic investigation in the area where the hydrocarbon column in the Brent Group terminates is conducted. Section X-X' and Y-Y' in Figure 5.26 runs through a fault

intersection in the northern part of the F-East structure. A dim zone overlain by brights is observed above the fault intersection. In section Z-Z', southwards along the structure, no amplitude anomalies are observed in the overburden.

5.4.5 C-West - 35/11-7

The C-West structure is located 2 km east of the F-East structure. Well 35/11-7 encountered oil and gas in two reservoirs: the Sognefjord Formation and the Brent Group (fluid contacts listed in Table 5.5). The Fensfjord Formation was found dry, with no residual hydrocarbons. The Brent Group spills towards the Troll field in the south at 2504 m. This corresponds with the depth of the gas-water contact, indicating that the Brent Group is filled to its capacity. Although the spill point of the Sognefjord Formation is unknown, it is believed to spill southwards into the Troll area as well. No residual hydrocarbons were recorded below any of the fluid contacts within this structure, indicating that it might be filled to its capacity (Fig. 5.24).

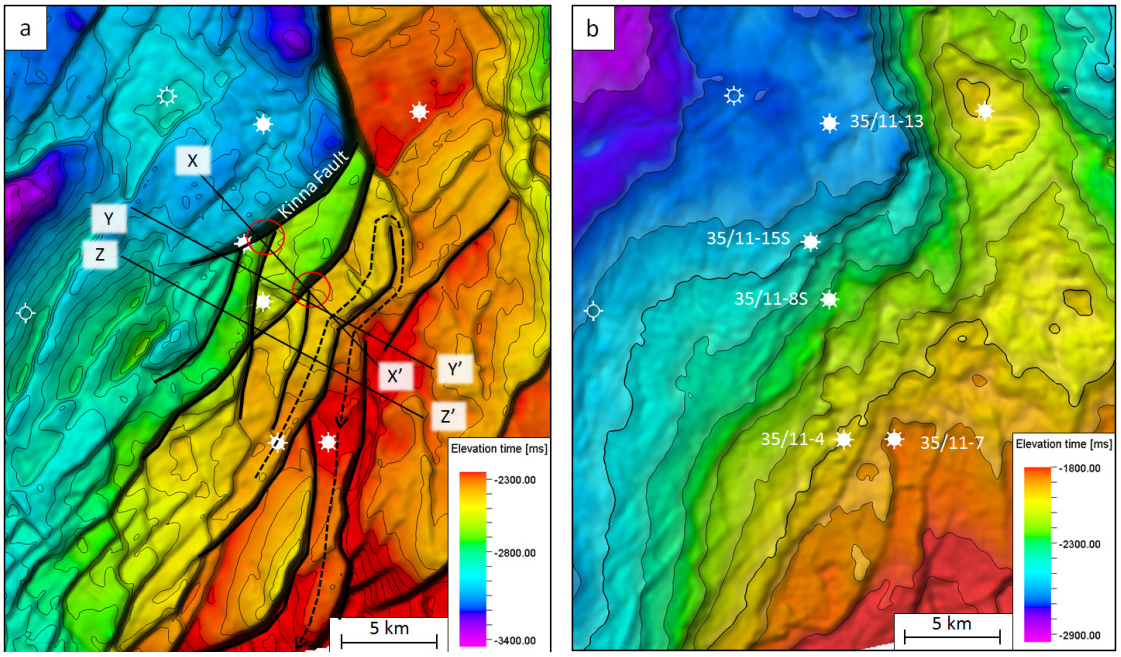

Figure 5.25: Close-up of the Farm area. **a:** Top Brent Group surface map (50 contour spacing) shows the structural configuration in the area and locations of seismic sections presented in Figure 5.26. **b:** Base Cretaceous surface map shows the unconformity between the Viking Group and the overlying Cretaceous shales. A possible migration route from 35/11-4 to 35/11-7 and further into the Troll area is marked dotted black arrows.

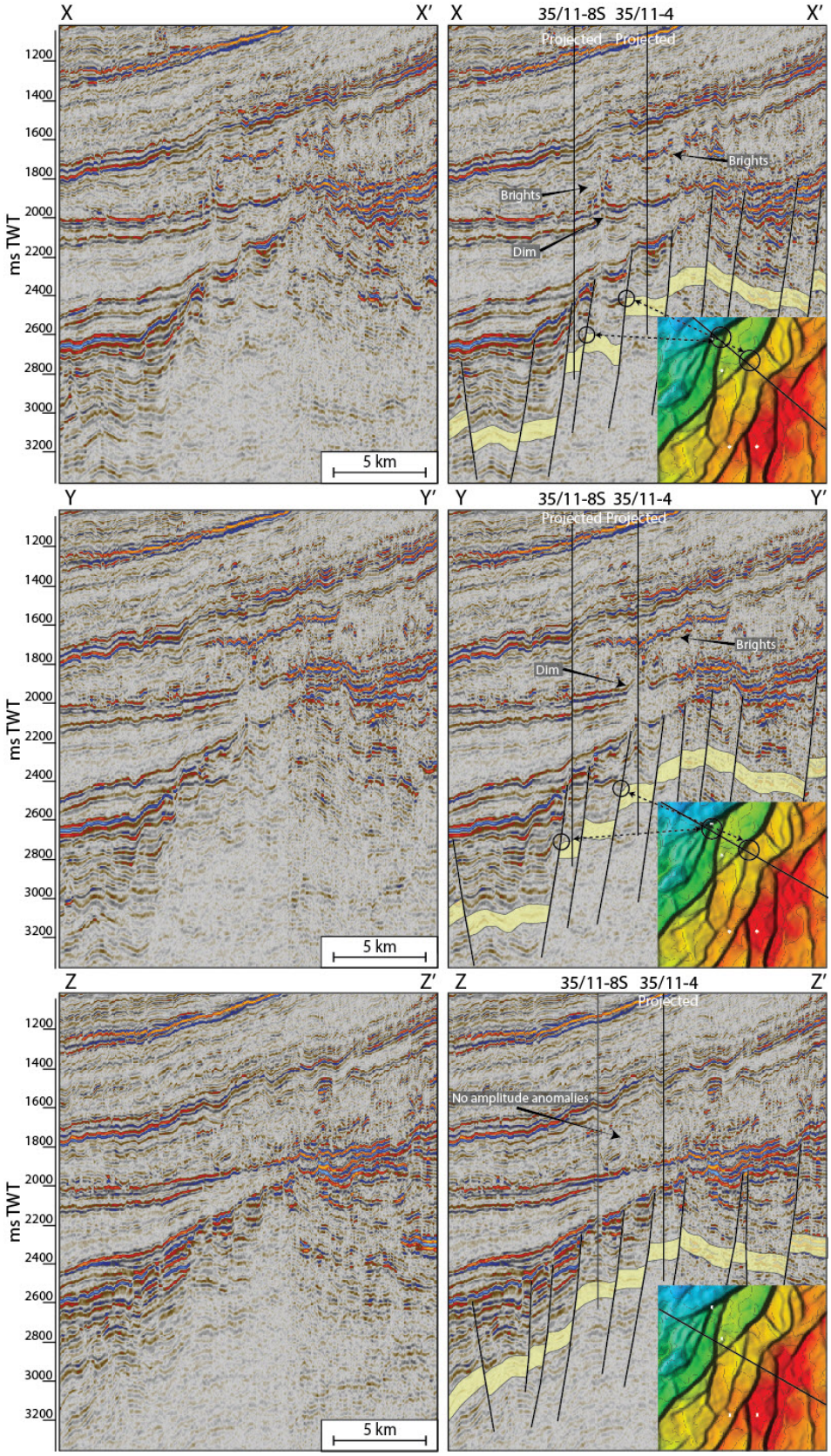

Figure 5.26: Seismic section X-X' and Y-Y' through the Fram area shows dim and brights above fault intersections, delineating the top Brent Group in both Fram H-South (35/11-8S) and Fram F-East (35/11-4). Further away from the fault intersections no strong amplitude anomalies are apparent.

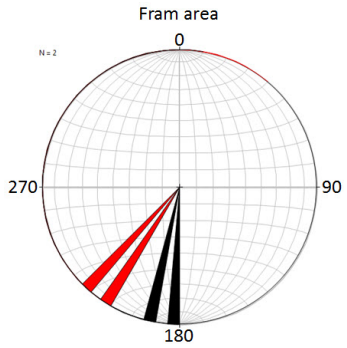

Figure 5.27: Rose diagram with the main fault trends in the Fram area. NE-SW trending faults that form fault intersections in the area is marked with red colour.

5.4.6 Summary of the Astero - Fram area

Spill points of the Sognefjord and Fensfjord Formations, including the Oxfordian turbidites could not be determined in this area. As a consequence, the uncertainty of whether these reservoirs are filled or underfilled is high. However, based on the presence of hydrocarbon shows beneath the fluid contacts, the following can be deduced:

- Astero and Fram C-West are suggested to be filled to their capacity. Although highly uncertain, Fram H-North is also suggested to be filled, based on the absence of residual hydrocarbons below the oil-water contact.
- Fram H-South is suggested to be underfilled in the upper reservoir sequence (Intra Heather Formation sst.), while the Brent Group is dry with residual hydrocarbons. Seismic anomalies (dim and brights) are observed above a fault intersection, which delineates the northern part of the structure.
- Fram F-East is suggested to be underfilled in the Brent Group, while the filling of the upper reservoir sequences are unknown. However, no residual hydrocarbons are recorded below the oil-water contacts in these sequences, suggesting that they might be filled to their capacity. Similar to Fram H-South, seismic amplitude anomalies (dim and brights) are observed above a fault intersection, which delineates the northern part of the structure.

5.5 Afrodite - B-structure

These structures reside on the Flatsfisk Slope, in the western and deepest part of the study area (Fig. 5.28a). Well 34/12-1 encountered gas in the Afrodite structure with an unknown gas-water contact, and well 35/10-2 encountered a gas column of ca. 72 m in the B-structure (Table 5.6). The gas-bearing Brent Group is highly overpressured in this area, as shown in the pressure vs depth plot in Figure 5.28b. Seismic section G-G' in Figure 5.29 displays an interpretation from the Afrodite structure in the north to the B-structure in the south, including key observations in the overburden.

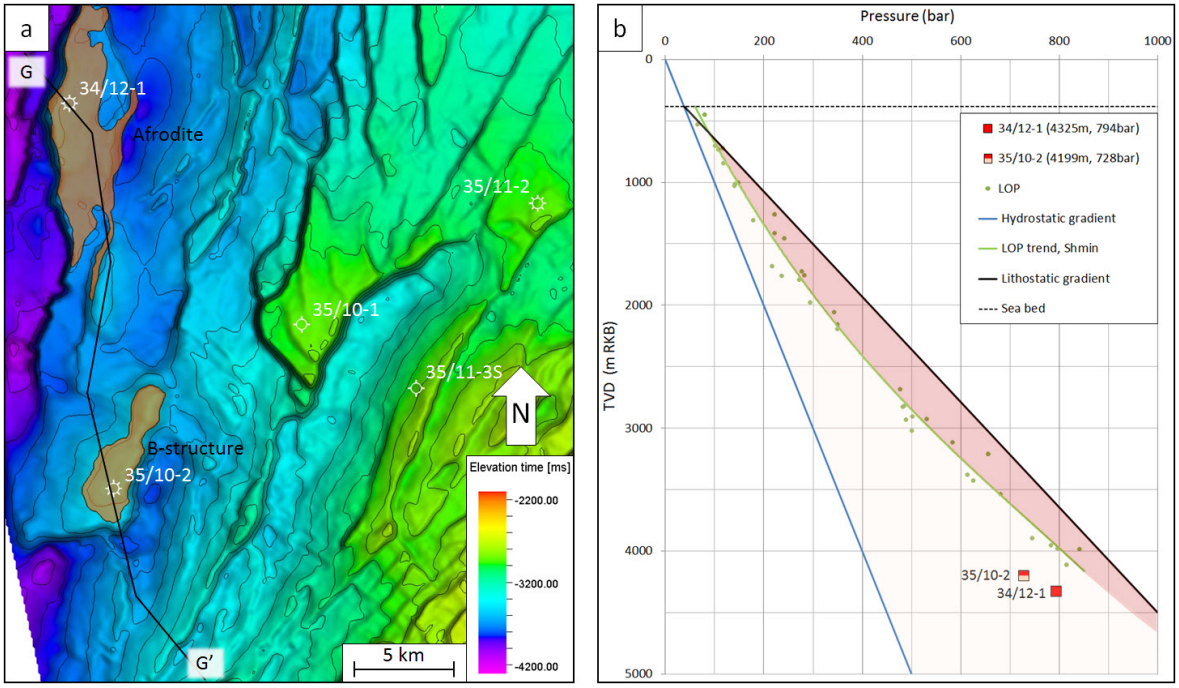

Figure 5.28: Overview of the Afrodite and B-structure. **a**: Top Brent Group surface map (100 m contour spacing) superimposed by red field outlines, based on gas-water contacts (outline of Afrodite accumulation is based on the field outline from NPD fact-maps). Black line represents the path of seismic section G-G'. **b**: Reservoir pressures in the Afrodite and B-structure presented in a pressure vs. depth plot.

Table 5.6: Summary of fluid contacts, spill points and pressure measurements close to top reservoir in the Afrodite and B-structure (note that no fluid contact were found in the Afrodite structure).

Well	GWC		Spill point		Pressure				
	TVD	TWT	TVD	TWT	TVD	Pore	Overpressure	RC	Op/LOT-Hydr
34/12-1	N/A		4482	-3710	4325	794	362	116	0.76
35/10-2	4221	-3520	4408	-3690	4199	728	308	132	0.70

Units: TVD (True Vertical Depth, m RKB); TWT (Two Way Time, ms); Pressure (bar)

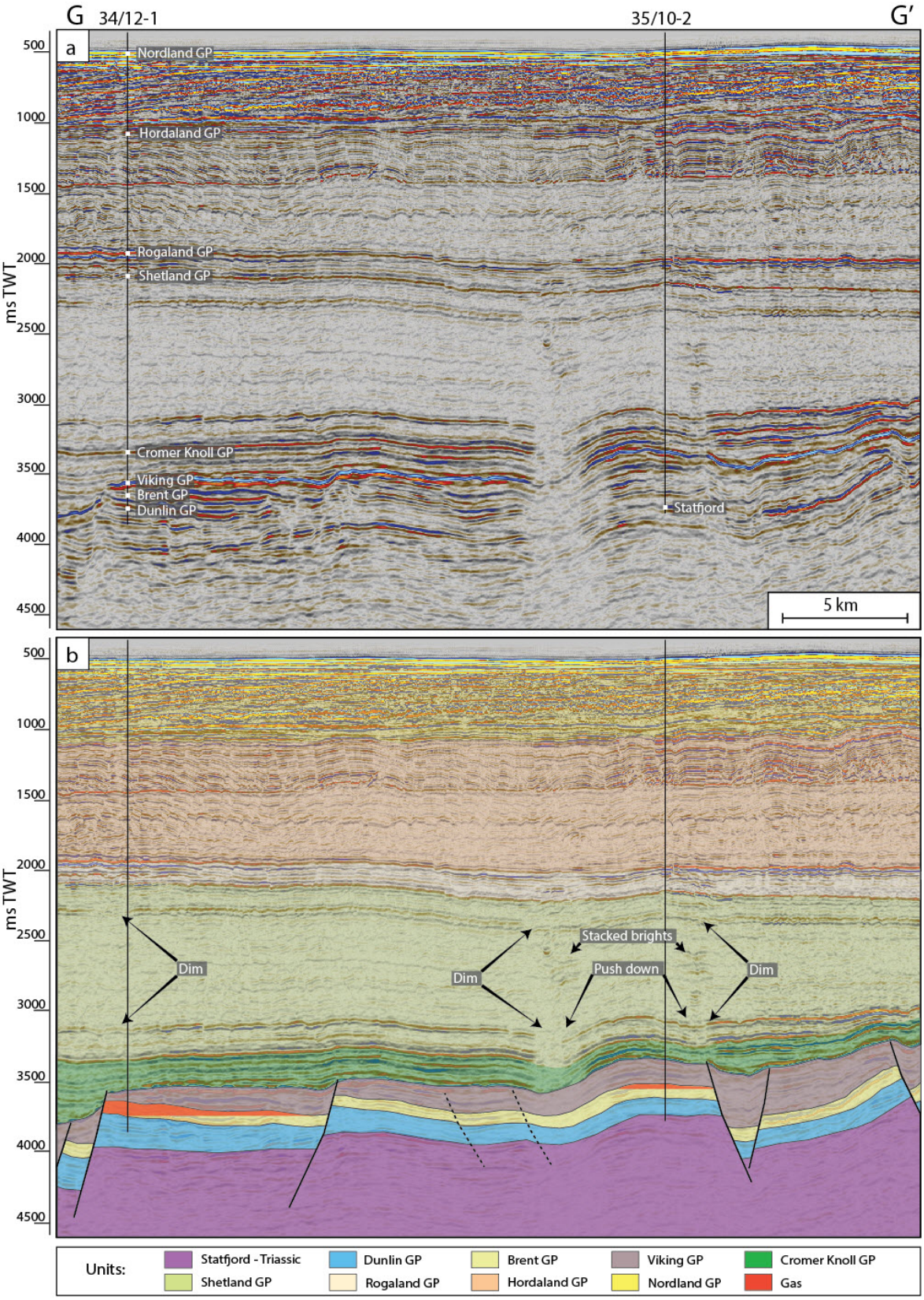

Figure 5.29: Seismic section G-G' shows an uninterpreted (**a**) and interpreted (**b**) section from N to S through the Afrodite and B-structure, including key observations in the overburden. Note the zones of reduced reflectivity over both structures and brights in vicinity of the B-structure.

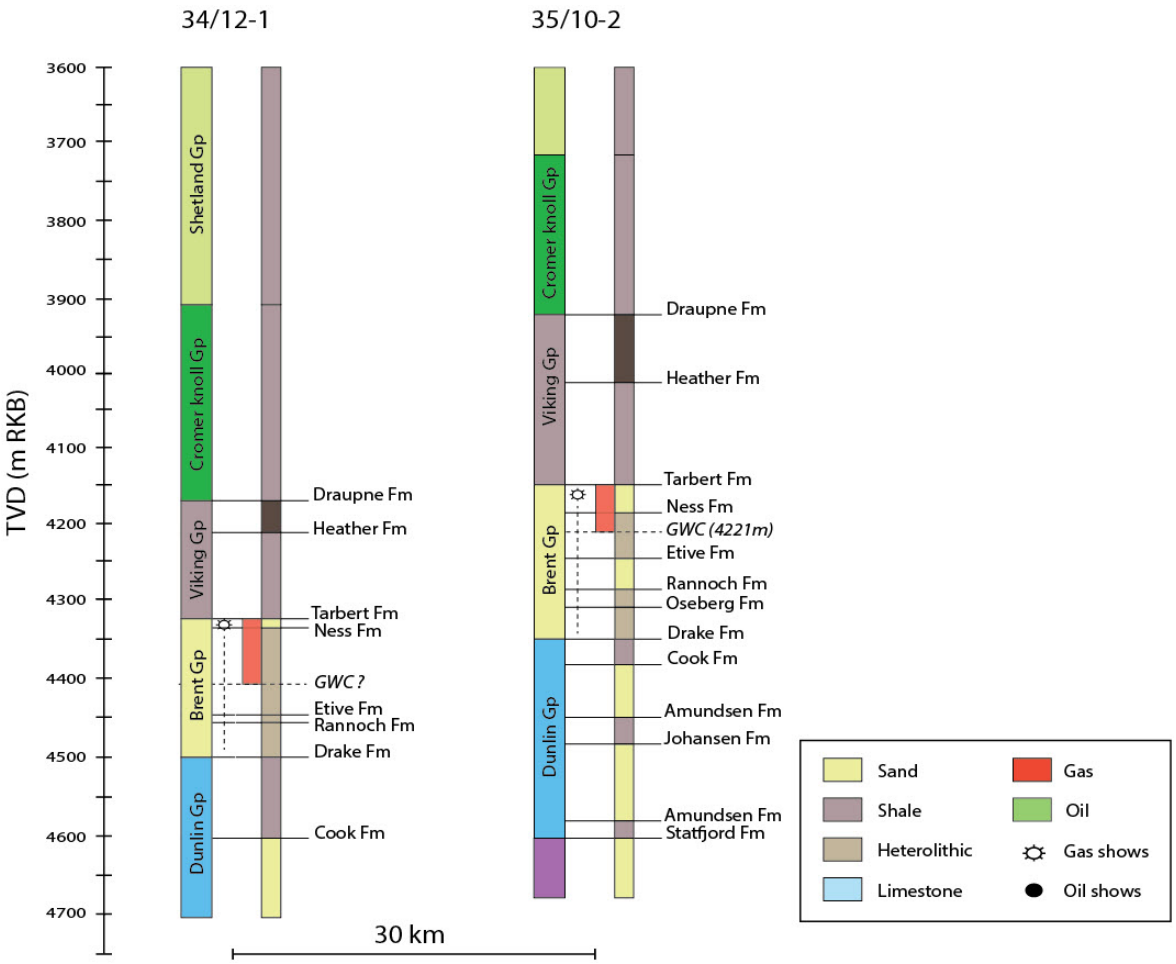

Figure 5.30: Lithological well logs corresponding to the wells in seismic section G-G', with recordings of hydrocarbon shows and fluid contacts. The gas-column in well 34/12-1 is for illustration only and should not be scaled. The gas-water contact in well 35/10-2 is based on a 72m gas-column (based on information from NPD).

5.5.1 Afrodite - 34/12-1

The Afrodite structure is an elongate horst, bound by two N-S trending normal faults, dipping to the east and west (Fig. 5.32a and 5.33). With top reservoir (Brent Group) at 4321 m and an overpressure of 362 bar, Afrodite is the deepest and highest pressured structure in the study area. The average permeability in the Brent Group is below 0,1 mD, resulting in uncertain RFT measurements and therefore uncertain identification of the gas-water contact (Table 5.6). As there is no information on the position of the gas-water contact in this structure, it is not possible to determine whether it is underfilled or not. However, according to the Norwegian Petroleum Directorate, high readings of background gas and gas peaks were recorded through the Brent Group. The Brent Group spills southwards at 4482 m towards the B-structure, as illustrated in Figure 5.32a.

A zone of reduced reflectivity (dim zone) is present in the seismic data through the Cromer Knoll and Shetland Groups, above the crest of the structure and the westerly

dipping fault (Fig. 5.29b). The lateral extent of this dim zone is displayed by an RMS amplitude map of the top Kyrre Formation reflector in Figure 5.32c. It is apparent that the area of reduced reflectivity is limited to an area of 3x3 km directly above the highest point of the structure along the westerly dipping fault plane.

5.5.2 B-structure - 35/10-2

The B-structure is a three-way fault bounded trap, confined by NE-SW, E-W and NW-SE -oriented normal faults (Fig. 5.32a and 5.33). Well 35/10-2 penetrated top reservoir at 4149 m and encountered a gas column of ca. 72 m through the Tarbert Formation and into the middle of the Ness Formation, followed by hydrocarbon shows to the base of the Brent Group. Based on this information, the gas-water contact is calculated to be located at 4221 m (Fig. 5.30). Pore pressure close to top reservoir is measured to 728 bar, which corresponds to an overpressure of 308 bar.

The structure has two possible spill points at different depths. The deepest spill point is located in the north-western part of the structure at 4408 m, where migration occurs northwards into a small rotated fault block (Fig. 5.32a). The vertical difference down to the gas-water contact is here 187 m. The second and shallowest spill point is located in the north-eastern end of the structure, at 4373 m, which is 152 m below the gas-water contact. However, this spill point is more uncertain as the Brent Group in this area is laterally juxtaposed with the Heather Formation. Residual hydrocarbons are recorded throughout the Brent Group, indicating that the structure is underfilled. Further investigation of the position of the fluid contact in this structure shows that it coincides with a fault intersection at top reservoir, bounding the south-eastern part of the structure (Fig. 5.31).

Reduced reflectivity (dim) followed by concentrated high amplitudes (brights) is observed in the Cromer Knoll and Shetland Groups, on the southern and northern flanks of the structure (Fig. 5.29b). The reflectors in the lower part of the Shetland Group down to the Viking Group in the north-eastern part of the structure are also markedly pushed down (Fig. 5.31). To display the brights in the Kyrre Formation (Shetland Group), a surface map generated from the top Kyrre reflector is lowered by -200 ms TWT, into the zone of brights. Thereby, RMS amplitude extraction of +/-15 ms TWT is processed on this surface. The extent of the bright events in the Intra Kyrre Formation (Shetland group) is displayed by the RMS amplitude map in Figure 5.32b. It is apparent that the high amplitudes are highly concentrated and limited to an area directly above the southern fault intersection where the gas-water contact terminates. The amplitude map of the top Kyrre Formation reflector in Figure 5.32c also shows an area of reduced reflectivity above the bright events.

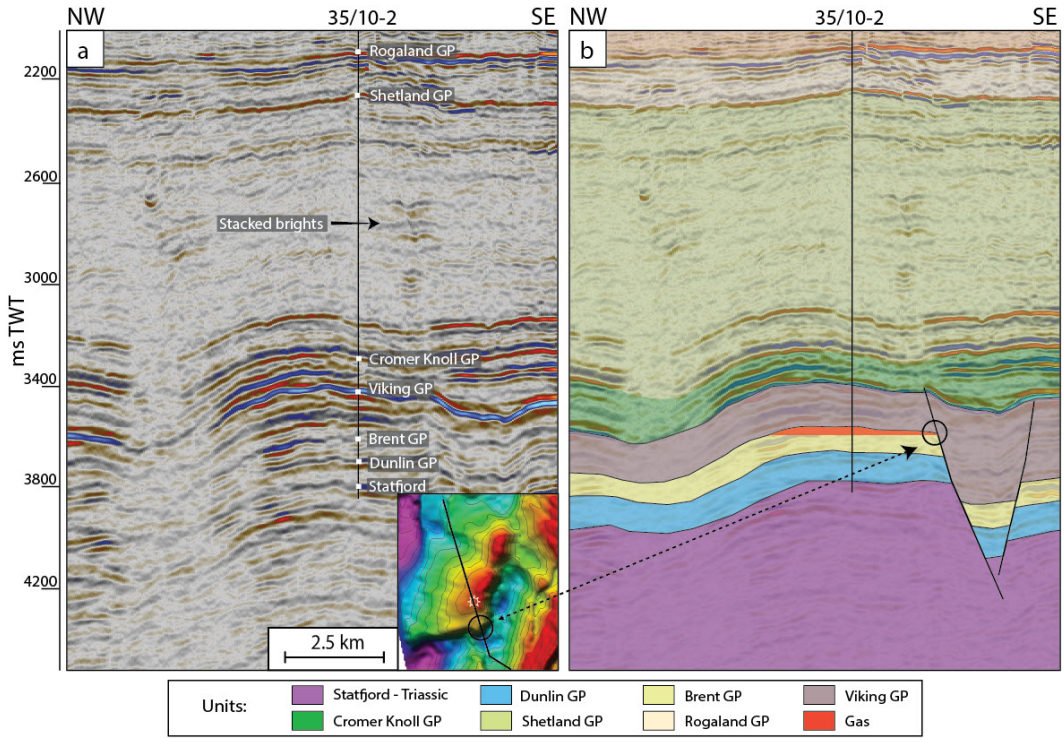

Figure 5.31: Seismic section of the B-structure, showing the depth of the gas-water contact coinciding with a fault-intersection at top reservoir.

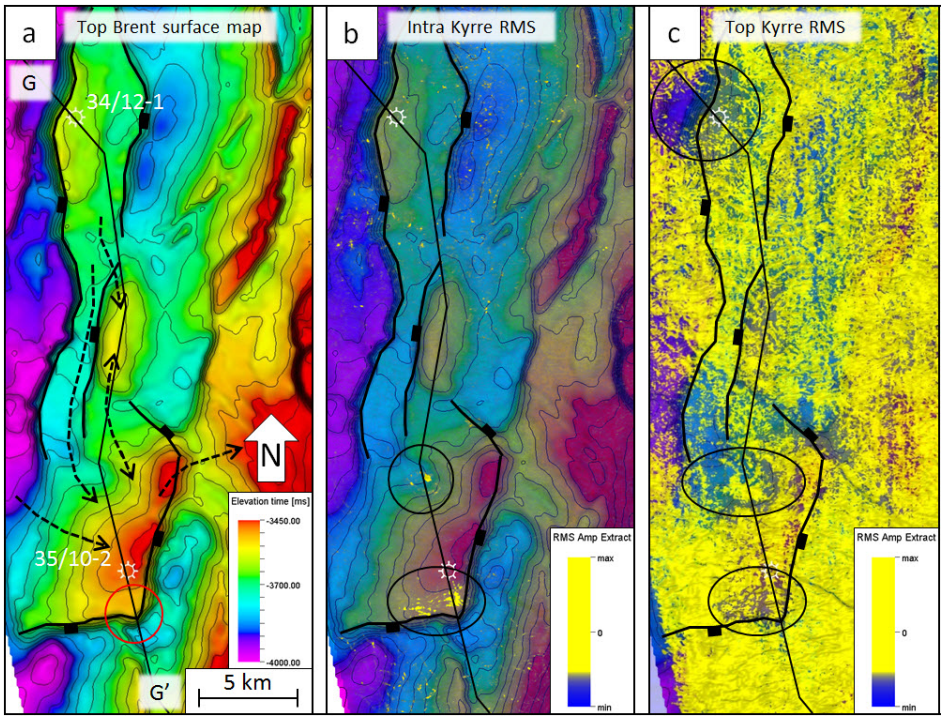

Figure 5.32: Close-up of the Afrodite and B-structure. **a**: Top Brent Group surface map (50 m contour spacing) shows the structural configuration and spill routes from Afrodite to the B-structure. **b**: Superimposed RMS amplitude map of the observed brights in the Kyrre Formation (note the increased reflectivity above the two intersecting faults confining the B-structure, marked by black circle). **c**: Superimposed RMS amplitude map of the top Kyrre Formation reflector, including outline of main faults (note the reduced reflectivity concentrated above the W-dipping fault of the Afrodite structure and above the faults of the B-structure. Reduced reflectivity is also apparent down-flank of the B-structure).

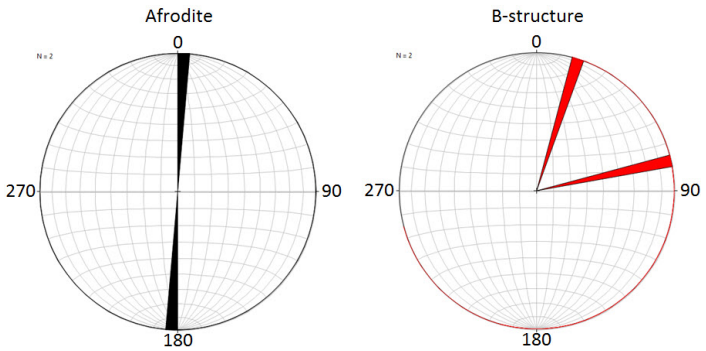

Figure 5.33: Rose diagram with the main fault trends in the Afrodite and B-structure. Note the red fault trends in the B-structure, which intersects and coincide with the gas-water contact.

5.5.3 Summary of Afrodite and B-structure

Based on analysis of spill-points and fluid contacts in the Afrodite and B-structure, the following can be deduced:

- The fluid contact in the Afrodite structure is unknown and it is not possible to determine whether the structure is filled to its structural capacity or not. A 3x3km zone of reduced reflectivity (dim) is observed above the westerly dipping fault bounding the structure.
- The B-structure is most likely underfilled, with the gas-water contact coinciding with a fault intersection bounding the south-eastern part of the structure. Bright amplitudes is observed in the overburden above the fault intersection. These observations are consistent with the work conducted by Teige & Hermanrud (2004), although they did not report anything on the brights observed in the Shetland Group.

5.6 Dry structures

Three dry structures that contain residual hydrocarbons are analysed in this study. These are not formally named by the Norwegian Petroleum Directorate, thus they are in this study named according to their respective exploration well. The overview map in 5.34a displays the location of each dry structure, represented by black outlines, as well as the path of seismic section I-I' and H-H'. Spill points and pressures in these structures are listed in Table 5.7. All dry structures are overpressured, whereas two of them, namely 35/4-1 and 35/10-1 plot close to the best fit leak-off pressure line (Fig. 5.34b).

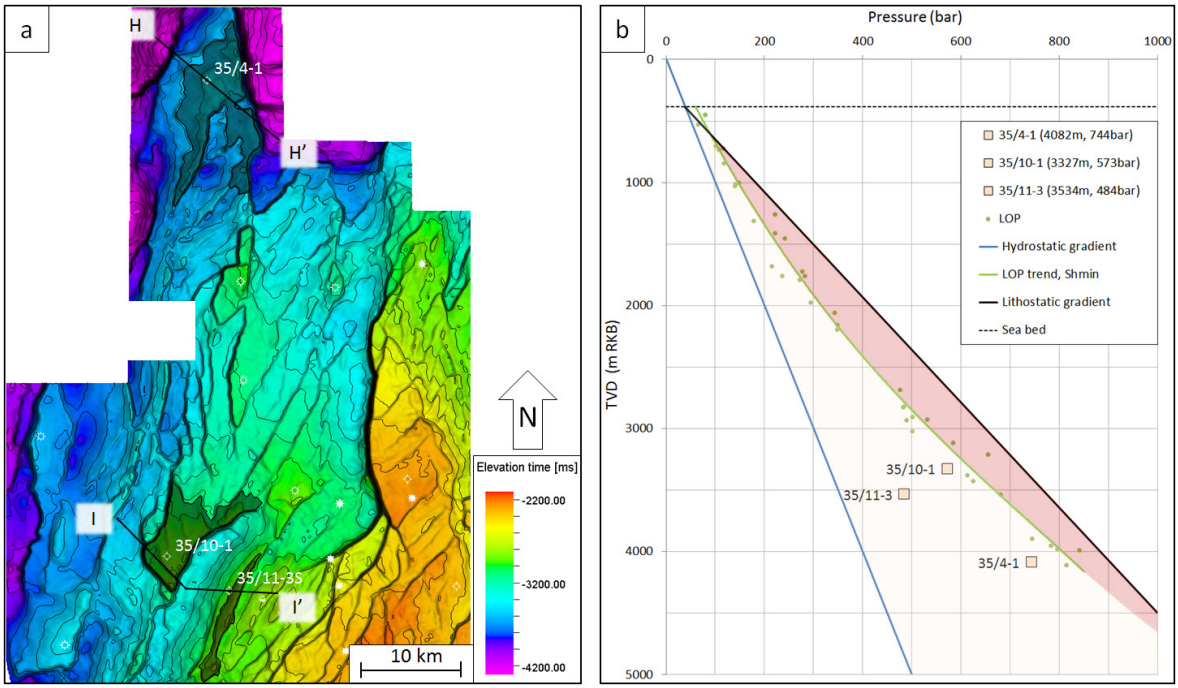

Figure 5.34: Overview of the dry structures in the study area. **a**: Top Brent surface map superimposed by black field outlines, based on the structural capacity of the dry structures. Black lines represents the path of seismic section H-H' and I-I', in the northern and southern area, respectively. **b**: Reservoir pressures in the dry structures presented in a pressure vs. depth plot (note the highly overpressured 35/4-1 and 35/10-1 plotting close to the best fit leak-off line.

Table 5.7: Summary of spill points and pressure measurements close to top reservoir in the dry structures.

Well	Spill point		Pressure				
	TVD	TWT	TVD	Pore	Overpressure	RC	Op/LOT-Hydr
35/4-1	4300	-3600	4028	744	341	86	0.80
35/10-1	3558	-3075	3327	573	240	47	0.84
35/11-3S	3355	-2925	3534	484	131	196	0.40

Units: TVD (True Vertical Depth, m RKB); TWT (Two Way Time, ms); Pressure (bar)

5.6.1 35/4-1

Well 35/4-1 was drilled on the Marflo Spur, targeting a large Middle Jurassic horst structure located between the Viking Graben and Sogn Graben. The structure is bound by two major normal faults (Fig. 5.36a). The first is the deeply seated, E-dipping Sogn Graben fault, which propagates NW-SE and links into the Tampen Spur to the north. The second major fault is a W-dipping, NE-SW-trending fault, separating the Marflo Spur from the deeper Mardoll sub-basin, which is part of the Northern Viking Graben to the west. The latter fault intersects with the Sogn Graben fault to the north and dies out, forming a transition between these major graben systems. The characteristic pointy geomorphology of the Marflo Spur is a result of this fault intersection. Smaller, ENE-WSW trending faults are disecting the top of the structure (Fig. 5.36a). The fault trends in structure 35/4-1 are displayed in the rose diagram in Figure 5.37.

While drilling, shows were recorded from the middle of the Hordaland Group through the entire underlying section and into the Statfjord Formation, with notably high gas peaks of up to 31% within the Shetland Group (Fig. 5.35c). The Brent Group equivalent was encountered at 4079 m but proved to contain mostly silts and very little sand of reservoir quality. High pressures were recorded from the upper part of Cretaceous (Shetland Group) to TD, with a maximum overpressure of 341 bar in the Brent Group (Table 5.7).

The seismic data quality in this area is very poor, thus the interpretation of this structure is highly uncertain. The seismic section H-H' in Figure 5.35 is oriented NW-SE over the structure and shows several amplitude anomalies in the overburden. Two distinct brights with soft responses (blue reflectors) are observed directly above the structure in the Kyrre Formation (Shetland Group), indicated in Figure 5.35b.

Chaotic reflection patterns and reduced reflectivity is concentrated vertically above the structure from the top of the Viking Group into the Hordaland Group. This might resemble a seismic chimney, as illustrated in Figure 5.35b. Figure 5.36b displays an RMS amplitude map of the top of the Cromer Knoll Group (top Rødby Formation) reflector, illustrating the extent of the reduced reflectivity in the deeper parts. The extent of the brights in the Kyrre Formation is shown with an attribute map in Figure 5.36c.

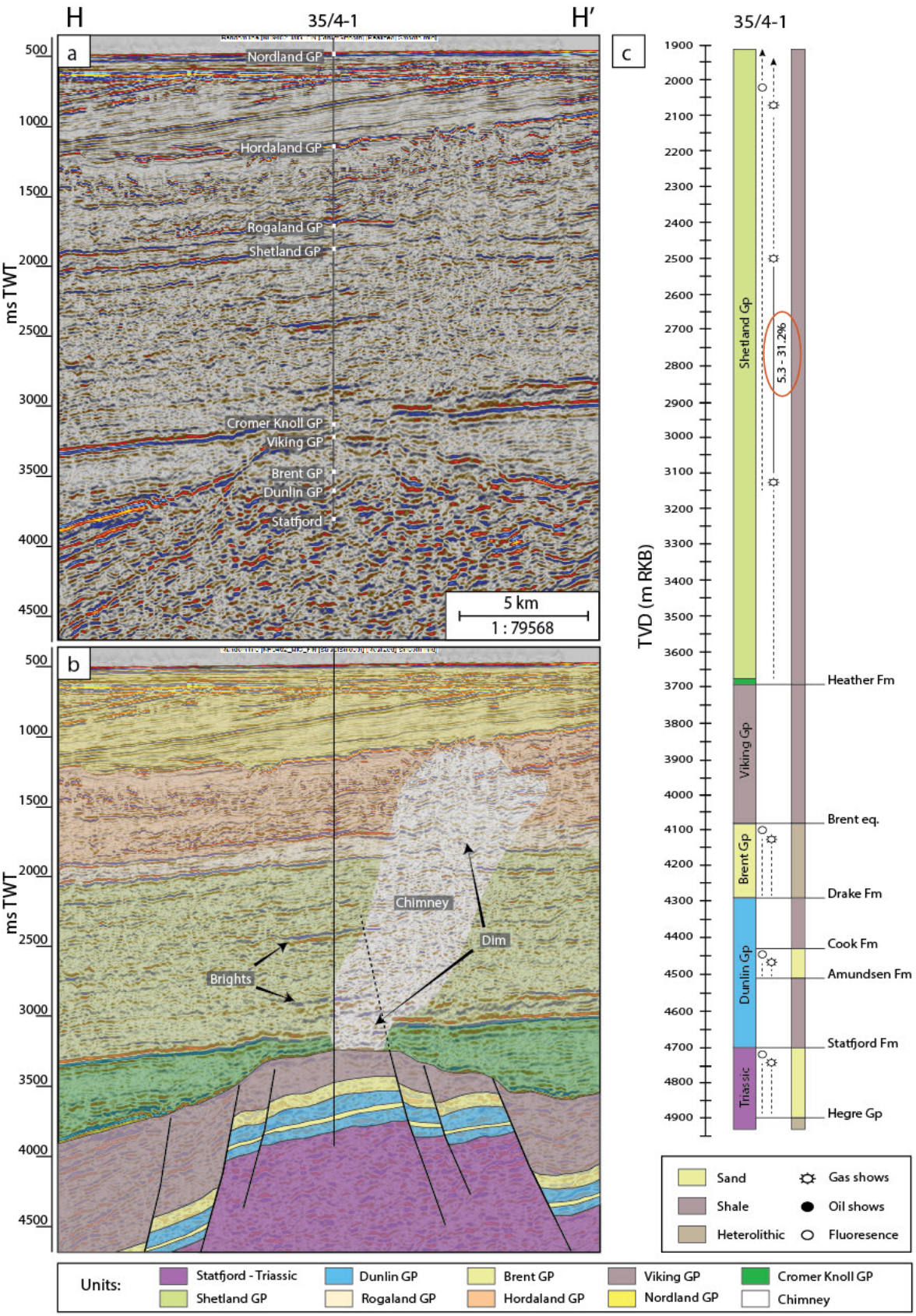

Figure 5.35: Seismic section H-H' shows an uninterpreted (**a**) and interpreted (**b**) version from NW to SE through the dry 35/4-1 structure. Note the large area of reduced and chaotic reflectivity (chimney) and brights above the structure. **c**: Lithological well log of well 35/4-1 with recordings of hydrocarbon shows. Note the high gas reading in the Shetland Group.

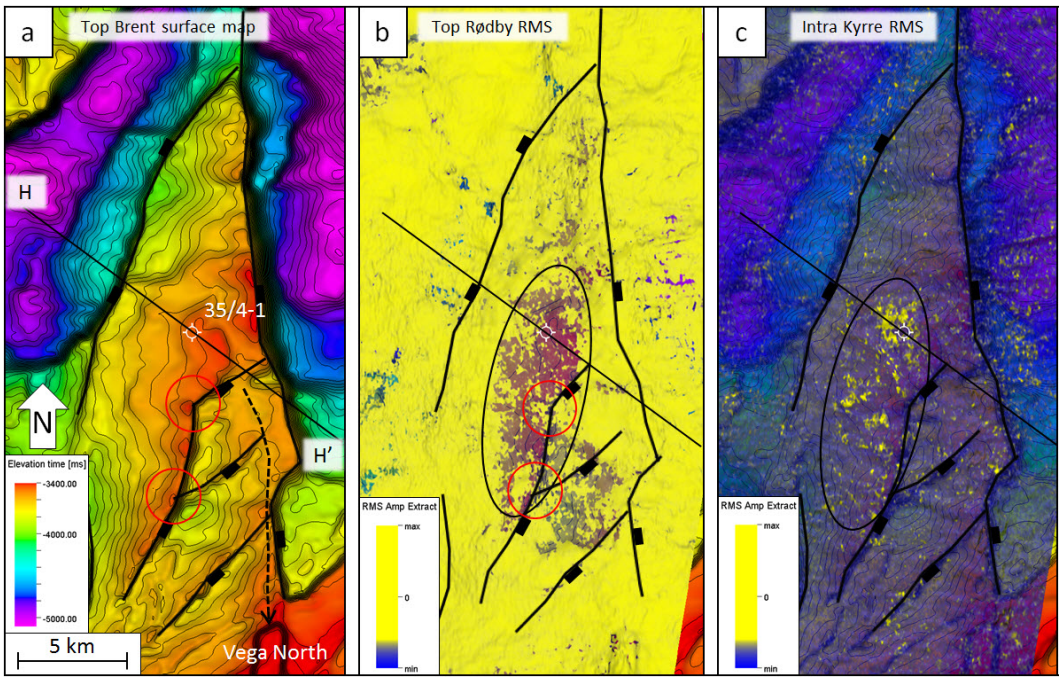

Figure 5.36: Close-up of structure 35/4-1 and outlines of main faults. **a**: Top Brent surface map (50 m contour spacing) shows the structural configuration and spill route towards Vega North. **b**: Superimposed RMS amplitude map of the top Rødby reflector (note the extent of the reduced reflectivity is limited the crest of the structure). **c**: Superimposed RMS amplitude map of brights Intra Kyrre Formation (-2400 ms TWT).

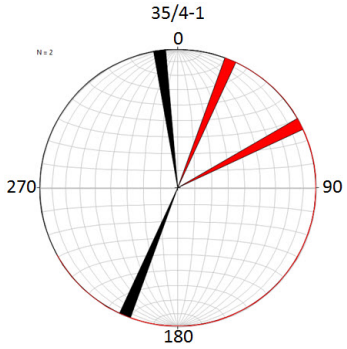

Figure 5.37: Rose diagram with the main fault trends in structure 35/4-1. Faults that intersects at the top of the structure is coloured red.

5.6.2 Summary of 35/4-1

- Residual hydrocarbons in the water bearing Jurassic reservoir sequences.
- Recordings of shows, high gas readings and high pressures throughout the overburden.
- The wide seismic chimney above the crest of the structure might be related to vertical migration of gas (gas chimney), which causes disturbed seismic signals.
- Two brights with negative amplitudes (blue reflectors) above the structure might indicate small, local accumulations of gas within the Shetland Group.

5.6.3 35/10-1

Well 35/10-1 targeted a relatively large horst-structure, located south of the Vega area. High displacement NE-SW and NW-SE trending normal faults forms a three way structural closure to the south and a dip closure to the north (Fig. 5.40a and 5.41). The well encountered a 2 m thick oil bearing sand in the Lista Formation, followed by oil shows in the Jorsalfare Formation, Brent Group and Cook Formation (Fig. 5.39c).

The Brent Group is highly overpressured, by a magnitude of 240 bar (Table 5.7). The structure spills north-east at 3558 m towards the lower pressured Vega South field (35/11-2), as illustrated by the stippled black line in Figure 5.40a.

Concentrated, stacked brights are observed in the Shetland Group (Intra Kyrre Formation), directly above the crest of the structure and in the vicinity of a fault intersection (Fig. 5.39b). These stacked brights are overlain by a slight push-down (velocity decrease) and dimming of the top Kyrre Formation reflector. Reflectors below this zone of brights are also markedly affected, showing reduced reflectivity and a slight push-down of the Brent and Dunlin Groups reflectors (Fig. 5.39a).

Figure 5.40b displays and RMS attribute map of the bright in the Kyrre Formation. It becomes evident that this bright is located above the crest of the structure and in the vicinity of two intersecting faults, concentrated in an area of 1x1 km. Figure 5.40c shows the extent of the dimming feature of the top Kyrre Formation reflector. This event is concentrated above the brights in a larger area, of ca. 2x2 km.

5.6.4 35/11-3S

Well 35/11-3S was spudded in a rotated fault block, located east of structure 35/10-1. The structure is formed by an easterly dipping, NE-SW-striking normal fault, forming a fault-bounded dip closure (Fig. 5.40a and 5.41). Unlike well 35/10-1, well 35/11-3S did not encounter oil in the Lista Formation, however, strong oil shows were recorded in Early Cretaceous limestones (Rødby and Mime Formations) and in a 15m thick silty Sognefjord Formation. Gas and oil shows were also recorded in the Brent Group (Fig. 5.39c).

Based on organic geochemical analysis, the Draupne Formation shales was found to be immature, while the deeper Heather formation has reached sufficient thermal maturity and probably expelled some of its potential. The Brent Group is overpressured by 131 bar, which is significantly lower than the other dry structures (Table 5.7).

As mentioned previously in chapter 5.1.3, the higher pressured Vega South structure spills towards 35/11-3S at 3550 m. Furthermore, this structure is interpreted to spill from the southern part at 3355 m, into an adjacent rotated fault block to the east, as illustrated by the stippled black line in Figure 5.40a. This fault block was proven to be gas and oil bearing by well 35/11-5. Moreover, if the structure spills at 3355 m, there might be an up-dip potential ca. 100 m laterally from the well location. This is illustrated in Figure 5.38, where the apparent position of well 35/11-3S is located outside the structural closure.

Except for a slight dim of the top Kyrre Formation reflector, no amplitude anomalies are observed in the overburden above this structure (Fig. 5.40c)

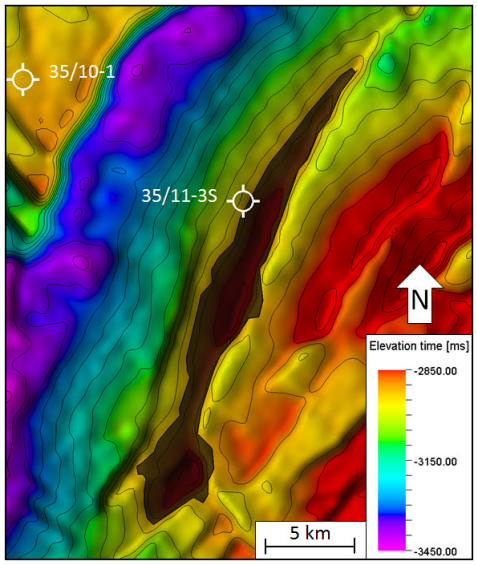

Figure 5.38: Top Brent Group surface map (50 contour spacing) with suggested structural closure of structure 35/11-3S, based on eastward fill-spill scenario. Note that the well is drilled outside the closure.

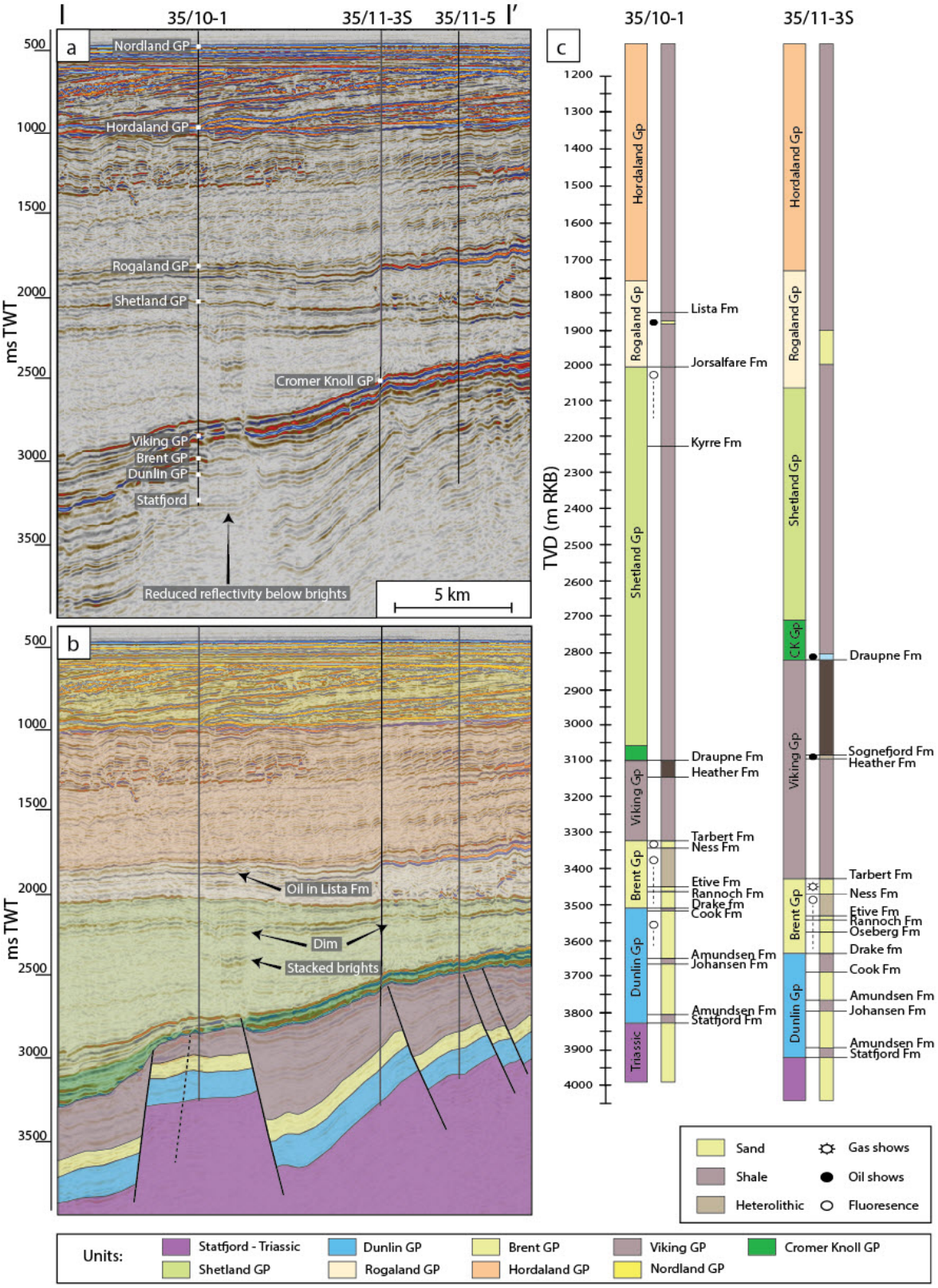

Figure 5.39: Seismic section I-I' shows an uninterpreted (**a**) and interpreted (**b**) version from NW to SE through the dry structures 35/10-1 and 35/11-3S, including the hydrocarbon filled structure 35/11-5. Not the increased reflectivity (stacked brights) locally above structure 35/10-1 in the Kyrre Formation and the dimming of the top Kyrre Formation reflector directly above this event and above structure 35/11-3S. **c**: Lithological well logs of well 35/10-1 and 35/11-3S with recordings of shows.

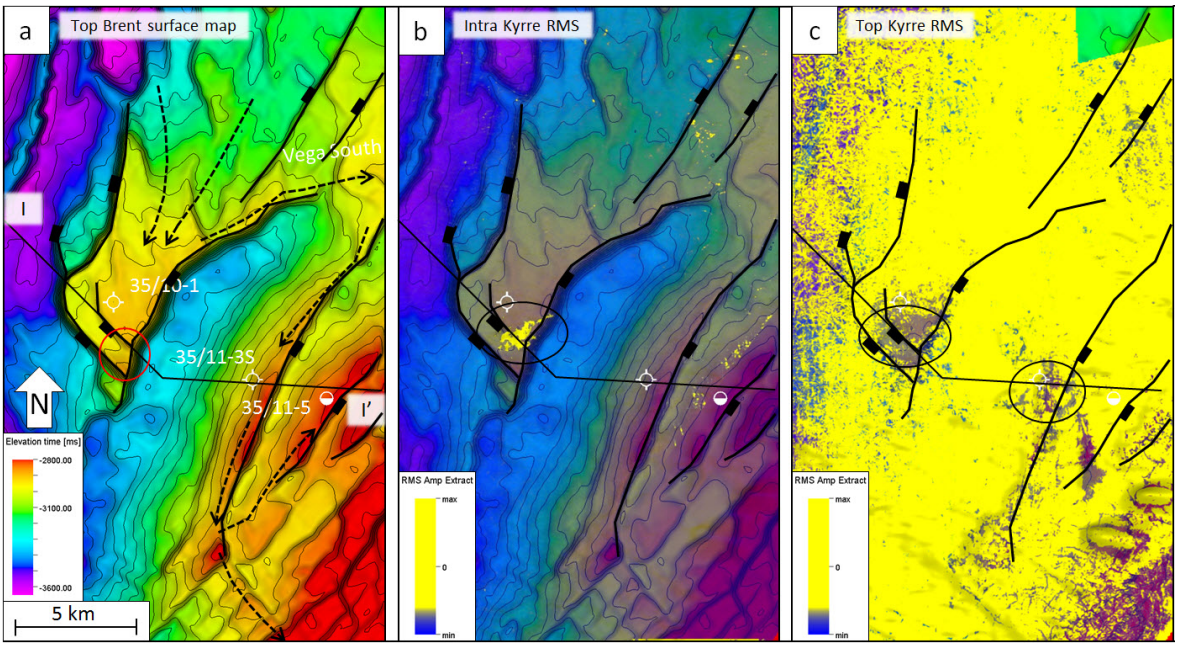

Figure 5.40: Close-up of the dry south area. **a**: Top Brent Group surface map (50 m contour spacing) shows the structural configuration and spill routes from 35/10-1 to Vega South, and further into 35/11-3S. The latter structure has two possible spill directions. One is north-eastwards into the hydrocarbon-bearing 35/11-5 structure, while the other is south-east towards the Fram and Troll area. **b**: Superimposed RMS amplitude map of the observed brights in the Kyrre Formation (note the increased reflectivity above the crest of structure 35/10-1, marked by black circle). **c**: Superimposed RMS amplitude map of the top Kyrre Formation reflector, including outline of main faults (note the reduced reflectivity above the crest of structure 35/10-1 and 35/11-3S).

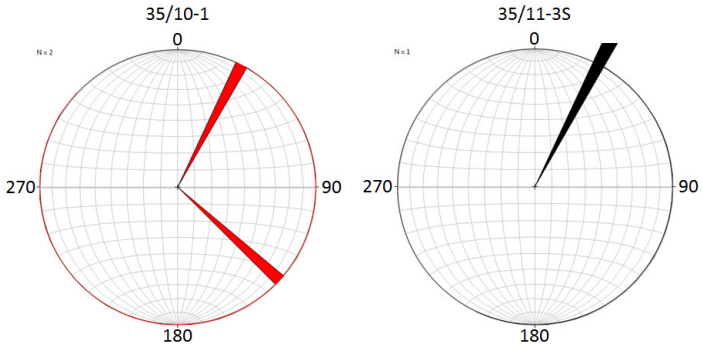

Figure 5.41: Rose diagram with the main fault trends in structure 35/10-1. Faults that intersects at the top of the structure is coloured red.

5.6.5 Summary of 35/10-1

- Oil shows recorded in the water bearing Brent Group and gas shows in the Cook Formation.
- Oil in a 2m sandstone in the Lista Formation (Rogaland Group) and oil shows in the Jorsalfare Formation (Shetland Group), directly above the structure.
- Stacked brights with soft responses in the Kyrre Formation (Shetland Group), concentrated above a fault intersection.
- Dim zone in the top Kyrre Formation reflector (top Shetland Group), directly above the brights.

5.6.6 Summary of 35/11-3S

- Mature Heather Formation
- Shows recorded in the Mime (Lower Cretaceous), Sognefjord Formation and in the Brent Group
- Reduced reflectivity of the top Kyrre reflector observed above the structure.
- Suggested structural closure is located above the well location (might be an up-dip potential).

6 Discussion

The purpose of this study was to investigate the controls on hydrocarbon column-heights in the north-eastern Viking Graben. A large variety of traps with different pressure regimes, fluid contacts and hydrocarbon types have been identified with 3-D seismic data and well data. This chapter is divided into five sections. First a discussion on migration routes and fluid contacts, followed by an analysis on the oil and gas distribution in the area. Further on, observations (e.g. pressures, fault orientations and seismic attributes) that might characterize underfilled and dry traps will be addressed. This is vital for the next section, where the causes for leakage will be discussed. Finally, a discussion on of to what extent whether these results can be helpful in exploration and prospect evaluation is included.

The previous analyses of the location of fluid contacts and hydrocarbon shows relative to the mapped spill points in 13 hydrocarbon bearing structures, suggest that at least four structures are underfilled, of which one also comprises a dry reservoir sequence (Table 6.1). Five out of 13 structures are suggested to be filled to their structural capacity, whereas the column heights relative to the spill points of the last four hydrocarbon bearing structures are unknown. The remaining three structures are known to be dry with residual hydrocarbons in the Brent reservoir. In total, there are at least seven of 16 structures in the study area of which hydrocarbon columns have been reduced or lost. The colour coding in Table 6.1 will be used later in this chapter to distinguish the different types of structures.

Table 6.1: Summary of observations in the study area

Structure	Well	Type	HC	Brent pressure
Vega North	35/8-1	Underfilled (B)	Gas	Overpressured
Vega Central	35/8-2	Filled (B)	Gas	Overpressured
Vega South	35/11-2	Filled (B)	Gas	Overpressured
Aurora	35/8-3	N/A (B, H)	Gas	Overpressured
Titan	35/9-6S	N/A (D, B, H)	Gas/oil	Hydrostatic
Grosbeak	35/12-2	Filled (B) / NA (F, S)	Gas/oil	Hydrostatic
Astero	35/11-13	Filled (H)	Gas/oil	Hydrostatic
Fram H-North	35/11-15S	N/A (H)	Gas/oil	Hydrostatic
Fram H-South	35/11-8S	Underfilled (H) / dry w/shows (B)	Gas/oil	Hydrostatic
Fram F-East	35/11-4	Underfilled (B) / NA (F, S)	Gas/oil	Hydrostatic
Fram C-West	35/11-7	Filled (B, S)	Gas/oil	Hydrostatic
Afrodite	34/12-1	N/A (B)	Gas	Overpressured
B-structure	35/10-2	Underfilled (B)	Gas	Overpressured
	35/4-1	Dry w/shows (B)	-	Overpressured
	35/10-1	Dry w/shows (B)	-	Overpressured
	35/11-3S	Dry w/shows (B)	-	Overpressured

D (Dunlin Gp); B (Brent Gp); H (Heather Fm sst.); F (Fensfjord Fm); S (Sognefjord Fm)

6.1 Spill routes, fluid contacts and pressure regimes

The organic rich Upper Jurassic shales, which are presented by the Draupne and Heather Formations, are at present time mature and even over-mature in the deep parts of the Viking and Sogn Graben (Goff, 1983). Based on a transition ratio of 0.3, which is assumed to be the upper limit for expulsion of oil, Hermanrud *et al.* (1991) suggested that the approximate location of the oil window in this area is between 3400 m and 4500 m. Below this depth, generation of gas and cracking of oil into gas will initiate (Goff, 1983). Based on simple depth conversion from wells, the approximate extent of the oil window of the Upper Jurassic Draupne and Heather Formations in the area is outlined with white colour on the Base Cretaceous time map in Figure 6.1a. Due to the thick Upper Jurassic sequences in this area, the oil-window covers large parts of the study area. Furthermore, as the Heather Formation is deeper buried than the Draupne Formation, these are capable of generating both oil and gas in some areas (outlined with red colour in Figure 6.1a).

From the source rock map in Figure 6.1a, it is evident that accumulation of hydrocarbons in the shallow situated traps in the study area is dependent on successful migration from the deep parts of the Viking Graben and/or Sogn Graben. Numerous discoveries towards the basin flanks, namely the Fram fields on the shallow part of the Lomre Terrace and the Troll field on the Horda Platform, demonstrate that migration towards these areas has been efficient. Moreover, several investigated structures, both in the deep and shallow areas, are filled to their structural capacity. Also, in most dry and underfilled structures, residual hydrocarbons are recorded in the water-bearing parts of the reservoirs. This may further imply that supply of hydrocarbons is not a significant restricting factor on hydrocarbon column heights in the study area.

As part of explaining the present day fluid contacts, analysis of fill-spill routes between the structures will be conducted in this section. Suggested spill-routes between the studied structures are marked with dotted white lines in Figure 6.1b, and presented with interpreted sections in Figure 6.2, 6.3 and 6.4. These routes are selected to illustrate the fluid contacts relative to the structural spill points throughout the study area. Additional migration routes in the area are indicated with black arrows in Figure 6.1b. In general, a regional drainage pattern from the Viking Graben in the west and Sogn Graben in the north, towards the Fram area in the south-east is apparent. Further migration from the Fram area seems to be directed towards the Troll field in the south. However, this cannot be confirmed by the present data set. Water gradients within the studied reservoirs are displayed in Figure 6.1c. Their implications on fluid flow and migration will also be discussed in this section.

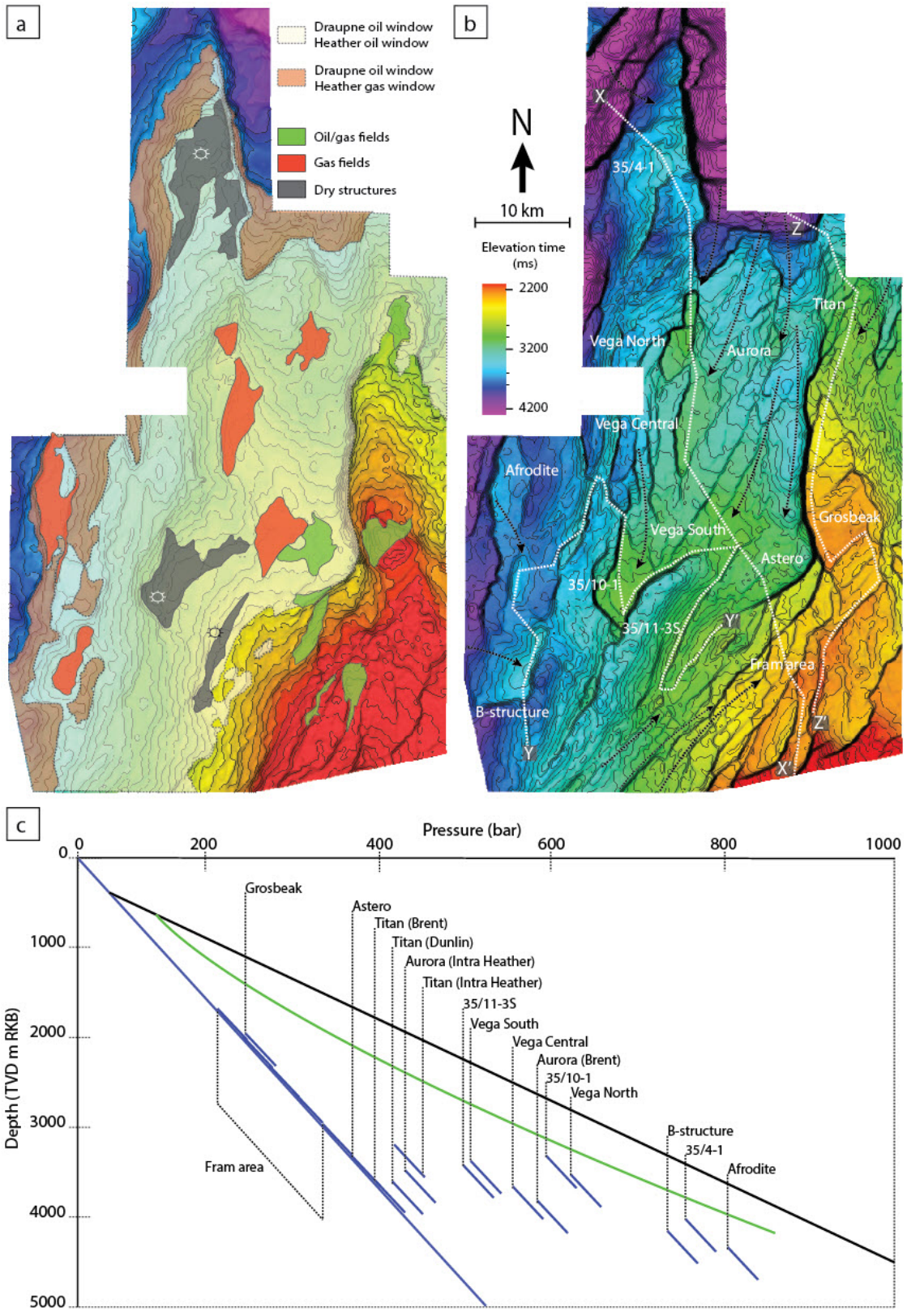

Figure 6.1: a: Regional Base Cretaceous surface map with approximate location of the oil window of the Draupne and Heather Formation (white outline). The red outline represents the area where the Draupne Foramtion is oil generating and the Heather Foramtion is gas generating. Combined these intervals stretches from 3400 - 4500 m depth. **b:** Regional Top Brent Group surface map with suggested migration routes. Suggested fill-spill routes: X-X', Y-Y' and Z-Z', between the studied structures are shown with dotted white lines. Interpreted sections through these routes are shown in Figure 6.2, 6.3 and 6.4. **c:** Pressure vs. depth plot with water gradients from all the investigated structures in the study area. A general observation is that the water gradients of the deep overpressured structures are separated, while the shallower structures are close to hydrostatic pressured.

6.1.1 Fill-spill route X-X'

Section X-X' (Fig. 6.2) presents a NW-SE migration route from the Viking/Sogn Graben, through 35/4-1, Vega North, Vega Central and Vega South. Although not part of the migration route, the Fram area is here included for illustration of reservoir juxtaposition and fluid contacts. A transition from highly overpressured gas-bearing reservoirs in the deep areas to normally pressured oil- and gas-bearing reservoirs in the shallow areas is evident in this section. All the overpressured structures along this section are located within the oil window, implying that local source rocks as well as migration from distal sources in the north, east and west may charge the Middle Jurassic Brent Group reservoirs. The shallow, normally pressured structures are located up-dip from the oil window, which indicates that migration must have occurred from distant sources.

Overpressured region

Dry structure 35/4-1 is situated in the lower part of the oil window, indicating that supply of oil and gas to the Brent Group reservoir should be sufficient. However, only residual hydrocarbons were encountered in this structure, suggesting that leakage has occurred. The structure forms a relative large closure, which is capable of holding large volumes. As no Upper Jurassic or Cretaceous sands have been recorded in this area, leakage is suggested to have occurred vertically. This is also supported by seismic observations, which will be discussed later.

Vega North is most likely charged from adjacent, down-faulted Draupne shales, juxtaposed to the Brent Group or from the Sogn Graben in the north. Hydrocarbon charge into Vega North should therefore be more than adequate to fill the structure to its structural capacity. However, as there is a large vertical distance from the gas-water contact to the mapped spill point, it is inferred that this structure is underfilled. The gas-water contact in the Vega North structure was found to coincide with a fault intersection (Fig. 5.6 in section 5.5.1). Furthermore, seismic amplitude anomalies were observed directly above this location. This might indicate that the hydrocarbon column height in this structure is controlled by vertical leakage through this very fault intersection. As section X-X' runs through the very crest of Vega North, this fault intersection is not displayed in Figure 6.2.

A 40 m thick Intra Heather Formation sand was recorded in the upper part of the Viking Group in this structure, of which the lateral extent is unknown due to the few number of wells in the area. If this sand is juxtaposed with the Brent Group reservoir in a favourable position, it could explain the underfilling of the structure. However, as residual hydrocarbons were recorded below the gas-water contact down to the base of the Brent Group, this presumably means that the structure previously contained

a much larger hydrocarbon column. A scenario were the Intra Heather Formation sand caused the underfilling is therefore unlikely, as this would probably not allow for accumulation down the the base of the Brent Group.

Further spill from Vega North is directed into the lower pressured Vega Central. The gas-water contact is here located at the same depth as the structural spill point, which indicates that Vega Central is filled to its capacity. Further migration from Vega Central is directed into Vega South, which also, based on the depth of the gas-water contact and mapped spill point, is suggested to be filled to its structural capacity. Although the top of the Draupne Formation is located shallower than the suggested oil window in this area (Fig. 6.2a), the organic rich part of the more deeply buried Heather Formation could potentially function as a proximal source. As for Vega South, the penetrated source intervals in the Draupne and Heather Formations were immature to marginally mature, and certainly less mature than the sampled petroleum in the Brent Group (well 35/11-2). This suggests that hydrocarbons in Vega South have migrated from areas down-dip of the structure and from distant sources. Aside from a fill-spill route from Vega North, suggested migration routes are indicated with black arrows in Figure 6.1b. In section X-X', the apparent fill-spill route terminates at Vega South. Further fill-spill from Vega South is displayed in Figure 6.3 and will be discussed in the next section.

Normally pressured region

Further along section X-X', the Astero and Fram fields are displayed. This area comprises oil and gas in different stratigraphic levels: the Middle Jurassic Brent Group, and Upper Jurassic Fensfjord Formation, Sognefjord Formation and Intra Heather Formation sandstones, separated by the silty to shaly Heather Formation. These reservoirs are all close to normally pressured, indicating an open system with possible communication between the hydrocarbon bearing units. Several down faulted terraces, of which many are slightly tilted to the south-east, form traps in which hydrocarbons have accumulated. Judging from the top Brent Group surface map, displacements along many of these faults are high enough to form juxtaposition between the different reservoir units. As no detailed mapping of the Upper Jurassic units have been performed in this study, interpretations of the controls on hydrocarbon column heights in this area should be considered highly uncertain.

The Astero field is an oil and gas accumulation in Intra Heater sandstones. Although the Draupne Formation is located above the oil window in this area, the more deeply buried Heather Foramtion could potentially charge this reservoir. Also, judging from the migration map (Fig. 6.1b), long-distant migration have most likely occurred from the Sogn Graben in the north. Based on the absence of residual hydrocarbons below the oil-water contact, the structure is suggested to be filled to its structural capacity.

However, as no spill point was mapped in this reservoir, this interpretation is uncertain. Based on the low reservoir pressure of the Astero field, communication and fill-spill towards the Fram H-North structure is proposed as likely. The hydrocarbon column in the Fram H-North sandstones is suggested to be controlled by lateral juxtaposition to the Brent Group or by episodic vertical leakage along the Kinna Fault, into the Fram H-South structure or overburden. However, no amplitude anomalies above this fault indicate vertical leakage. And as no residual hydrocarbons were reported below the oil-water contact, the structure could be filled to the structural spill point. Although, this is highly uncertain, as no spill point has been mapped. In a fill-spill scenario, lateral spill into the Brent Group is the most favourable suggestion, due to the large displacement of the Kinna Fault.

The reservoir in the Fram H-South structure is, like Astero and Fram H-North, comprised of Intra Heather sandstones. In addition, the Brent Group was penetrated in this structure. Judging by the location of this structure, which is on the westernmost down-faulted terrace in this area, hydrocarbon charge could occur both from the west, through juxtaposed sands; south-west, along the terrace; or north, through Astero and Fram H-North (Fig. 6.1a and b). Residual hydrocarbons were recorded below the oil-water contact in the upper reservoir sequence (Intra Heather sst.) and in the water bearing Brent Group. This suggests that some recent process has caused reduction of the hydrocarbon column in the upper reservoir and emptied the lower reservoir. One process which could explain this is lateral or vertical leakage caused by fault reactivation. Compartments that previously were laterally sealed off by the Heather Formation shales could by fault reactivation be juxtaposed to other, adjacent sands. Leakage could then occur laterally though the fault. Whether the in-place volumes becomes fully or party reduced, depends on the geometry of the juxtaposed sand relative to the reservoir. However, if this was the case, significant fault reactivation and displacement would be needed to cause the emptied Brent Group. Thus, one would expect an offset be apparent in seismic data, all the way up in the Cenozoic sequences. No such features, which indicate recent high displacement along these faults, are observed in the area, suggesting that this is not the case.

Fault reactivation could also lead to vertical leakage along one or several faults that delineate the structure. Only a small displacement or movement could be sufficient to reduce the permeability along the fault, and especially within fault intersections (Gartrell *et al.*, 2004). Seismic amplitude anomalies (dim and brights) were observed in the overburden above one of the fault intersections that bounds the northern part of the structure. The fault intersection happens to delineate the shallowest part of the Brent Group, which implies that if leakage took place in this area, the reservoir could potentially be emptied. As only residual hydrocarbons were recorded in this

reservoir sequence, vertical leakage caused by fault reactivation could be the case. As for the underfilled Intra Heather Formation reservoir, the cause of leakage is more uncertain. It could be speculated that the fault intersection which emptied the Brent Group delineates the Intra Heather Formation at a deeper point. Thus, allowing for an accumulation up-flank of the point of leakage.

Fram F-East, which is situated further south, contains oil and gas in three stratigraphic levels: the Sognefjord and Fensfjord Formations, and the Brent Group. The Brent Group was suggested to be underfilled based on the presence of residual hydrocarbons below the oil-water contact (section 5.4.4). The filling of the shallowest reservoirs is unknown, as no residual hydrocarbons were recorded below the oil-water contacts and no spill points have been mapped. The underfilling of the Brent Group in this structure could be explained by the same processes as in Fram H-South. Also in this structure, seismic amplitude anomalies are observed above a fault intersection in the northern part of the structure. However, this fault intersection delineates top of the Brent Group reservoir in a down flank position, which explains that a hydrocarbon column is preserved in this structure. Although uncertain, hydrocarbons in the Brent Group in Fram F-East are suggested to spill northwards along the terrace and into a relay ramp, before migrating southwards into the Fram C-West structure. The Brent Group in this structure is suggested to be filled to its capacity, as the oil-water contact coincides with the spill point in the southern part of the structure. Due to poor seismic data in this area, it is highly uncertain whether the upper reservoir sequence in the Sognefjord Formation is filled or underfilled. However, as no residual hydrocarbons were reported beneath the oil-water contact in this reservoir, this may imply that the structure is filled to its structural capacity. Further migration from Fram C-West is suggested to occur southwards into the Troll area, both in the Brent Group and in the Sognefjord Formation.

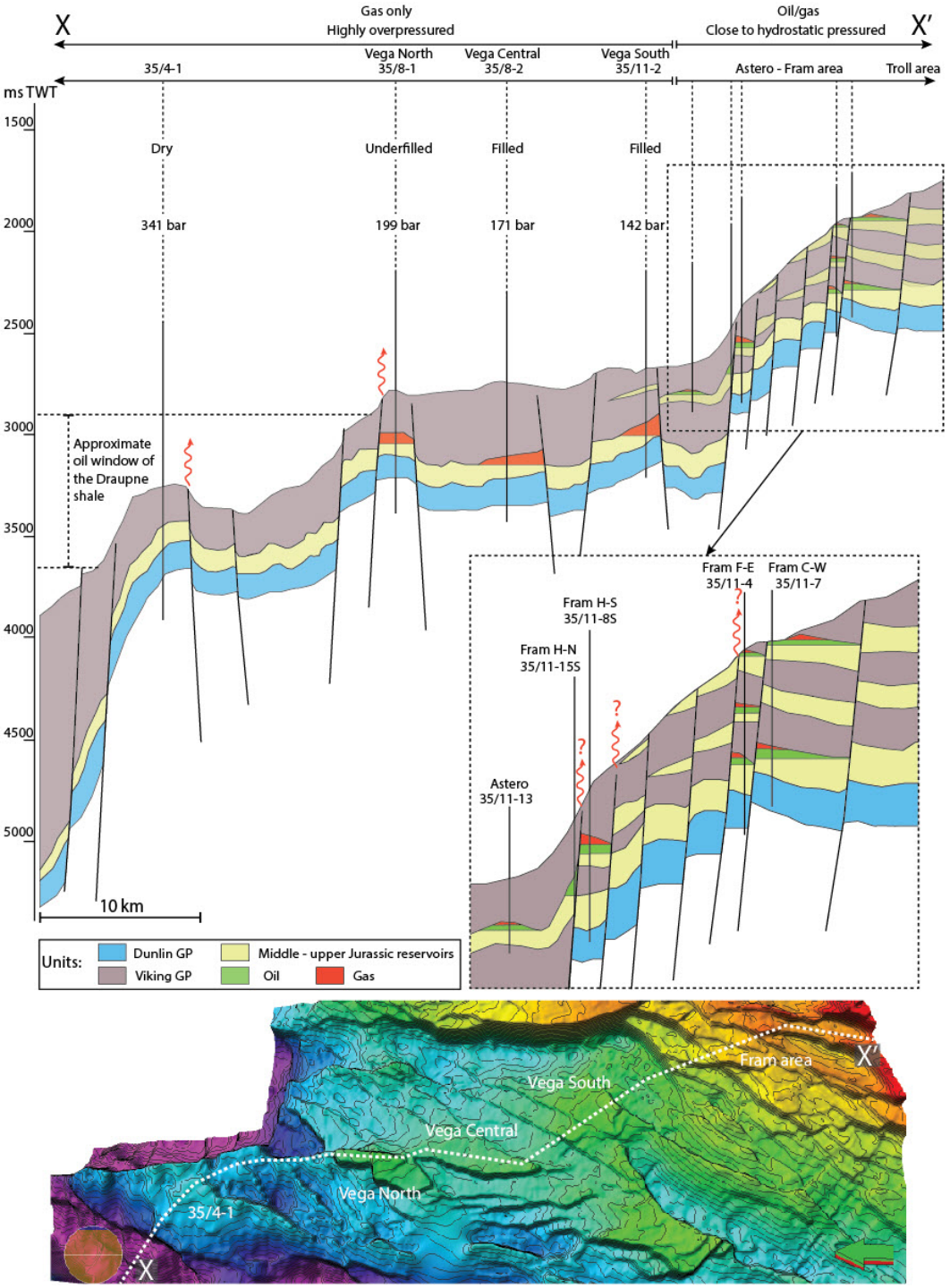

Figure 6.2: Migration route from NW to SE through dry structure 35/4-1, underfilled Vega North, and filled Vega Central and Vega South. The Astero field and Fram area is also presented in this section. Migration in this area does not necessarily occur along this section in the Fram area. However, this section illustrates that many of the hydrocarbon column-heights within the Fram area might be controlled by juxtaposition between the reservoirs. Vertical red arrows indicate possible locations of leakage.

6.1.2 Fill-spill route Y-Y'

Section Y-Y' (Fig. 6.3) presents a suggested fill-spill route from east to west, starting in the B-structure, through 35/10-1, Vega South, 35/11-3S and into the lower part of the Fram area. Between the B-structure and 35/10-1, hydrocarbons are believed to have migrated through a couple of small undrilled closures. The Afrodite structure is not included in the displayed migration route, as the gas-water contact and spill direction from this structure is unknown. In this area, the oil window of the Draupne Formation is located approximately from the top of structure 35/10-1 and down below the shallowest part of the reservoir in the B-structure. Also, in the half-graben between 35/10-1 and 35/11-3S, organic intervals of the Heather Formation are reported by well 35/11-3S to be oil mature. A decrease in overpressure is evident towards the shallower areas in this section.

The B-structure is located in the lower part of the present day oil window. In the surrounding sub-basins, both oil and gas generation may occur from the Draupne and Heather Formations, respectively. Aside from primary migration from juxtaposed Draupne shales in the south and east, secondary, long-distance migration is believed to occur from the deep Viking Graben in the west and probably from the higher pressured Afrodite structure. This, along with observations of residual hydrocarbons throughout the Brent Group, indicates that hydrocarbon charge can be considered sufficient to fill the structure to its capacity.

The large vertical distance between the gas-water contact and the spill point of the B-structure, suggest that the structure is underfilled. As there is not reported or observed any Upper Jurassic or Cretaceous thief sands in this area, which potentially could cause the underfilling, vertical leakage is suggested to be the main cause of the reduced hydrocarbon column-height in this structure. The depth of the gas-water contact coincides with a fault intersection, delineating the south-eastern part of the structure (Fig. 6.3). This, combined with the observation of seismic amplitude anomalies (brights) in the overburden, directly above the faults, suggest that the hydrocarbon column height is controlled by vertical leakage through the fault intersection. This is in agreement with the results from Teige & Hermanrud (2004).

The B-structure might spill in two directions, either to the east or to the north. Section A-A' in Figure 6.3 illustrates that eastward migration from this structure is most likely hindered by lateral seal of the Heather Formation. Further spill from the B-structure is therefore suggested to be directed northwards, through two small undrilled structural closures, before encountering dry structure 35/10-1. This structure is situated in the upper part of the oil window. In addition to supply from the north, the structure might be charged by adjacent, down-faulted Draupne and Heather Formation shales. This is

highly likely, as distinct oil- and gas shows were recorded in this structure, both in the Brent Group and in the Cook Formation of the Dunlin Group.

Either lateral or vertical leakage is suggested to be the cause of emptied reservoirs in structure 35/10-1, of which vertical leakage is considered most likely. This is mainly due to the observation of seismic amplitude anomalies (brights) in the overburden above the south-eastern fault intersection, which delineate the structure. This fault intersection is also located at the crest of the top Brent Group, which might explain why this structure is dry, while the B-structure still contains a hydrocarbon column. Furthermore, a small accumulation of oil is recorded in the Lista Formation, directly above the structure. Although uncertain, it is possible that this oil is derived from the underlying structure by vertical leakage.

Structure 35/10-1 is located closer to the Farm area, in which several Upper Jurassic sands exists: Fensfjord and Sognefjord Formations, and Intra Heather Formation sandstones. A 15 m sand, which is suggested to be part of the Sognefjord Formation is recorded in well 35/11-3S, situated further to the east. As no well is drilled between the 35/10-1 and 35/11-3S, it is not known whether Upper Jurassic sands are present further west into the basin, towards 35/10-1. If this is the case, contact between the Brent Group reservoir and Upper Jurassic thief sands might result in lateral leakage out of the structure. However, as the sand recorded in well 35/11-3S is only 15 m thick, it is highly unlikely that it stretches 10 km further west. Also, most of the Intra Heather Formation sandstones encountered in the Fram area, are interpreted as local turbidites derived from the Sognefjord delta in the east. Due to the prevalence of the Sognefjord Formation, the likeliness of encountering Intra Heather Formation sandstones in the distal parts of the basin is low. Furthermore, as discussed in section 6.1.1, the presence of deep shows in the reservoir, could indicate that the lateral and vertical seals has been sufficient in the past and allowed for accumulation of hydrocarbons. Based on this, it is suggested that structure 35/10-1 is sealed laterally by the Heather Formation and/or the Draupne Formation shale and that leakage has occurred vertically.

Further spill from structure 35/10-1 is directed into the lower pressured Vega South, which has already been discussed in section 6.1.1. Vega South is believed to spill south-westwards, into a lower pressured, westerly dipping rotated fault block, which were proven dry by well 35/11-3S. The structural closure of this rotated fault block was estimated based on a spill point to the east, through juxtaposition of the Brent Group. If this spill point is correct, well 35/11-3S is placed outside the structural closure by a few 100 metres (Fig. 5.38 in section 5.6.4). However, residual hydrocarbons were recorded in the Brent Group, indicating a palaeo-fluid contact which is deeper than the estimated spill point. A few mechanisms which could explain this observation is discussed below.

According to the well report of 35/11-3S, an organic interval in the deeper part of the Heather Formation has reached sufficient maturity and probably expelled some of its potential. Primary migration from this interval into the Brent Group could therefore explain the observed residual hydrocarbons below the spill point. A second explanation could be that the fault was sealing in the past, which allowed for a larger accumulation. Subsequent seal-breach through the fault, due to pressure build-ups, could have resulted in lateral leakage through this spill point, towards the north-east. In this case, a potential reduced hydrocarbon column could be present up-dip from the well location. Although no strong indications of vertical leakage is observed in the seismic data (small dim), oil shows were recorded in the Upper Jurassic Sognefjord Formation and the Lower Cretaceous Mime Formation. Therefore, the possibility of vertical leakage from this structure cannot be excluded.

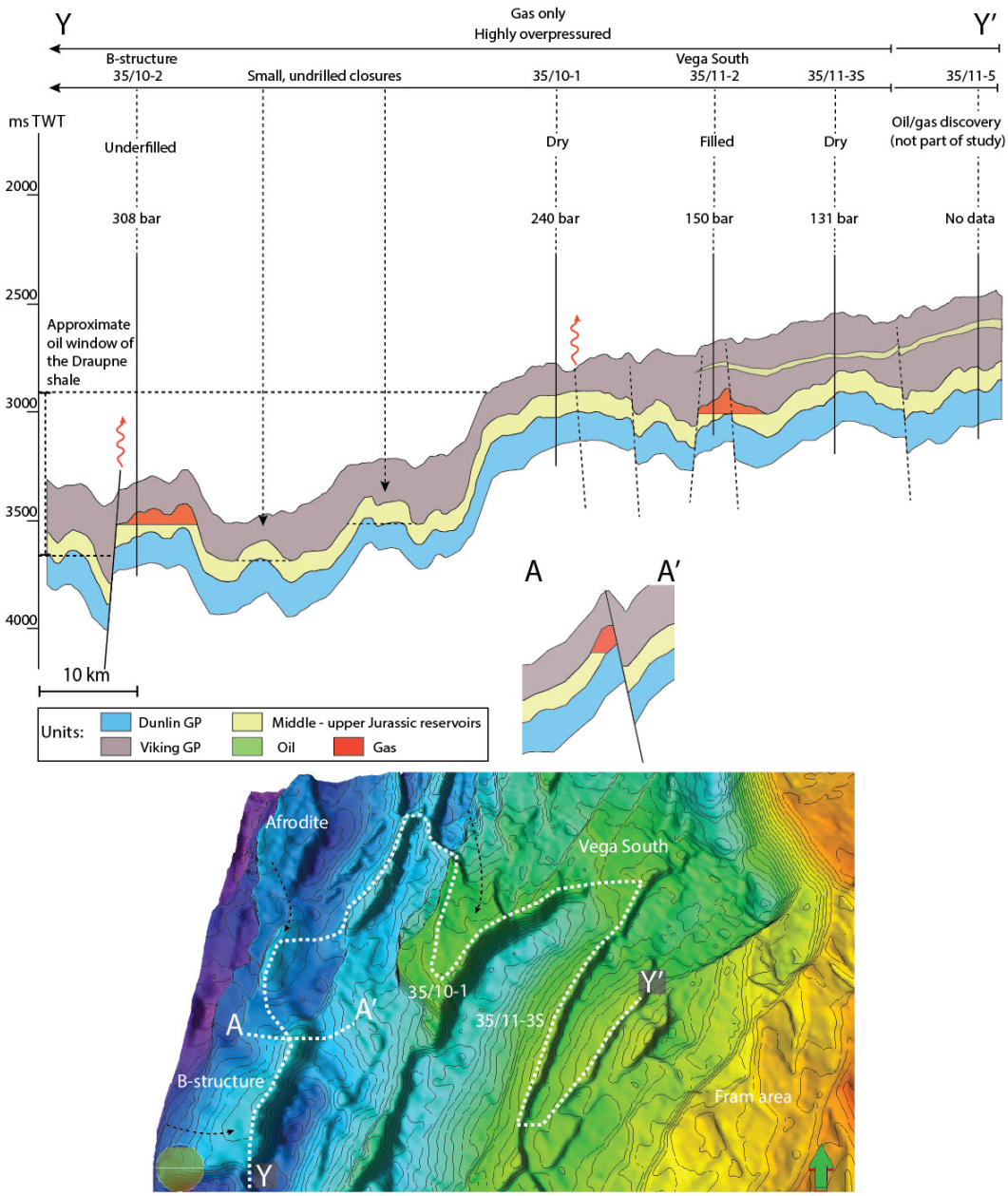

Figure 6.3: Suggested W-E fill-spill route from the underfilled B-structure, dry structure 35/10-1, filled Vega south, dry 35/11-3S and into 35/11-5. The overpressure is decreasing towards east. Probable vertical leakage is here indicated with red arrows.

6.1.3 Fill -spill route Z-Z'

Section Z-Z' (Fig. 6.4) presents a N-S migration route from the Sogn Graben to Titan and along the Ryggstein Ridge, into the Grosbeak structure. The oil window is here located approximately from the middle of the Titan structure, down into the upper part of the Sogn Graben. The Brent Group is in this area close to normally pressured, indicating that there might be communication between the Titan and Grosbeak structures in this unit. No fluid contacts were reported in Titan, therefore, analysis of the controls on hydrocarbon column-heights in this structure will not be conducted.

The Grosbeak structure comprises three reservoir units: the Upper Jurassic Sognefjord and Fensfjord Formations and the Middle Jurassic Brent Group. Gas was encountered down to the base of the Sognefjord Formation, which is unconformable overlain by Cretaceous shales. Oil was encountered in the two deepest reservoirs (Fensfjord Formation and Brent Group). As the Grosbeak structure is located well above the oil window, hydrocarbons must migrate from the the deeper areas, along the Ryggstein Ridge, before reaching the structure. Alternatively, migration could also occur from the deeper areas in the east or vertically along the Ryggstein Fault from the deeper basin in the west. However, there are no data available to confirm this. These migration routes are, however, only applicable for the Brent Group. As the Sognefjord and Fensfjord Formations are eroded in the north, east and west, lateral migration into these reservoirs is more likely to have occurred from the Fram area in the south. Vertical migration could, alternatively, occur through faults from the Brent Group.

Based on the mapped spill point of the Brent Group and the depth of the oil-water contact, this interval is suggested to be underfilled. However, there is no information on hydrocarbon shows being present below the oil-water contact in well 35/12-2. Moreover, well 35/11-1, which is situated slightly further to the north on the Ryggstein Ridge did not record any residual hydrocarbons in the Brent Group. This may indicate that supply in this area is a restricting factor for accumulation in the Brent Group. However, judging by the location of the Grosbeak structure relative to other discoveries in the area (e.g. Titan, Skarfjell and Fram), this seems unlikely.

High, positive seismic amplitudes (red reflections) were observed in the Jurassic section, adjacent to the faulted Brent Group in the Grosbeak structure. These were interpreted as sands, which potentially could be part of the down-faulted Fensfjord Formation. If juxtaposition exists between the Brent Group in the Grosbeak structure and the Fensfjord Formation (or Cretaceous sands), this would only allow for accumulation down to the shallow-most part of the down-faulted sand (section A-A' in Figure 6.4). Such a scenario could explain the underfilling and absence of residual hydrocarbons in the Brent Group reservoir. Furthermore, if this is the case, migration from the Grosbeak structure would have a different route (dotted black line in Figure 6.4)

The fault intersection, bounding the south-western part of the structure could be a good candidate for vertical leakage. However, the hydrocarbon column in the Brent Group does not seem to be restricted by any faults. Furthermore, this fault intersection delineates the shallowest part of the Brent Group, implying that if it would leak, the reservoir could potentially be emptied. As no hydrocarbon shows are recorded below the oil-water contact, the Grosbeak structure is interpreted to be filled to its structural capacity, by fill-spill into the Fensfjord Formation.

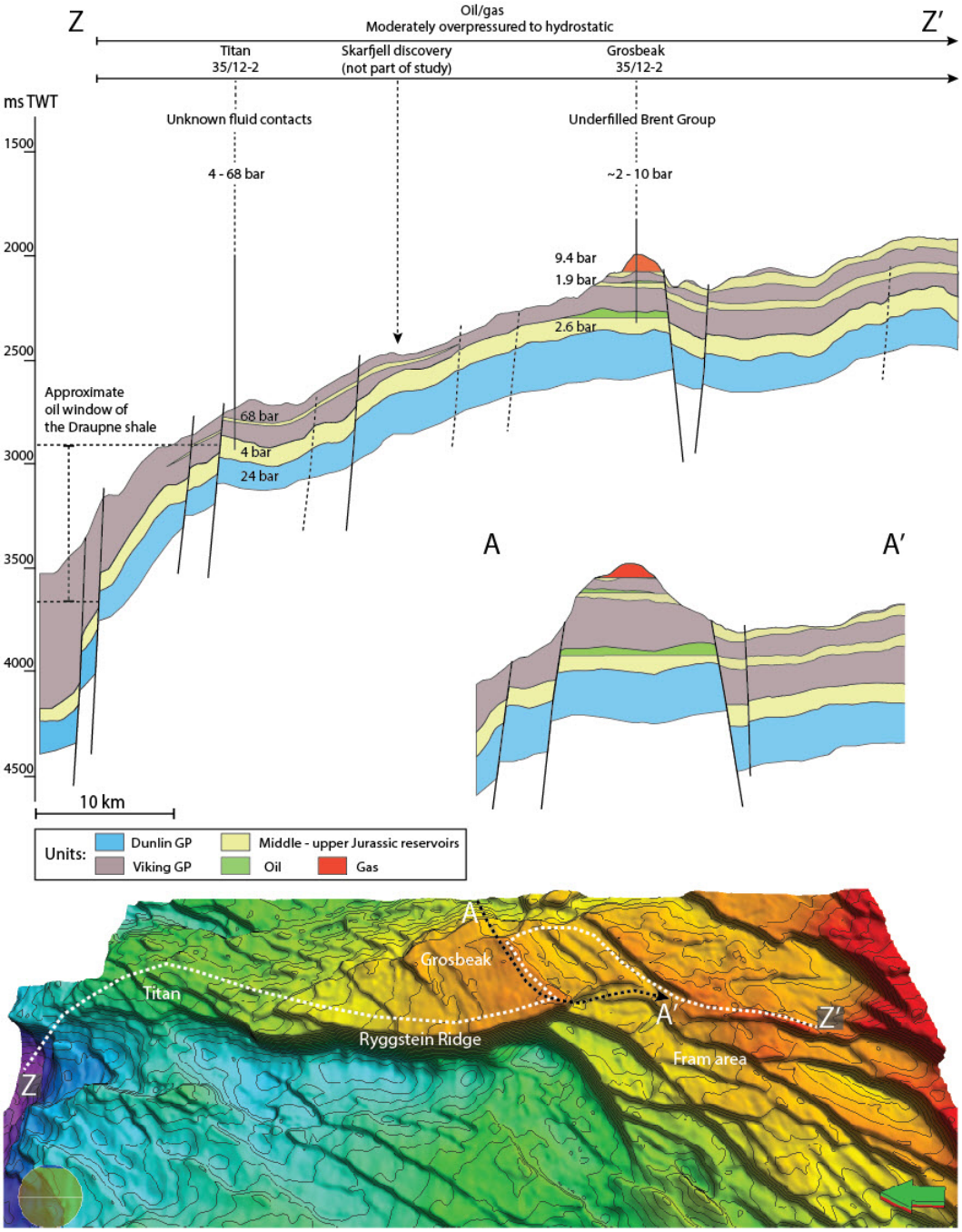

Figure 6.4: Suggested migration route form the Sogn Graben, through Titan and into the Grosbeak structure. Migration could occur through the Brent group towards the south, as juxtaposition exists here, however, it is proposed that Upper Jurassic sands (or Cretaceous) control the hydrocarbon column in the Grosbeak structure.

6.1.4 Summary of fill-spill routes

Based on three suggested fill-spill routes throughout the study area and fluid contacts within the hydrocarbon-bearing structures, five structures of which hydrocarbons have accumulated down to the spill points are identified (Vega Central, Vega South, Grosbeak, Astero and Fram C-West). The hydrocarbon column-heights in four of the suggested underfilled structures seems to be controlled by vertical leakage through faults (the B-structure Vega North, Fram H-South and Fram F-East). Vertical leakage through faults or cap rock is also suggested to be the cause of emptied reservoirs in two of the dry structures (35/10-1 and 35/4-1). The third dry structure 35/11-3S, could still contain a potential hydrocarbon column, up-dip from the well.

A large difference in overpressures between the Brent Group reservoirs of the deep situated structures: Afrodite, B-structure, 35/10-1, 35/4-1, Vega North, Vega Central, Aurora and Vega South, indicates a lack of present communication between these structures (Fig. 6.1c). The presence of compartmentalized reservoirs, where present day fluid flow is hindered by lateral barriers, most likely sealing faults, could explain this observation. Also, the Brent group, which constitutes most of the deep reservoirs in this area, is located in the very northern part where the Brent delta prograded (Helland-Hansen *et al.*, 1992). Because of this, poor developed reservoirs and discontinuous sands, could also affect the pressure distribution in this area. However, sedimentological and petrophysical investigation in the area is not part of the scope of this study.

The displacement of the faults along the suggested spill-routes are not high enough to result in lateral sealing of the Brent Group reservoirs, by juxtaposition between the Brent Group and Heather Formation shales. Furthermore, the gas-water contacts in the suggested filled Vega Central and Vega South structures, are located at the same depth as the mapped spill points in these structures. Together with the absence of residual hydrocarbons below the gas-water contacts, these observations suggests that the spill route between Vega Central, Vega South and 35/11-3S was previously open. The present state of this spill route could be explained by a dynamic system, where migration routes in the deep areas gradually became less permeable with increased burial.

If the spill route was open in the past, one mechanism which could explain the present day impermeable barriers, is quartz cementation. It is widely agreed that quartz cementation is a late diagenetic process which initiates between $70 - 80°C$ (Bjørlykke *et al.*, 1986; Walderhaug, 2000). According to Hermanrud (1988)'s temperature depth correlation, which is based on more than 400 wells in the North Sea basin, this corresponds to a depth of approximately 2 km. Most of the overpressured fields in the study area are located below 3500 m, implying that quartz cementation has been ongoing for a while. This has most likely contributed to reduction of permeability and porosity

in these reservoirs, and along faults. This is in agreement with Borge (2000), which suggested that quartz cementation was the dominating pressure generating mechanism during Tertiary (66 - 2.58 Ma).

However, when hydrocarbon generation and migration commenced in Early Cenozoic (Goff, 1983), the structures were not as deeply buried. At this time, the Rogaland, Hordaland and Nordland Groups were not yet deposited. Above Vega Central, these groups together constitutes almost 1950 m of sediments. Even if the Rogaland Group were deposited, which corresponds to mid-Eocene times, there would still be almost 1700 m of sediments less than at present day. At this time most of the now deeply buried structures were above the depth where quartz cementation initiates (2000 m). The structures could probably still be extensively buried before cementation would significantly reduce the permeability. It its therefore suggested that a fill-spill system within the study area could exist in the past, at shallower burial depths, during generation and migration of hydrocarbons.

6.2 Oil versus gas distribution

During basin subsidence in the Early Cenozoic, when generation of oil initiated in the deepest parts of the Viking Graben and Sogn Graben, migration routes were probably less restricted (as discussed in section 6.1). Large quantities of oil could therefore migrate from the kitchen area and towards the shallow terraces and platform areas. In addition to the oil- and gas-bearing shallow traps (e.g. Astero, Fram and Grosbeak), oil shows are recorded in the Brent Group of the gas-bearing Vega North and Vega South, and dry structure 35/10-1. This indicates that many of the deep traps contained oil at an earlier stage, and that the shallow traps might also have contained larger proportions of oil relative to gas.

With further basin subsidence, much of the previously oil-generating shales reached sufficient temperatures to initiate generation of gas and cracking of oil into gas. Most of the deep situated structures, except for Afrodite, are still located above the depth where generation of gas occurs, which is approximately at 4500 m (Goff, 1983). Gas must therefore have migrated from distant sources and replaced the oil in the deep structures. As gas has lower density than oil, it will continuously migrate towards the top of the reservoir, driven by buoyancy. Sufficient supply of gas into the trap will therefore push the oil-column downwards below the spill point, causing the oil to migrate towards shallower areas, and eventually leave a pure gas-column behind in the deep trap. This scenario is likely for most of the deep gas-bearing structures in the study area, and a fill-spill system in the past, as presented in section 6.1, would allow for this.

The shallow traps in the area, namely Astero, the Fram fields, and the Grosbeak structure, are all located above the present day oil-window of the Draupne Formation. At an early stage, the accumulated hydrocarbons in these traps must therefore migrate over longer distances from the generating grabens. However, the presence of both oil and gas in these structures is more difficult to explain than the presence of pure gas columns in the deep area. If the migration of oil and gas were infinite towards the shallow areas, the shallow traps would most likely suffer the same fate as the deep structures, where gas eventually replaces the oil column. As this is not the case, some processes or mechanisms must have allowed for the oil to be preserved.

As discussed in section 6.1, migration routes that were previously open, could by basin subsidence and cementation become less permeable. Thus such a change in permeability along migration routes in the deep basin could potentially result in reduced supply of gas towards the shallow areas. The presence of oil in the shallow structures might therefore be explained by the closed, compartmentalized system in the deep parts of the study area that is observed today. Although mature source rocks in the Heather Formation may exists close to the shallow terraces, theses are situated well within the present day oil window, and are thus not capable of generating gas.

6.3 Characteristics of underfilled and dry traps

Several leaking structures are identified within the study area. In this section, attributes which may characterize these structures will be discussed, with the purpose of: a) provide an understanding of where and how leakage occurred, and b) investigating if these results can contribute in detection/identification of leaking structures and restricted hydrocarbon column-heights. These attributes include pressures and retention capacities, fault orientations, and seismic amplitude anomalies in the overburden above the structures. Relationships between these characteristics and leaky structures may contribute to recognition of dry traps and better prediction of column heights in potentially hydrocarbon bearing structures before drilling.

6.3.1 Pressure and retention capacities

Retention capacities have for several decades been considered a measure on the likeliness for formation pressures to induce tensile failure in the cap rock (Gaarenstroom *et al.*, 1993; Bolås *et al.*, 2005). Calculations of retention capacities have therefore been conducted on all the structures in order to look for potential relationships between high formation pressures and leaking structures (Fig. 6.5a).

Two of the dry structures, namely 35/10-1 and 35/4-1, have retention capacities below 100 bar, whereas the calculated retention capacity of the third dry structure, 35/11-3S, is close to 200 bar. This structure is here coloured orange, as the hydrocarbon column-height in this structure might be spill-point controlled. The suggested underfilled structures, Vega North, B-structure, Fram H-South and Fram F-East, have retention capacities between 100 and 155 bar. Two of the structures that are suggested to be filled, namely Fram C-West and Vega South, also have retention capacities between 100 and 155 bar. Aside from low retention capacities of structure 35/10-1 and 35/4-1, there is no clear relationship between calculated retention capacities and leaky structures in this diagram (Fig. 6.5a). In structures with more than one reservoir unit, only the upper unit is presented is this diagram (this also applies to the diagram in Figure 6.5b)

The retention capacity is the difference between the pore pressure of given structure and the calculated magnitude of the least principal stress at the same depth (Bolås & Hermanrud, 2003), which in this case is based on leak-off pressure measurements (section 4.2.3). In a sedimentary basin, the least principal stress magnitude is much lower at shallow depths than in deep areas. Thus, shallow, close to normally pressured structures, such as the Fram fields, will therefore have more or less the same retention capacities as the deep, overpressured structures. This is well illustrated in the digram in Figure 6.5a. As the likeliness for normal pore pressures to induce failure is low

compared to overpressured reservoirs, using retention capacities to distinguish leaking structures from non-leaking structures is not sufficient in this area.

In an attempt to separate the normally pressured structures from the overpressured structures, calculations of overpressure factors have been conducted for all the structures (see section 4.2.3 for definition and formula). In the diagram in Figure 6.5b, all the structures are represented with a value from 0 to 1, where 0 corresponds to no overpressure and 1 corresponds to the largest overpressure possible before failure. Here, the dry and underfilled structures, which had the same retention capacities as the filled, normally pressured structures, now stand out with much higher values. Although some filled structures, namely Vega Central and Vega South has relative high values, the dry and underfilled structures: 35/10-1, 35/4-1, B-structure and Vega North, are clearly separated with much higher values. Dry structure 35/11-3S, here marked with orange colour, does not separate much from the other filled structures. Also, the suggested underfilled structures in the Fram area have overpressure factors close to 0, due to the normally pressured reservoirs.

Although analysis of reservoir pressures might contribute in distinguishing leaky structures from non-leaky structures, it cannot single-handedly be used as a tool for this purpose. Other attributes which might contribute in distinguishing these structures must therefore be included.

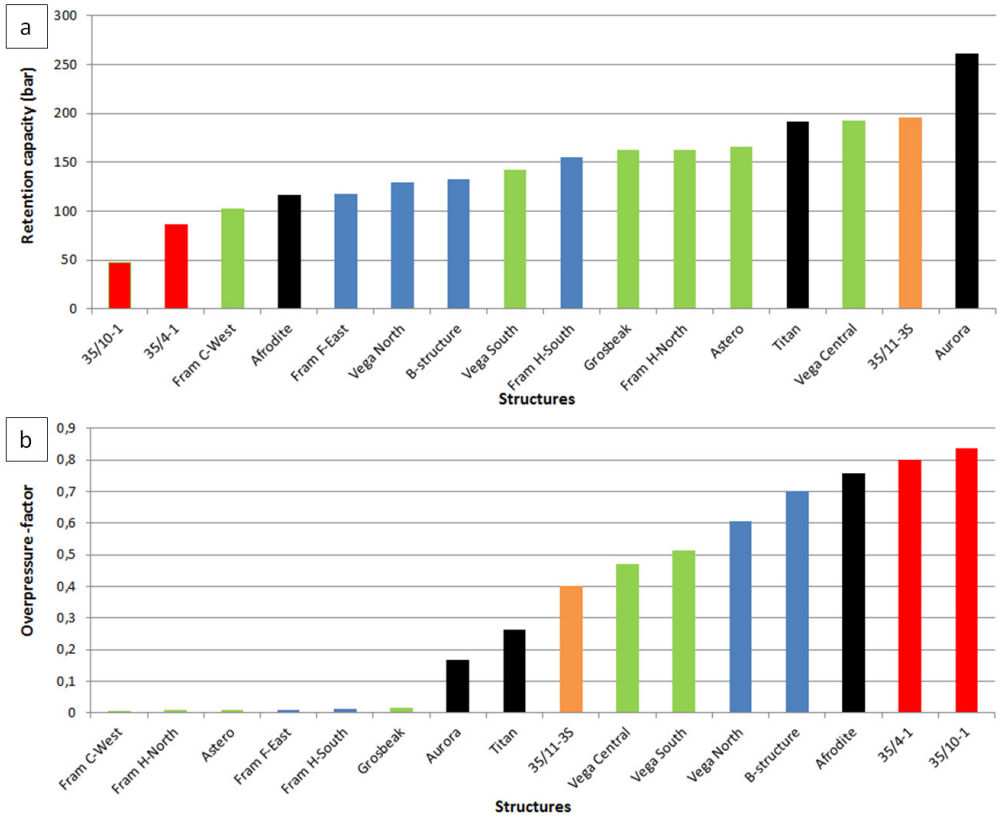

Figure 6.5: a: Retention capacities and **b:** overpressure factors of the studied structures. Colour codes: green (filled), blue (underfilled), red (dry), black (N/A).

6.3.2 Orientation of faults and fault intersections

Along with other authors, Wiprut & Zoback (2002) suggested that faults which are optimally oriented towards the maximum horizontal stress in the Northern North Sea, would have increased probability of reactivation and vertical leakage. In general, failure is most favourable initiated at +/-30° to the maximum principal stress (S_1). Whether the present day S_1 in the Northern North Sea corresponds to the maximum horizontal stress (S_H) or the vertical stress (S_V), is disputed. Aadnoy *et al.* (1994) suggested that the Northern North Sea is currently in a normal-fault regime, which implies that $S_V > S_H$, while Wiprut (1998) suggested that $S_1 = S_H$, implying that the Northern North Sea is currently in a strike-slip fault regime.

The orientation of the maximum horizontal stress in the Northern North Sea is less disputed. Brudy & Kjørholt (2001) suggested this orientation to be WNW-ESE (N100°E) on the western flank of the Viking Graben, and ENE-WSW (N80°E) on the eastern flank. This is consistent with the World Stress Map (WSM, 2009). If Wiprut (1998)'s suggestion of $S_1 = S_H$ is followed, one would expect faults that are oriented +/-30° on N80°E to be critically stressed within the study area, considering the present day stress state.

The stress state along the Norwegian Continental Shelf has, however, changed several times during Pliocene and Pleistocene, due to repeated glacial advance and withdrawal (Doré & Jensen, 1996; Fjeldskaar *et al.*, 2000; Grollimund & Zoback, 2000, 2003; Bolås *et al.*, 2005). This caused increased stress variations through time, especially in the sediments under the hinge zone where the crustal flexuring was most influencing. The position of this hinge zone, is located more or less above the study area (Doré & Jensen, 1996)(Fig. 3.5a, section 3.3.4). Increased stress anisotropy is something that could potentially lead to trap failure, most likely by fault reactivation (Bolås *et al.*, 2005). Therefore, fault orientations of all the filled, underfilled and dry structures have been investigated. These are here compiled and presented in rose diagrams to see if there is any relationships between fault orientations and leaking structures (Fig. 6.6 and 6.7).

A general observation is that faults bounding the structures that are suggested to be filled, are dominantly oriented N-S and slightly NE-SW (Fig. 6.6a). These fault orientations are described in literature as the most common fault trends formed under the Permo-Triassic and Late Jurassic rifting phases (Færseth, 1996). These faults seem to be oriented close to perpendicular to the present day maximum horizontal stress orientation in the area. There is, however, one exception. One of the faults that delineate the Grosbeak structure is oriented more towards ENE-WSW, and thereby seems to be critically stressed in the present day stress field. The fault orientations of the structures where the fluid contacts are unknown, are presented in Figure 6.6b. These orientations

do not deviate much from the fault orientations of the filled structures are also very consistent with the main fault trends (N-S and NE-SW) in the study area (Fig. 6.6c). If failure were to initiate at +/-30° to the maximum horizontal stress in the present day stress field on the eastern flank of the Viking Graben (N80°E), only the fault that delineate the Grosbeak structure seems to be critically stressed. However, if the stress field on the western flank of the Viking Graben (N100°E) were to be considered, none of the faults that delineate the filled structures or the structures with unknown fluid contacts, seems to be critically stressed.

In Figure 6.7, rose diagrams with fault orientations of the underfilled and dry structures are presented. Like the filled structures, many of the faults that delineate the underfilled and dry structures, are oriented NE-SW. In order to display the deviating fault orientations, which are of most interest, NE-SW -oriented faults that delineate structures with fault intersections, have been excluded in these diagrams.

All the underfilled structures are bound by one or more fault intersections. A general trend of NE-SW to ENE-WSW -oriented faults is apparent in the rose diagram which presents the underfilled structures (Fig. 6.7a). Considering a N80°E -orientation of the maximum horizontal stress, which is suggested for the eastern flank of the Viking Graben (Brudy & Kjørholt, 2001), the suggested column restricting faults of Vega North and the B-structure are not favourable oriented for shear failure (+/-30°). However, both of the suggested column restricting faults in the Fram area are close to favourable oriented for shear failure in this stress field. On the other hand, if a N100°E -orientation of the maximum horizontal stress were considered, which is suggested for the western flank of the Viking Graben, all the suggested column restricting faults of the underfilled structures are close to favourable oriented for shear failure.

The fault orientations of the dry structures are more varying than for the underfilled structures (Fig. 6.7b). 35/11-3S is only delineated by one NE-SW -oriented fault, which is very similar to the faults delineating the filled structures. Therefore, this fault is not favourable oriented for shear failure, neither for the maximum horizontal stress orientation on the eastern or the western flank of Viking Graben. The intersecting fault that delineates top of structure 35/4-1 is oriented more towards ENE-WSW, which is close to favourable oriented for shear failure, considering an N80°E -orientation of the maximum horizontal stress. However, in this scenario, the suggested leaky fault of structure 35/10-1, is not favourable oriented. On the other hand, a N100°E -orientation of the maximum horizontal stress would favour reactivation of both 35/4-1 and 35/10-1.

A general observation for the faults that are suggested to leak, is that they are more favourable oriented for reactivation when the present day maximum horizontal stress is oriented N100°E (Fig. 6.7c). The reported orientation of the maximum horizontal stress within the study area, which is N80°E, cannot explain the column restricting

faults as well. Most of the faults that delineate the filled structures are not critically stressed, which could explain why these faults are not leaking.

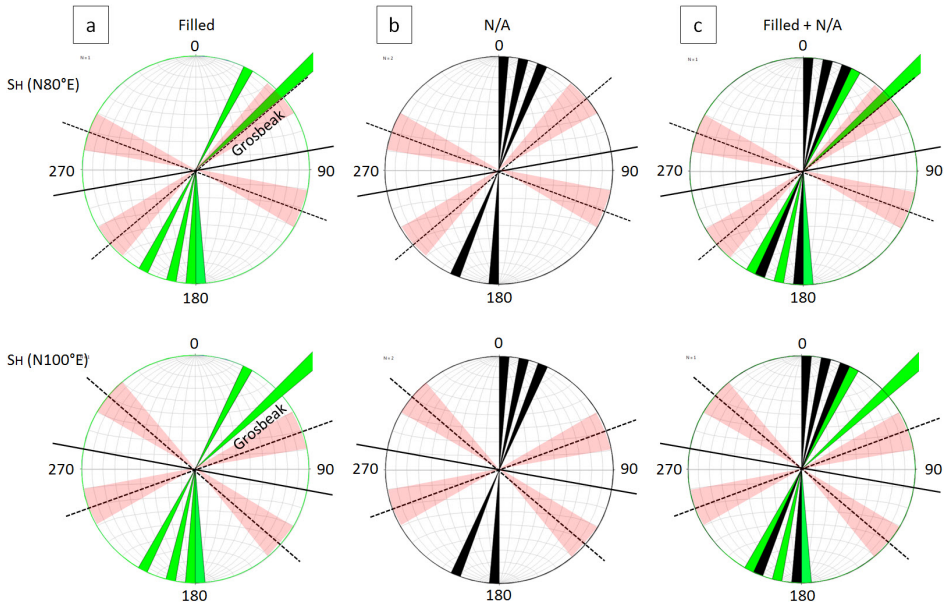

Figure 6.6: Rose diagrams with fault orientations of the filled structures (green) and the structures with unknown fluid contacts (black). The orientation of the maximum horizontal stress is indicated with black lines (N$80°$E for the eastern flank and N$100°$E for the western flank of the Viking Graben). The stippled lines represents a +/-$30°$ angle to the stress orientation. The red zone marks the area of (+/-$10°$) to the critically stressed orientation. Note that the faults are mostly oriented N-S or NE-SW, which are the main fault trends formed under the Jurassic rifting phases. Only the fault the delineate the Grosbeak structure is critically stressed in the present day stress field.

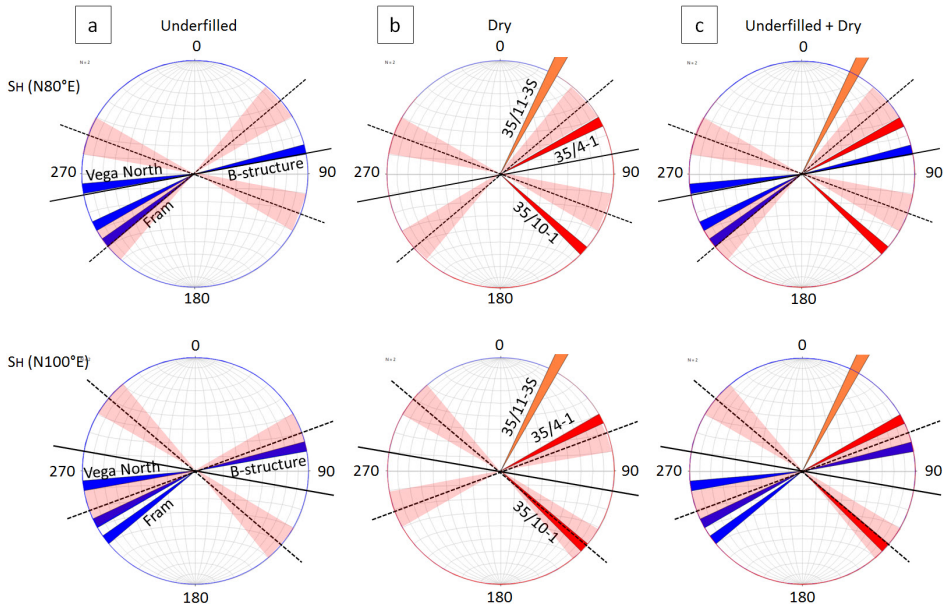

Figure 6.7: Rose diagrams with fault orientations of underfilled (blue) and dry structures (red and orange). The orientation of the maximum horizontal stress is indicated with black lines. (N$80°$E for the eastern flank and N$100°$E for the western flank of the Viking Graben). The stippled lines represents a +/-$30°$ angle to the stress orientation. The red zone marks the area of (+/-$10°$) to the critically stressed orientation. Note that these fault orientations are more varying than the faults delineating the filled traps. Also a trend slightly more towards ENE-WSW is apparent.

6.3.3 Seismic amplitude characteristics in the overburden

Seismic amplitude anomalies in the overburden can often be associated with hydrocarbon leakage (Avseth *et al.*, 2005; Ligtenberg, 2005; Arntsen *et al.*, 2007; Løseth *et al.*, 2009; Heggland, 2013). Throughout this study, the overburden above all the structures has been thoroughly investigated for amplitude anomalies that might indicate potential hydrocarbon leakage. Brights (strong amplitudes), dim zones (weak amplitudes) and seismic chimneys (columns of noisy seismic character) have been observed above many structures in the study area. Their presence and relation to suggested leaky structures will be discussed here.

The most pronounced features which are observed above most of the dry and underfilled structures in the study area, are brights in the Kyrre Formation. These amplitude anomalies can be characterized as concentrated, stacked features. Due to the alternation between high and low amplitudes, it is difficult to determine whether these features reflect a decrease or increase in acoustic impedance. Whether they can be defined as small gas accumulations (decrease in acoustic impedance) or cemented areas (increase in acoustic impedance) is therefore uncertain. However, gas in overburden rocks may cause intense localized carbonate cementation, in which case such areas of local high amplitudes can be interpreted as hydrocarbon-related diagenetic zones (HDRZ). HDRZ are reportedly often observed above local fluid conduits, such as faults and fault-intersections (O'Brien *et al.*, 2002; Ligtenberg, 2005). However, subtle local push down effects of the reflectors below the brights zones is evident both in 35/4-1, 35/10-1 and the B-structure. This could imply that the overlaying brights reflects the presence of gas, which causes reduced seismic velocity in the underlying sections.

The Kyrre Formation consist primarily of shales, deposited by hemipelagic clay (Bugge *et al.*, 2001), making the Kyrre Formation homogeneous and without strong internal reflectors in seismic data. Some sandstones are found in parts of the Agat area, which is located outside of the study area (Bugge *et al.*, 2001). Because of the shaly character of this formation, it is not capable of preserving large quantities of hydrocarbons, nor is it permeable enough to allow for lateral migration of hydrocarbons within the study area. Reactivation of faults or propagation of fractures would, however, form local conduits for fluid flow. Because of this, brights that are observed in vicinity of faults could potentially indicate vertical leakage from dry and underfilled structures. Furthermore, due to the lack of significant lithological differences within the Kyrre Formation (Bugge *et al.*, 2001), this makes it a very good candidate for analysis of brights by attribute extraction.

Figure 6.8a shows a regional attribute map of the Intra Kyrre Formation, superimposed on the top Brent Group surface map. This map is generated with an RMS attribute extraction interval of +/-15 ms TWT, -200 ms TWT below the top Kyrre Formation

reflector. As the Kyrre Formation onlap the shallow terraces, this map is only applicable in the deep, overpressured areas. It is evident that brights are concentrated above the crests of the dry structures, 35/4-1 and 35/10-1. No brights were observed above the third dry structure, 35/11-3S. Intra Kyrre Formation brights were also observed above the fault intersection of the underfilled B-structure and above the underfilled Vega North. It is hardly coincidental that brights only appear above the suggested dry and underfilled structures. Due to this reason, brights in the Kyrre Formation could be an indicator of leakage. Furthermore, these brights might also give an indication of where leakage is occurring from the dry and underfilled structures.

Brights were also observed in the Rogaland Group above the underfilled Fram structures, H-South and F-West. However, no attribute maps were generated in this area. Due to larger lithological variations within the Rogaland Group than in the Kyrre Formation, it would be difficult to distinguish between lithology variations and actual leakage within this sequence. Another attribute which were observed in the overburden in the shallow area, above the Grosbeak structure and in the Fram area, was V-shaped brights. These features were by Løseth *et al.* (2003, 2009) suggested to be associated with sand-injections, triggered by internal generation of overpressure, which could be caused by invasion of fluids. Also the chaotic reflection patterns observed in the upper part of the Hordaland Group are by Løseth *et al.* (2003, 2009) described as remobilized sediments, triggered by the same mechanisms as the sand injections. However, in a recent study on remobilized sediments in the Johan Sverdrup area in the Northern North Sea, Christensen (2015) suggested that remobilization of sediments were mainly caused by gravitation sliding and not necessarily by invasion of fluids. It is therefore highly uncertain whether these seismic features reflect hydrocarbon leakage from underlying traps.

In addition to brights, dim features and seismic chimneys were observed in the overburden throughout the study area. The definition of a seismic chimney is very broad, and some might categorize dim features as seismic chimneys as well (Heggland, 2013). However, in this study, only near-vertical columns of noisy seismic character, as described by Ligtenberg (2005), are referred to as seismic chimneys. Dim zones are here attributed to more subtle and local observations. Figure 6.8b shows a regional attribute map of the top Kyrre Formation reflector, superimposed on the top Brent Group surface map. It is here evident, by the stronger amplitudes, that the top Kyrre Formation reflector is much more continuous than the bright features within the Kyrre Formation. As previously mentioned, the Kyrre Formation is absent in the shallow most area in the east, and is therefore not included here.

Dim features are observed above the dry structures 35/4-1 and 35/10-1, and also above the underfilled B-structure. However, other large dim areas are also present in the

western area, partly above the Afrodite structure, and above the Ryggstein Ridge to the north-east, covering parts of the Aurora and Titan structures. The relationship between the top Kyrre Formation attribute map and leaky structures is therefore not as consistent as the Intra Kyrre Formation attribute map. It is unclear if these features are directly related to leakage, as the filling of the Afrodite structure, Aurora and Titan is unknown. Also, as the top of the Kyrre Formation is located 1-1.5 km above these structures, seismic amplitude anomalies observed in this interval is not necessarily directly related to vertical leakage from the underlying structures. Low concentrations of gas, derived from other areas, might be present over large parts of the study area.

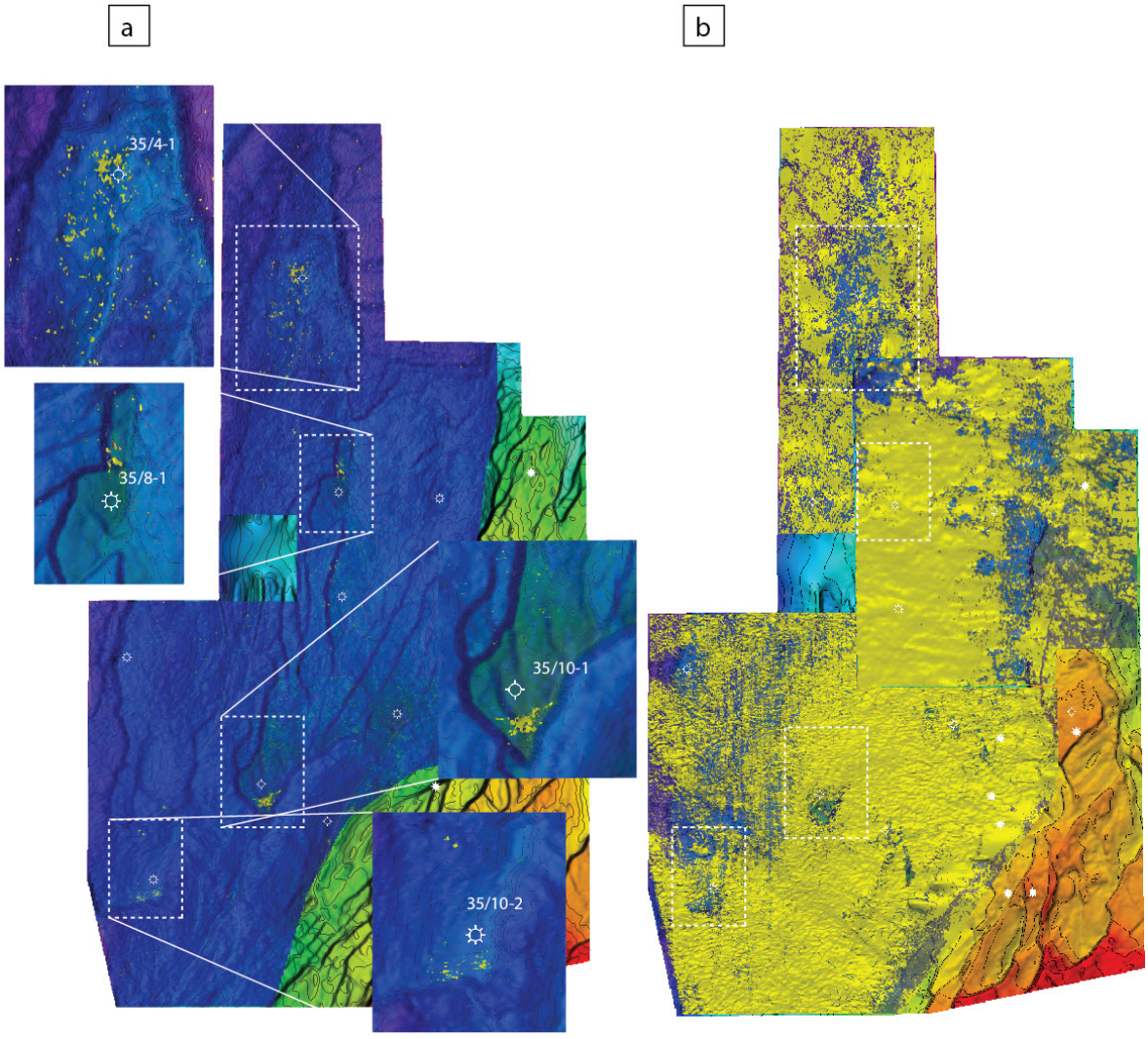

Figure 6.8: a: RMS attribute map of the Intra Kyrre Formation. This is lowered -200 ms TWT from the top Kyrre Formation reflector and the interval of RMS extraction is +/-15 ms TWT. Note the brights above the deep dry and underfilled structures (35/4-1, 35/10-1, 35/8-1 and 35/10-2). **b:** RMS attribute map of the top Kyrre Formation reflector, with an extraction interval of +/-15 ms TWT. Note that the dim areas above the dry structures 35/4-1, 35/10-1 and underfilled structure 35/10-2. Also, note that the dim areas are more widespread and less consistent with the suggested leaky structures.

One seismic feature which here is defined as a seismic chimney was observed above the dry structure 35/4-1 (Figure 5.35, section 5.6.1). Here, a broad, near-vertical column of noisy seismic character was present directly above the crest of the structure. Adjacent to this seismic chimney, horizontal brights were apparent in the Kyrre Formation (Fig. 6.8a). The extent and position of this chimney is different from what is observed of seismic features above the other leaky structures, which are mostly of concentrated and local character. Although the chimney is located over a larger area, the brights could, like the seismic anomalies above the other leaky structures, originate from one of the faults that delineate the crest of the structure. However, due to the poor seismic resolution in this area, this is difficult to determine. Another alternative, is that the chimney is caused by leakage from the cap rock and not by leakage through faults.

In general, amplitude anomalies in the Kyrre Formation seem to be the most consistent seismic feature which could be related to hydrocarbon leakage. Dim zones, V-brights and chaotic reflection patterns in the upper Hordaland Group seems to be less consistent, as they are also observed above filled structures.

6.4 How did leakage occur?

Vertical leakage is recognized as the main cause for all the underfilled and emptied reservoirs in the investigated structures. This type of leakage is commonly associated with fractures and faults, caused by tensile failure and shear failure, respectively. Alternatively, hydrocarbons could leak vertically through the pore network of the cap rocks, which is also referred to as capillary leakage (Bolås & Hermanrud, 2003). In this section, a discussion of to what extent these mechanisms can explain leakage in the area will be conducted, with emphasis on the observations made in the study area.

For tensile failure and formation of new fractures in the cap rock to occur, the reservoir pressure must exceed the least principal stress and the tensile strength of the cap rock. Such failure is favoured at the apex of the structures, where the effective stress is the least (Bolås & Hermanrud, 2003). A common measure of the likeliness for this to occur is the retention capacity. A general observation is that the calculated retention capacities of the suggested leaky structures are significantly larger than zero, which indicates that current pore pressures in the investigated structures are not high enough to induce new tensile fractures. Bolås *et al.* (2005) suggested that areas with high retention capacities on the Continental Shelf can be associated with areas that have been affected by recent stress anisotropies, due to crustal flexuring as a response to glacial advance and retreat. Based on the location of the present day hinge zone of crustal flexuring in the Northern North Sea, outlined by (Doré & Jensen, 1996), this implies that the study area is at present day affected by high stress anisotropy (Fig. 3.5, section 3.3.4).

Based on 3D numerical modelling of glacially induced lithospheric flexure, Grollimund & Zoback (2003) estimated the stress changes through time in the Northern North Sea. They found that in areas completely covered by the ice sheets, the horizontal stress remained unchanged while the vertical stress increased drastically. Furthermore, as the ice retreated, the vertical stress decreased, causing the maximum horizontal stress to become the largest, which resulted in a strike-slip regime in the Northern North Sea (Grollimund & Zoback, 2003). This change in stress state and increased stress anisotropy can be demonstrated by the use of Mohr's diagram (Fig. 6.9). Here, circle 1 represents the stress state under glacial loading, which is a stable normal-faulting regime. Circle 2 represents the stress state in the study area under glacial retreat, where the maximum horizontal stress becomes the largest. Such increase of maximum horizontal stress relative to the vertical stress leads to increased stress anisotropy. As visualized by Mohr's diagram this will promote shear failure, which involves reopening of already existing faults or fractures. This is in agreement with Wiprut & Zoback (2002) and Bolås & Hermanrud (2002), which suggested that leakage by hydrofracturing in general is unlikely, as shear failure will occur before the pore pressure can rise to

the level of the minimum principal stress. Furthermore, leakage by shear failure could cause pressure release, and thereby reduce the pore pressure within the formations. This could also explain why the retention capacities are relatively low within the study area. Although this is not in agreement with Borge (2000)'s theory, that leakage in the Northern Viking Graben is caused by hydrofracturing (tensile failure), leakage induced by shear failure is still considered the most plausible cause in the study area.

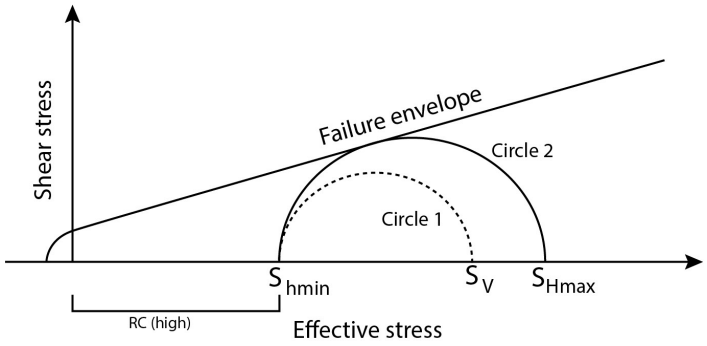

Figure 6.9: Mohr's diagram with failure envelope and Mohr' circle. Circle 1 illustrates the stress state under normal-faulting regime, where the rock is not critically stressed (the ice is stable over the study area, no crustal flexuring). Here, the vertical stress (S_V) is the largest, while the minimum horizontal stress (S_{hmin}) is the smallest. As the ice cap melts and retreats, crustal flexuring causes increased stress anisotropy and the maximum horizontal stress (S_{Hmax})) becomes the largest. This causes the circle to expand and intersect with the failure envelope (shear failure is induced). Shear failure due to increased stress anisotropy could explain the relative high retention capacities in the study area.

The two normally pressured structures Fram H-South and Fram F-East are both believed to have leaked vertically from faults that delineate the structures. Although no amplitude maps have been generated, amplitude anomalies are clearly concentrated above these faults (Fig. 5.26). Normally pressured reservoirs are not very prone to induce failure. However, the suggested leaky faults that delineate these structures are very close to being critically stressed in the current stress field. This could explain why these are the only leaking structures in the Fram area, as the faults that delineate the filled structures are not critically stressed. This is consistent with the suggestion made by Wiprut & Zoback (2002), that faults which are optimal oriented in the present-day stress field are more prone to reactivate than others. It is therefore proposed that leakage from these structures have occurred in relative recent time, caused by crustal flexuring.

The overpressured and underfilled structures Vega North and the B-structure share the same characteristics. They have approximately the same retention capacities and orientations of suggested leaky faults. Furthermore, the gas-water contacts in these structures seem to coincide with fault intersections, which are overlain by seismic amplitude anomalies in the Kyrre Formation. Combined, these characteristics indicate vertical leakage, focused in fault intersections. These observations are similar to what Gartrell *et al.* (2004) reported from an underfilled oil field, offshore Australia. By 3D

numerical modelling of the faults that delineates this field, Gartrell *et al.* (2004) found that fault intersections which have gone through reactivation are likely to be sites of high permeability, due to the high concentration of fracture networks. Furthermore, Gartrell *et al.* (2003) suggested that continuous flow of hydrocarbons, at the expense of hydrothermal fluids, through such high permeability zones, may reduce the potential for mineral precipitation to occur. This could possible explain why the B-structure and Vega North are still underfilled, despite being surrounded by mature source rocks which could continuously charge the traps.

However, the suggested leaky faults which form the fault intersections of the underfilled B-structure and Vega North, are not critically stressed in the current stress field. Reactivation of these faults can therefore not be directly related to recent crustal flexuring. A stress state which could explain reactivation of these faults is a WNW-ESE -orientation of the maximum horizontal stress, which is currently present on the western flank of the Viking Graben and at the Halten Terrace (Brudy & Kjørholt, 2001). Both of these areas are located further west from the hinge zone caused by crustal flexuring than the eastern flank of the Viking Graben (Fig. 3.5, section 3.3.4) (Doré & Jensen, 1996). One could therefore speculate that if the hinge zone was located further east, the maximum horizontal stress orientation on the eastern flank of the Viking Graben would be similar to the present-day orientation on the western flank. However, as the stress state in the Northern North Sea probably is affected by other processes than crustal flexuring, such as ridge push from the North Atlantic rift margin (Grollimund & Zoback, 2003), the timing of reactivation of these faults remains inconclusive.

Similar seismic anomalies as in the B-structure and Vega North were observed above a fault intersection that delineates the apex of overpressured dry structure 35/10-1. Due to the location of the fault intersection, it is inferred that leakage in this location caused the emptied reservoir in this structure. If the seismic characteristics above this structure could be defined as a chimney, this would be in agreement with the "class A chimney" in Heggland (2013)'s chimney classification, where leaky fault that intersects the apex of the structure results in emptied reservoirs (Fig. 3.9). However, similar to the other underfilled overpressured structures, the suggested leaky fault in structure 35/10-1 is not favourably oriented in the present day stress field. It is therefore uncertain which event that caused the leakage.

The second overpressured dry structure, 35/4-1 has slightly different characteristics. The large chimney, which stretches along the entire crest of the structure, does not indicate a specific point source of concentrated leakage. Based on Heggland (2013)'s chimney classification, this type of chimney (type 2) is associated with hydrocarbon bearing structures with only minor leakage through the cap rock (Fig. 3.9). However, as this structure is proven dry with residual hydrocarbons, it is inferred that fatal

leakage has occurred, either by fault reactivation or fracturing of the cap rock. The suggested leaky fault, which delineates the apex of the structure, is close to favourable oriented for shear failure in the present day stress field. Furthermore, if this fault is extrapolated into the overburden with the same dip, it will encounter the observed brights in the Kyrre Formation (marked with dotted black line in Figure 5.35). This fault could therefore be a good candidate for the observed leakage. Based on this, it is suggested that leakage from this structure occurred through reactivation of this fault or shear fractures at top reservoir, caused by recent crustal flexuring.

Whether leakage occurred from the third dry structure, 35/11-3S, is more uncertain than the other dry structures, as the exploration well could have been drilled outside the structural closure. The fault that delineates this structure is oriented similar to the faults of the filled structures. These faults were not found to be critically stressed, neither for the stress field at the eastern or the western flank of the Viking Graben. Furthermore, the calculated retention capacity of this structure is the second highest of all the structures in the study area. Other than a subtle dim in the top Kyrre Formation reflector, there are no seismic observations that may indicate vertical leakage from this structure. The structure is therefore suggested to be spill-point controlled with up-dip volumes of the well location. Alternative explanations for this dry structure are discussed in section 6.1.2.

In general, leakage from the underfilled and emptied reservoirs is suggested to occur through faults, by fault reactivation or by opening of pre-existing fractures in faults. For the underfilled/dry Fram H-South and Fram F-East, this is favoured due to the orientations of the suggested leaky faults. Although the present day stress field cannot explain such fault reactivation in the B-structure, Vega North and 35/10-1, this is still favoured over hydraulic fracturing of the cap rocks. Dry structure 35/4-1 may have leaked due to reopening of pre-existing fractures in of the cap rock, judging by the wide seismic chimney. However, also in this structure, fault leakage is favoured due to the orientation of the fault that delineates the apex of the structure.

Vertical leakage through the pore network as cause for the observed emptied and underfilled reservoirs is considered unlikely due to following reasons. For hydrocarbons to leak through the pore network of the cap rock, the hydrocarbon phase (oil or gas) has to overcome the capillary entry pressure of the seal, which is determined by the size of of the largest interconnected pore throats of the seal (section 3.4.3) (Berg, 1975). The cap rocks in the study area are in most parts represented by the shaly Heather and Draupne Formations of the Viking Group. In the shallow most parts of the study area, reservoirs in Sognefjord Formation are in some places capped by the shaly Shetland Group. Nevertheless, filled structures are present in both the deep and shallow parts of the study area. As the caprocks of the filled structures are the same as for the

underfilled and dry structures, it is inferred that the size of the pore throats of these seals are small enough to withstand capillary leakage.

6.5 Practical significance of the results

Most of the leaking traps are delineated by faults which are oriented differently than the dominating fault trends in the area. Furthermore, almost all the leaking structures are bounded by fault intersections. However, the Grosbeak structure, which appears to be filled, falls within this category as well. Therefore, fault orientations that deviate from the most common strike in the area do not necessarily imply leakage. However, if combined with seismic observations of amplitude anomalies in the overburden above the structure, such observations could strengthen the possibility of identification of leaky structures. If amplitude anomalies, such as concentrated areas of brights, are present directly above faults or fault intersections, this could be diagnostic of leakage. The locations of the amplitude anomalies can also in many cases point to the locations where the leakage occurred, and could therefore potentially reveal the position of the fluid contact. The location of the fault intersections relative to the top of the reservoirs are also of vital importance, as structures with fault intersections that delineate the apex are proven dry. If the fault intersection delineates the top of the reservoir in a down-flank position, and if one of these faults were to be critically stressed in the current stress field, this could control the height of the hydrocarbon column. It is therefore suggested that such observations should be included when calculating in-place volumes and risking of the prospect.

7 Proposal for further work

There are many uncertainties related to the interpretations of fill-spill routes and column-height controls in this study. To reduce these uncertainties in a possible further work, the following is suggested:

- Utilization of 3D seismic data with improved quality would allow for more detailed interpretation in the deep areas, especially in the northernmost part where structure 35/4-1 is located. Also, by detailed mapping of Upper Jurassic reservoirs in the south-western shallow area, spill points could be obtained. This would allow for more precise analysis of column-height controls in this area.
- Evaluation of whether recent tilting of reservoirs (induced by uplift) has affected the column heights and oil/gas distribution in the area. This could be done by flattening of seismic horizons.
- Sedimentological and petrophysical investigation of the area should be conducted for a complete understanding of the pressure distribution and migration routes.
- Investigations of whether the chaotic reflection patterns (i.e. remobilized sediments) in the upper part of the Hordaland Group are caused by vertical leakage from underlying structures.
- Measurements of dip of faults and model of which faults are most likely to slip under normal faulting regime.

8 Conclusion

The main focus of this study was to investigate the controls on hydrocarbon column-heights and hydrocarbon distribution in the north-eastern Viking Graben. Analysis of 3D-seimsic data and exploration well data in the area has showed that the position of the structural spill points and vertical leakage are the main controlling factor on hydrocarbon column-heights in the investigated structures. The main conclusions are as follows:

- The north-eastern Viking Graben can be divided into an overpressured region and a close to- normally pressured region. The overpressured area is characterized by compartmentalization and a lack of lateral communication between the structures. Fill-spill routes in this area are therefore suggested to be closed at present day. In the normally pressured area, communication between the reservoirs and southwards to the Troll field seems to be present.

- The distribution between deep, overpressured gas fields and shallow, close to normally pressured oil/gas fields could be a result of reduced supply of gas into the shallow area. This is suggested to be related to closing of migration routes, caused by extensive cementation and sealing faults, between the deep gas-generating grabens and the shallow terraces. Hydrocarbon supply is considered to have been sufficient for all the structures in the study area, and hydrocarbon generation and migration is suggested to have occurred before extensive cementation initiated.

- Of a total of nine structures in the overpressured region, four structures are suggested to leak, of which two are underfilled and two are dry. One of the reportedly dry wells is suggested to be drilled outside the structural closure and the structure might therefore contain up-dip volumes. However, vertical leakage from this structure cannot be ruled out. Of the remaining four overpressured structures, two structures are suggested to be filled, while the fluid contacts in the last two structures are unknown. Of seven normally pressured structures, two structures are suggested to have leaked.

- Fault intersections are observed above the apex in three of four dry structures. In the dry structure without fault intersection, up-dip volumes from the well might be present. In the underfilled, overpressured structures, gas-water contacts coincide with fault intersections where they delineate the top reservoir surface. Leakage through faults, most probably fault intersections, is also suggested to control the hydrocarbon column-heights in the underfilled, normally pressured structures.

- Suggested leaky faults of the underfilled and dry traps have different orientations than the filled structures (with one exception, the Grosbeak structure). Considering a present day strike slip fault regime with maximum horizontal stress oriented N80°E in the study area, the suggested leaky fault orientations of the underfilled, normally pressured structures are close to critically stressed. No clear relationship have been found between this stress state and the suggested leaky fault orientations of the dry and underfilled, overpressured structures. A N100°E -orientation of the maximum horizontal stress, as is present at the western flank of the Viking Graben, would generally be a better fit for reactivation of these faults. All the faults that delineates the filled structures (with one exception, the Grosbeak structure) seem to be stable in both of these stress fields.

- Brights are observed in the Rogaland Group above the suggested leaky structures in the normally pressured area. Also, brights in the Kyrre Formation are observed above all the suggested leaky structures in the overpressured, deep part of the study area. Judging by the location of these seismic amplitude anomalies relative to the suggested leaky faults, they could give an indication of the point source of vertical leakage. Furthermore, if such amplitude anomalies are found to be related to specific faults, and these faults are critically stressed in the current stress field, this should be included when calculating in-place volumes and risking of the prospect.

References

Aadnoy, Bernt S, Bratli, Rolf K, & Lindholm, Conrad D. 1994. In-situ stress modelling of the Snorre field. *In: Rock Mechanics in Petroleum Engineering.* Society of Petroleum Engineers.

Anderson, Ernest Masson. 1905. The dynamics of faulting. *Transactions of the Edinburgh Geological Society*, **8**(3), 387–402.

Arntsen, Børge, Wensaas, Lars, Løseth, Helge, & Hermanrud, Christian. 2007. Seismic modeling of gas chimneys. *Geophysics*, **72**(5), SM251–SM259.

Avseth, Per, Mukerji, Tapan, & Mavko, Gary. 2005. *Quantitative seismic interpretation: Applying rock physics tools to reduce interpretation risk.* Cambridge University Press.

Badley, ME, Price, JD, Dahl, C Rambech, & Agdestein, T. 1988. The structural evolution of the northern Viking Graben and its bearing upon extensional modes of basin formation. *Journal of the Geological Society*, **145**(3), 455–472.

Badley, Michael E. 1985. *Practical seismic interpretation.* IHRDC Press, Boston, MA.

Bartholomew, ID, Peters, JM, & Powell, CM. 1993. Regional structural evolution of the North Sea: oblique slip and the reactivation of basement lineaments. *Geology of Northwest Europe: proceedings of the 4th Conference*, **4**, 1109–1122.

Berg, Robert R. 1975. Capillary pressures in stratigraphic traps. *AAPG bulletin*, **59**(6), 939–956.

Bjørlykke, K, Aagaard, P, Dypvik, H, Hastings, DS, & Harper, AS. 1986. Diagenesis and reservoir properties of Jurassic sandstones from the Haltenbanken area, offshore mid-Norway. *Habitat of hydrocarbons on the Norwegian continental shelf*, 275–286.

Bjørlykke, Knut. 2010. *Petroleum geoscience: From sedimentary environments to rock physics.* Springer Science & Business Media.

Bluck, BJ. 2000. Caledonian and related events in Scotland. *Transactions of the Royal Society of Edinburgh: Earth Sciences*, **91**(3-4), 375–404.

Bolås, Hege M Nordgård, & Hermanrud, Christian. 2003. Hydrocarbon leakage processes and trap retention capacities offshore Norway. *Petroleum Geoscience*, **9**(4), 321–332.

Bolås, Hege M Nordgård, Hermanrud, Christian, & Teige, Gunn MG. 2005. The Influence of Stress Regimes on Hydrocarbon Leakage. *AAPG Hedberg Series*, **2**, 109–123.

Bolås, Hege Marit Nordgård, & Hermanrud, Christian. 2002. Rock stress in sedimentary basins – Implications for trap integrity. *Norwegian Petroleum Society Special Publications*, **11**, 17–35.

Borge, Hans. 2000. *Fault controlled pressure modelling in sedimentary basins.* Ph.D. thesis, Department of Mathematical Sciences, Norwegian University of Science and Technology, Trondheim, Norway.

Brudy, M, Zoback, MD, Fuchs, K, Rummel, F, & Baumgärtner, J. 1997. Estimation of the complete stress tensor to 8 km depth in the KTB scientific drill holes: Implications for crustal strength. *Journal of Geophysical Research: Solid Earth (1978–2012)*, **102**(B8), 18453–18475.

Brudy, Martin, & Kjørholt, Halvor. 2001. Stress orientation on the Norwegian continental shelf derived from borehole failures observed in high-resolution borehole imaging logs. *Tectonophysics*, **337**(1), 65–84.

Bugge, Tom, Tveiten, Bjarne, & Bäckström, Sven. 2001. The depositional history of the Cretaceous in the northeastern North Sea. *Norwegian Petroleum Society Special Publications*, **10**, 279–291.

Buhrig, C. 1989. Geopressured Jurassic reservoirs in the Viking Graben: modelling and geological significance. *Marine and Petroleum Geology*, **6**(1), 31–48.

Cartwright, Joe, Huuse, Mads, & Aplin, Andrew. 2007. Seal bypass systems. *AAPG Bulletin*, **91**(8), 1141–1166.

Christensen, Elisa. 2015. *The geological evolution of the Oligocene to Middle Miocene Hordaland Group, from deposittion to present day geometries, based on data from the Johan Sverdrup.* Petroleum geology, Department of Earth Science, University of Bergen.

Dahl, N, & Solli, T. 1993. The structural evolution of the Snorre Field and surrounding areas. *Pages 1159–1166 of: Geological Society, London, England, Petroleum Geology Conference series*, vol. 4. Geological Society of London.

Doré, AG, & Jensen, LN. 1996. The impact of late Cenozoic uplift and erosion on hydrocarbon exploration: offshore Norway and some other uplifted basins. *Global and Planetary Change*, **12**(1), 415–436.

Eidvin, T, Riis, F, Rasmussen, ES, & Rundberg, Y. 2013a. Investigation of Oligocene to lower pliocene deposits in the Nordic area. *NPD Bull*, **10**, 59.

Eidvin, Tor, & Rundberg, Yngve. 2007. Post-Eocene strata of the southern Viking Graben, northern North Sea; integrated biostratigraphic, strontium isotopic and lithostratigraphic study. *Norwegian Journal of Geology/Norsk Geologisk Forening*, **87**(4), 391–450.

Ersland, Remi Anthoni. 2014. *Vertikal forkastningslekkasje på Haltenbanken: Sammenligning mellom lekkende of hydrokarbonfylte strukturer.* M.Phil. thesis, Department of Earth Science, University of Bergen.

Faleide, Jan Inge, Kyrkjebø, Rune, Kjennerud, Tomas, Gabrielsen, Roy H, Jordt, Henrik, Fanavoll, Stein, & Bjerke, Morten D. 2002. Tectonic impact on sedimentary processes during Cenozoic evolution of the northern North Sea and surrounding areas. *Geological Society, London, Special Publications*, **196**(1), 235–269.

Fjeldskaar, Willy, Lindholm, Conrad, Dehls, John F, & Fjeldskaar, Ingrid. 2000. Postglacial uplift, neotectonics and seismicity in Fennoscandia. *Quaternary Science Reviews*, **19**(14), 1413–1422.

Færseth, RB. 1996. Interaction of Permo-Triassic and Jurassic extensional fault-blocks during the development of the northern North Sea. *Journal of the Geological Society*, **153**(6), 931–944.

Fyfe, JA, Gregersen, U, Jordt, H, Rundberg, Y, Eidvin, T, Evans, D, Stewart, D, Hovland, M, & Andresen, P. 2003. *Millenium Atlas: Petroleum geology of the Central and Northern North Sea.* The Geological Society of London, England. Chap. Oligocene to holocene, pages 279–285.

Gaarenstroom, L, Tromp, RAJ, BRANDENBURG, AM, *et al.* 1993. Overpressures in the Central North Sea: implications for trap integrity and drilling safety. *Geological Society, London, Petroleum Geology Conference series*, **4**, 1305–1313.

Gabrielsen, Roy H, Kyrkjebø, Rune, Faleide, Jan Inge, Fjeldskaar, Willy, & Kjennerud, Tomas. 2001. The Cretaceous post-rift basin configuration of the northern North Sea. *Petroleum Geoscience*, **7**(2), 137–154.

Galloway, WE. 2002. Paleogeographic setting and depositional architecture of a sand-dominated shelf depositional system, Miocene Utsira Formation, North Sea Basin. *Journal of Sedimentary Research*, **72**(4), 476–490.

Gartrell, Anthony, Zhang, Yanhua, Lisk, Mark, & Dewhurst, David. 2003. Enhanced hydrocarbon leakage at fault intersections: an example from the Timor Sea, Northwest Shelf, Australia. *Journal of Geochemical Exploration*, **78**, 361–365.

Gartrell, Anthony, Zhang, Yanhua, Lisk, Mark, & Dewhurst, David. 2004. Fault intersections as critical hydrocarbon leakage zones: integrated field study and numerical modelling of an example from the Timor Sea, Australia. *Marine and Petroleum Geology*, **21**(9), 1165–1179.

Georgescu, Lidia. 2013. *Vertical Fault Leakage in the Western Part of the Hammerfest Basin.* M.Phil. thesis, Department of Earth Science, University of Bergen.

Gluyas, J, & Swarbrick, R. 2003. *Petroleum Geoscience.* Wiley: Blackwell Publishing, Oxford, England.

Goff, JC. 1983. Hydrocarbon generation and migration from Jurassic source rocks in the E Shetland Basin and Viking Graben of the northern North Sea. *Journal of the Geological Society*, **140**(3), 445–474.

Graham, C, Armour, Andrew, Bathurst, Paul, Evans, Daniel, & Petroleumsforening, Norsk. 2003. The millennium atlas: Petroleum geology of the central and northern North Sea. *In: The millennium atlas: Petroleum geology of the central and northern North Sea*. Geological Society of London.

Graue, K. 2000. Mud volcanoes in deepwater Nigeria. *Marine and Petroleum Geology*, **17**(8), 959–974.

Gregersen, U, & Johannessen, PN. 2007. Distribution of the Neogene Utsira Sand and the succeeding deposits in the Viking Graben area, North Sea. *Marine and Petroleum Geology*, **24**(10), 591–606.

Grollimund, Balz, & Zoback, Mark D. 2000. Post glacial lithospheric flexure and induced stresses and pore pressure changes in the northern North Sea. *Tectonophysics*, **327**(1), 61–81.

Grollimund, Balz, & Zoback, Mark D. 2003. Impact of glacially induced stress changes on fault-seal integrity offshore Norway. *AAPG bulletin*, **87**(3), 493–506.

Head, Martin J, Riding, James B, Eidvin, Tor, & Chadwick, R Andrew. 2004. Palynological and foraminiferal biostratigraphy of (upper Pliocene) Nordland Group mudstones at Sleipner, northern North Sea. *Marine and Petroleum Geology*, **21**(3), 277–297.

Heggland, Roar. 1998. Gas seepage as an indicator of deeper prospective reservoirs. A study based on exploration 3D seismic data. *Marine and Petroleum Geology*, **15**(1), 1–9.

Heggland, Roar. 2005. Using gas chimneys in seal integrity analysis: A discussion based on case histories. *AAPG Hedberg Series*, **2**, 237–245.

Heggland, Roar. 2013. Hydrocarbon Trap Classification Based on Associated Gas Chimneys. *Hydrocarbon Seepage: From Source to Surface. SEG AAPG Geophysical Developments*, **16**, 221–230.

Helland-Hansen, W, Ashton, M, Lømo, L, & Steel, R. 1992. Advance and retreat of the Brent delta: recent contributions to the depositional model. *Geological Society, London, Special Publications*, **61**(1), 109–127.

Hermanrud, Christian. 1988. *Determination of formation temperature from downhole measurements*. Tech. rept. South Carolina Univ., Columbia, SC (USA).

Hermanrud, Christian, & Bolås, Hege Marit Nordgård. 2002. Leakage from overpressured hydrocarbon reservoirs at Haltenbanken and in the northern North Sea. *Norwegian Petroleum Society Special Publications*, **11**, 221–231.

Hermanrud, Christian, Eggen, Svein, & Larsen, Rolf Magne. 1991. Investigation of the thermal regime of the Horda platform by basin modelling: implications for the hydrocarbon potential of the Stord basin, northern North Sea. *Generation, Accumulation and Production of*

Europe's Hydrocarbon. European Association of Petroleum Geoscientists, Special Publication, **1**, 65–73.

Hermanrud, Christian, Bolås, Hege M Nordgård, & Teige, Gunn MG. 2005. Seal failure related to basin-scale processes. *AAPG Hedberg Series*, **2**, 13–22.

Hermanrud, Christian, Halkjelsvik, Malene Eikås, Kristiansen, Kine, Bernal, Asdrúbal, & Strömbäck, Anna Christiana. 2014. Petroleum column-height controls in the western Hammerfest Basin, Barents Sea. *Petroleum Geoscience*, **20**(3), 227–240.

Holgate, Nicholas E, Jackson, Christopher A-L, Hampson, Gary J, & Dreyer, Tom. 2013. Sedimentology and sequence stratigraphy of the Middle-upper Jurassic Krossfjord and Fensfjord formations, troll Field, northern North Sea. *Petroleum Geoscience*, **19**, 237–258.

Huuse, Mads, & Mickelson, Marit. 2004. Eocene sandstone intrusions in the Tampen Spur area (Norwegian North Sea Quad 34) imaged by 3D seismic data. *Marine and Petroleum Geology*, **21**(2), 141–155.

Huuse, Mads, Duranti, Davide, Steinsland, Noralf, Guargena, Claudia G, Prat, Philippe, Holm, Kristine, Cartwright, Joseph A, & Hurst, Andrew. 2004. Seismic characteristics of large-scale sandstone intrusions in the Paleogene of the south Viking Graben, UK and Norwegian North Sea. *Geological Society, London, Memoirs*, **29**(1), 263–278.

ICS. 2014. *International Chronostratigraphic Chart, 2014.* Tech. rept. International Comission on Stratigraphy (ICS), Available from the internet: http://www.stratigraphy.org/ICSchart/ChronostratChart2014-10.jpg.

Isaksen, D, & Tonstad, Ke. 1989. *A revised Cretaceous and Tertiary lithostratigraphic nomenclature for the Norwegian North Sea.* NPD Bulletin No. 5.

Jordt, Henrik, Faleide, Jan Inge, Bjørlykke, Knut, & Ibrahim, Maged T. 1995. Cenozoic sequence stratigraphy of the central and northern North Sea Basin: tectonic development, sediment distribution and provenance areas. *Marine and Petroleum Geology*, **12**(8), 845–879.

Keym, Matthias, Dieckmann, Volker, Horsfield, Brian, Erdmann, Michael, Galimberti, Roberto, Kua, Lung-Chuan, Leith, Leslie, & Podlaha, Olaf. 2006. Source rock heterogeneity of the Upper Jurassic Draupne Formation, North Viking Graben, and its relevance to petroleum generation studies. *Organic Geochemistry*, **37**(2), 220–243.

Kjennerud, T, Faleide, JI, Gabrielsen, RH, Gillmore, GK, Kyrkjebø, R, Lippard, SJ, & Løseth, H. 2001. Structural restoration of Cretaceous-Cenozoic (post-rift) palaeobathymetry in the northern North Sea. *Norwegian Petroleum Society Special Publications*, **10**, 347–364.

Kristiansen, Kine. 2011. *Vertical Fault Leakage in the Western Part of the Hammerfest Basin.* M.Phil. thesis, Department of Earth Science, University of Bergen.

Kyrkjebø, R, Kjennerud, T, Gillmore, GK, Faleide, JI, & Gabrielsen, RH. 2001. Cretaceous-Tertiary palaeo-bathymetry in the northern North Sea; integration of palaeo-water depth estimates obtained by structural restoration and micropalaeontological analysis. *Norwegian Petroleum Society Special Publications*, **10**, 321–345.

Ligtenberg, JH. 2005. Detection of fluid migration pathways in seismic data: implications for fault seal analysis. *Basin Research*, **17**(1), 141–153.

Lothe, AE, Sylta, Ø, Lauvrak, O, & Sperrevik, S. 2006. Influence of fault map resolution on pore pressure distribution and secondary hydrocarbon migration; Tune area, North Sea. *Geofluids*, **6**(2), 122–136.

Løseth, H, Raulline, B, & Nygård, A. 2013. Late Cenozoic geological evolution of the northern North Sea: development of a Miocene unconformity reshaped by large-scale Pleistocene sand intrusion. *Journal of the Geological Society*, **170**(1), 133–145.

Løseth, Helge, Wensaas, Lars, Arntsen, Børge, & Hovland, Martin. 2003. Gas and fluid injection triggering shallow mud mobilization in the Hordaland Group, North Sea. *Geological Society, London, Special Publications*, **216**(1), 139–157.

Løseth, Helge, Gading, Marita, & Wensaas, Lars. 2009. Hydrocarbon leakage interpreted on seismic data. *Marine and Petroleum Geology*, **26**(7), 1304–1319.

Martinsen, OJ, Bøen, F, Charnock, MA, Mangerud, G, & Nøttvedt, A. 1999. Cenozoic development of the Norwegian margin 60–64 N: sequences and sedimentary response to variable basin physiography and tectonic setting. *Proceedings of the Fifth Conference*, **5**, 293–304.

Minescu, Florea, Popa, Constantin, & Grecu, Dumitru. 2010. Theoretical and practical aspects of tertiary hydrocarbon migration. *Petroleum Science and Technology*, **28**(6), 555–572.

NPD. 2015. *The NPD fact pages and maps.* Tech. rept. Norwegian Petroleum directorate, Available from the internet: http://npd.no/.

Nøttvedt, A, Gabrielsen, RH, & Steel, RJ. 1995. Tectonostratigraphy and sedimentary architecture of rift basins, with reference to the northern North Sea. *Marine and Petroleum Geology*, **12**(8), 881–901.

O'Brien, GW, Cowley, R, Quaife, P, & Morse, M. 2002. Characterizing hydrocarbon migration and fault-seal integrity in Australia's Timor Sea via multiple, integrated remote-sensing technologies. *Surface exploration case histories: applications of geochemistry, magnetics and remote sensing. AAPG Stud Geol*, **48**, 393–413.

Odinsen, Tore, Reemst, Paul, Van Der Beek, Peter, Faleide, Jan Inge, & Gabrielsen, Roy H. 2000. Permo-Triassic and Jurassic extension in the northern North Sea: results from

tectonostratigraphic forward modelling. *Geological Society, London, Special Publications*, **167**(1), 83–103.

Osborne, Mark J, & Swarbrick, Richard E. 1997. Mechanisms for generating overpressure in sedimentary basins: a reevaluation. *AAPG Bulletin*, **81**(6), 1023–1041.

Rasmussen, Erik S, Heilmann-Clausen, Claus, Waagstein, Regin, & Eidvin, Tor. 2008. The tertiary of Norden. *Episodes*, **31**(1), 66.

Ravnaas, R, Nottvedt, A, Steel, RJ, & Windelstad, J. 2000. Syn-rift sedimentary architectures in the Northern North Sea. *Geological Society, London, Special Publications*, **167**(1), 133–177.

Rundberg, Yngve, & Eidvin, Tor. 2005. Controls on depositional history and architecture of the Oligocene-Miocene succession, northern North Sea Basin. *Norwegian Petroleum Society Special Publications*, **12**, 207–239.

Skibeli, M, Barnes, K, Straume, T, Syvertsen, SE, & Shanmugam, G. 1995. A sequence stratigraphic study of Lower Cretaceous deposits in the northernmost North Sea. *Norwegian Petroleum Society Special Publications*, **5**, 389–400.

Skogseid, Jakob, Planke, Sverre, Faleide, Jan Inge, Pedersen, Tom, Eldholm, Olav, & Neverdal, Flemming. 2000. NE Atlantic continental rifting and volcanic margin formation. *Geological Society, London, Special Publications*, **167**(1), 295–326.

Steel, R, & Ryseth, A. 1990. The Triassic - Early Jurassic succession in the northern North Sea: megasequence stratigraphy and intra-Triassic tectonics. *Geological Society, London, Special Publications*, **55**(1), 139–168.

Steel, RJ. 1993. Triassic - Jurassic megasequence stratigraphy in the Northern North Sea: rift to post-rift evolution. *Geological Society, London, Petroleum Geology Conference series*, **4**, 299–315.

Stewart, Simon A, & Davies, Richard J. 2006. Structure and emplacement of mud volcano systems in the South Caspian Basin. *AAPG bulletin*, **90**(5), 771–786.

Teige, Gunn MG, & Hermanrud, Christian. 2004. Seismic characteristics of fluid leakage from an underfilled and overpressured Jurassic fault trap in the Norwegian North Sea. *Petroleum Geoscience*, **10**(1), 35–42.

Teige, Gunn MG, Hermanrud, Christian, Kløvjan, Oddbjørn S, Eliassen, Per Emil, Løseth, Helge, & Gading, Marita. 2002. Evaluation of caprock integrity in the western (high-pressured) Haltenbanken area: a case history based on analyses of seismic signatures in overburden rocks. *Norwegian Petroleum Society Special Publications*, **11**, 233–242.

Thyberg, B, Jordt, H, Bjorlykke, K, & Faleide, JI. 2000. Relationships between sequence stratigraphy, mineralogy and geochemistry in Cenozoic sediments of the northern North Sea. *Geological Society, London, Special Publications*, **167**, 245–272.

Tissot, Bernard P, & Welte, Dietrich H. 1984. *Petroleum formation and occurrence*. Springer-Verlag, New York, NY.

Walderhaug, Olav. 2000. Modeling quartz cementation and porosity in Middle Jurassic Brent Group sandstones of the Kvitebjørn field, northern North Sea. *AAPG bulletin*, **84**(9), 1325–1339.

Whipp, PS, Jackson, C, Gawthorpe, RL, Dreyer, T, Quinn, D, *et al.* 2014. Normal fault array evolution above a reactivated rift fabric; a subsurface example from the northern Horda Platform, Norwegian North Sea. *Basin Research*, **26**(4), 523–549.

Wiprut, David, & Zoback, Mark D. 2000. Fault reactivation and fluid flow along a previously dormant normal fault in the northern North Sea. *Geology*, **28**(7), 595–598.

Wiprut, David, & Zoback, Mark D. 2002. Fault reactivation, leakage potential, and hydrocarbon column heights in the northern North Sea. *Norwegian Petroleum Society Special Publications*, **11**, 203–219.

Wiprut, DJ. 1998. High horizontal stress in the Visund field, Norwegian North Sea: consequences for borehole stability and sand production. *SPE/ISRM*, **47255**, 199–208.

WSM. 2009. *World Stress Map database*. Tech. rept. Helmholtz Centre Potsdam - GFZ German Research Centre for Geosciences, Available from the internet: www.world-stress-map.org.

Zachos, James, Pagani, Mark, Sloan, Lisa, Thomas, Ellen, & Billups, Katharina. 2001. Trends, rhythms, and aberrations in global climate 65 Ma to present. *Science*, **292**(5517), 686–693.

Ziegler, PA. 1975. Geologic evolution of North Sea and its tectonic framework. *AAPG Bulletin*, **59**(7), 1073–1097.

Ziegler, PA. 1992. North Sea rift system. *Tectonophysics*, **208**(1), 55–75.

Zoback, Mark D, Moos, Daniel, Mastin, Larry, & Anderson, Roger N. 1985. Well bore breakouts and in situ stress. *Journal of Geophysical Research: Solid Earth (1978–2012)*, **90**(B7), 5523–5530.

Zoback, MD, Barton, C, Brudy, M, Chang, C, Moos, D, Peska, P, & Vernik, L. 1995a. A review of some new methods for determining the in situ stress state from observations of borehole failure with applications to borehole stability and enhanced production in the North Sea. *Pages 13–14 of: Proceedings of the Workshop on Rock Stresses in the North Sea, Trondheim, Norway, Feb.*

Zoback, MD, Barton, CA, Brudy, M, Chang, C, Moos, D, Peska, P, & Vernik, L. 1995b. Utilization and analysis of multiple modes of borehole failure for estimation of in situ stress. *In: Proceedings of the International Symposium on Rock Mechanics, Tokyo, Japan, 25–30 September.*